Water Resources Research Institute
of The University of North Carolina

Report No. 445

GEOPHYSICAL AND WATER QUALITY CHARACTERIZATION OF ON-SITE WASTEWATER PLUMES

By
Charles Humphrey[1], M. O'Driscoll[2], D. Mallison[2], and S. Hardison[2]

[1]Environmental Health Sciences
East Carolina University
Greenville, NC

[2]Department of Geological Sciences
East Carolina University
Greenville, NC

UNC-WRRI-445

The research on which this report is based was supported by funds provided by the North Carolina General Assembly and/or the US Geological Survey through the NC Water Resources Research Institute.

This report fulfills the requirements for a project completion report of the Water Resources Research Institute of The University of North Carolina. The authors are solely responsible for the content and completeness of the report.

WRRI Project No. 12-07-W
July 2013

Abstract
The objectives of this study were to evaluate the effectiveness of the geophysical techniques ground penetrating radar (GPR) and electrical resistivity (ER) surveys in delineating groundwater influenced by onsite wastewater system discharges (plumes) in coastal NC. Another objective was to assess the effectiveness of the onsite systems in reducing wastewater nitrogen and phosphorus concentrations. Four sites that utilized on-site wastewater systems (OWS) were instrumented with piezometers for groundwater characterization and sample analysis. The sites included two schools in Craven County, NC, a new environmental education center in Pitt County, NC, and a private residence in Pitt County. ER and GPR surveys were conducted three times at each site. Groundwater environmental readings were recorded during the surveys including depth to water, pH, specific conductivity, temperature, and dissolved oxygen. Grab samples were collected from septic tanks, groundwater beneath the OWS, from up and down-gradient from the OWS, and nearby surface waters. The results indicated that GPR was effective at locating OWS components such as drainfield trenches and distribution boxes at each of the settings. ER was successful at delineating groundwater influenced by OWS at the two schools, and was moderately successful at the residential site. Some differences in soil and groundwater specific conductance and resistance were observed at the environmental education center after the system start up, but wastewater generation and discharge to the subsurface was limited, and thus plume development and distinct observation was not significant. The four OWS were more effective at reducing phosphorus concentrations and mass loads in comparison to nitrogen. The site that performed the best for reducing nutrient concentrations and loads had a riparian buffer between the OWS and a nearby stream. Nitrogen and phosphorus concentrations were reduced by 90% or more when groundwater moved through the buffer. However, groundwater that discharge to a spring at the same site had elevated nitrogen and phosphorus concentrations. Groundwater beneath the OWS typically had elevated specific conductivity and pH. Therefore, the OWS were influencing groundwater properties. More research is needed to determine the applicability of GPR and ER for detecting OWS components and groundwater plumes in different geologic settings. More work in determining the processes responsible for reduction in nitrogen and phosphorus mass loadings from the OWS is also suggested.

Acknowledgements
The authors would like to acknowledge the efforts of students and staff including: Matt Smith, Guy Iverson, Eliot Anderson-Evans, John Woods, Jim Watson, Rob Howard, Jonathan Harris, and others for assistance with the project. The study would not have been possible without cooperation from the Craven County Public School System and Craven County School Maintenance Department, Dr. John Bray with A Time For Science, and the homeowner for allowing us to instrument their properties and have access for data collection. We acknowledge and thank the NC Water Resources Research Institute for providing funds to complete this study. We also thank the ECU Research and Graduate Studies for providing a seed grant to help collect data from some of the sites, and the NC Department of Environment and Natural Resources 319 Program for providing funding via a different project to instrument one of the sites used for this study. General acknowledgements to Department of Geological Sciences and Environmental Health Sciences faculty and staff for continued support.

1. Introduction

On-site wastewater treatment systems (OWS) treat and disperse wastewater to the subsurface. Improperly functioning OWS may contribute elevated concentrations of nutrients, pathogens, and other contaminants to water resources, thus influencing water quality. Studies in North Carolina have shown elevated nutrient and/or pathogen concentrations in groundwater (Humphrey et al.. 2010; Humphrey et al., 2011; Humphrey and O'Driscoll, 2012; Sobsey and Scandura, 1997; Cogger et al., 1988) and in surface waters (Cahoon et al., 2006) in close proximity to OWS. Efforts to identify and remediate OWS-related water contamination require a comprehensive understanding of how wastewater is transported and behaves in the subsurface. A better understanding of wastewater migration in the subsurface will allow scientists, resource managers, and policy-makers to effectively address water quality issues, particularly non-point source pollution. The objectives of this study were to test the effectiveness of the geophysical techniques ground penetrating radar (GPR) and electrical resistivity (ER) surveys in delineating groundwater influenced by wastewater discharges (plumes) in variable soil and water depth conditions in coastal NC. Another objective was to assess the effectiveness of the OWS in reducing wastewater nitrogen and phosphorus concentrations.

1.1. Background

1.1.1 On-site Wastewater System Components

OWS typically include 4 components: 1) septic tank, 2) effluent distribution device, 3) drainfield trenches, and 4) soil beneath the trenches (Figure 1).Septic tanks provide primary treatment via sedimentation and retention of solids, and an environment for the anaerobic digestion of organic matter. Liquid effluent is conveyed from the tank to the distribution device, where the effluent is distributed to each of the drainfield trenches. The trenches provide storage area until wastewater infiltrates the soil. The soil beneath the trenches is where most of the wastewater treatment occurs before the effluent reaches groundwater (Figure 1).

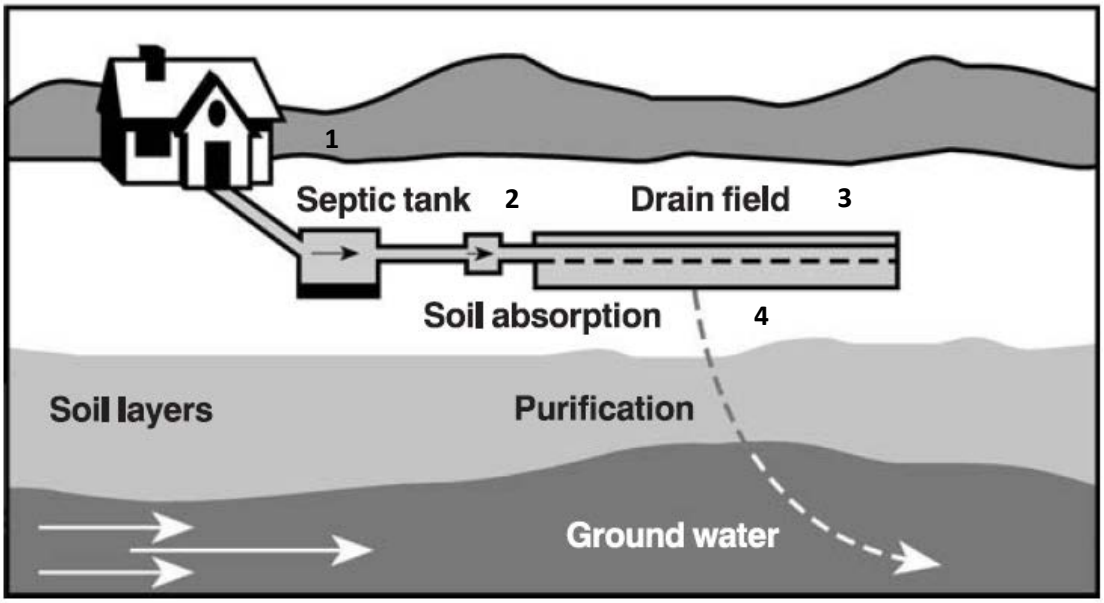

Figure 1. Conventional on-site wastewater treatment system including the 4 major components (septic tank, distribution device, trench, and soil). Modified from: NSFC/EPA (2002).

1.1.2. On-site Wastewater System Treatment Performance

In North Carolina (NC), approximately 50% of the total population uses OWS, with an even higher percentage (~60%) of residences in coastal areas served by these technologies (NC NERR, 2003; Hoover, 2004). OWS treat raw sewage with elevated concentrations of pollutants such as nitrogen, phosphorus, dissolved solids and salts, and pathogenic microorganisms (US EPA, 2002). Many of the contaminants found in high concentrations in wastewater such as nitrogen and phosphorus, are also common in surface waters and have led to degradation of water quality in North Carolina and other states (Fear et al., 2004; Humphrey et al., 2010). If OWS malfunction, or are not effective at reducing nutrient concentrations, then groundwater and nearby surface waters may be negatively impacted. OWS malfunctions occur when 1) wastewater surfaces, 2) wastewater backs up in a plumbing system and/or 3) when the wastewater is inadequately treated in the subsurface (US EPA, 2002). OWS are the third most common reported cause of groundwater contamination in the US (US EPA, 2002).

In coastal NC, approximately 5,000 repair permits are issued each year because of OWS that have experienced hydraulic failures (Humphrey et al., 2012). Information regarding inadequate OWS treatment is not as available, because most OWS are not monitored for treatment performance after the initial permitting process. However, numerous studies have shown that OWS can contribute elevated concentrations on nitrogen and/or phosphorus to groundwater beneath and/or adjacent to OWS. More specifically, studies by Robertson (1991), Aravena et al. (1993); Harman et al. (1996), and Ptacek (1998) in Canada, Corbett et al. (2002) in Florida; and Humphrey et al. (2010; 2012) in coastal North Carolina showed elevated nutrient concentrations adjacent to OWS. Some studies located and tracked wastewater plumes for varying distances away from the systems and determined that nutrient concentrations remained elevated more than 30 m from the source (Robertson et al., 1991; Harman et al., 1996; Ptacek, 1998; Corbett et al. 2002.).

Setback distances between OWS and water bodies are implemented to provide more time and opportunity for OWS contaminant reduction. In North Carolina, a minimum setback of 15 -30 m between OWS and surface water bodies is required for systems depending on the size of the OWS and surface water classification (15A NCAC 18A .1950a-d). These setbacks are based on the assumption that a 15 – 30+ m subsurface flow path will provide adequate treatment of wastewater constituents necessary to prevent contamination of surface water bodies. Research has shown wastewater nutrient migration distances can exceed the 15m offset distance in sandy coastal plain settings (Robertson et al., 1991; Harmon et al., 1996; Corbett et al., 2002; Humphrey et al., in press). Therefore, a 15m offset distance may be inadequate for preventing high concentrations of OWS derived nutrients from discharging to adjacent surface waters. More research regarding OWS pollutant fate and transport conducted in settings with variability in geology, soils, and with different OWS technologies is needed to help environmental agencies and policy developers determine what steps should be taken (if any) to address OWS nutrient contributions to ground and surface waters.

Because OWS are non-point sources of pollution, quantifying their influence on water resources is more difficult than with point sources of pollution. The installation of many groundwater monitoring wells installed down-gradient and within the groundwater flow path of OWS with routine sample collection and analyses can help determine contaminant fate and transport. However, this methodology requires installing a network of monitoring wells, and thus is labor intensive, costly, and disruptive. The number of monitoring wells installed for data collection is often limited by these constraints. Furthermore, groundwater flow direction, magnitude, and the concentration of pollutants and area of influence can vary with time, adding to the complexity of characterizing groundwater pollution and surface water impacts. Determining the impacts of groundwater transported OWS sources of pollution requires accurate delineation of plumes. If monitoring wells are installed in areas outside the major zone of influence, or the zone of influence changes over time, the actual impacts of the pollution source may be underestimated. It is challenging to find property owners that use OWS and will allow researchers to install an intensive network of monitoring wells. Non-intrusive techniques that can provide evidence of OWS impacted groundwater with minimal site disturbance would be very beneficial to scientists, regulators and resource managers by allowing more focused groundwater monitoring network installations, thus reducing the number of wells needed for the research.

1.2.1. Geophysical Technologies

Two non-intrusive geophysical techniques, electrical resistivity (ER) surveys and ground penetrating radar (GPR), are sensitive to changes in electrical properties in the subsurface and may be applied toward locating and delineating wastewater plumes. Dissolved solids, especially salts, are good conductors of electricity. Wastewater effluent is characterized by elevated concentrations of dissolved salts, and thus elevated electrical conductivity relative to fresh groundwater and surface waters (Lee et al., 2006; Humphrey and O'Driscoll 2012). Often groundwater influenced by OWS wastewater will also have higher concentrations of dissolved salts compared to groundwater not influenced by OWS (Humphrey et al., 2010; Humphrey and O'Driscoll, 2012). Spatial differences in the concentration of dissolved salts results in variations in the electrical properties of the subsurface. Contaminant plumes with elevated salt concentrations will conduct electricity better than the surrounding media and water. Previous studies have been conducted in which geophysical methods have been applied to locate various waste plumes in the subsurface (Porsani et al. 2004; Adepelumi et al., 2001; Lee et al., 2006; Humphrey et al., 2010)

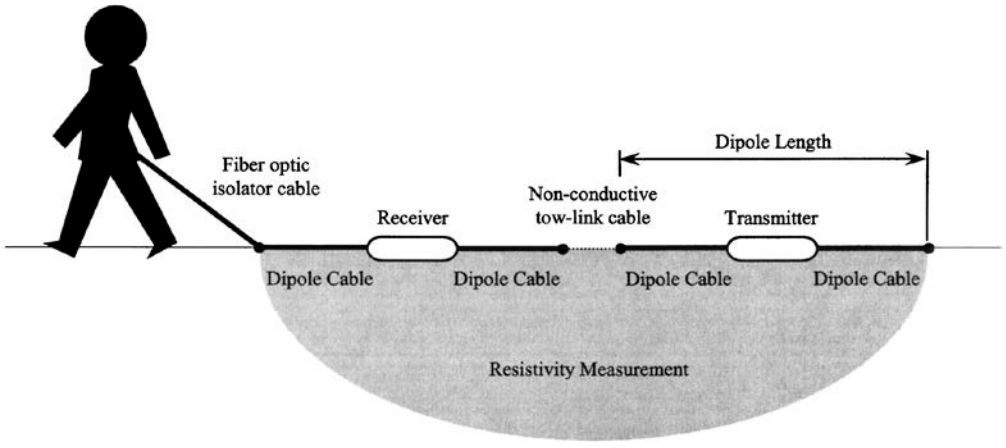

Figure 2. OhmMapper (Geometrics, Inc.) connects a transmitter and receiver with dipole cables.

1.2.2. Electrical Resistivity

Electrical resistivity mapping is a geophysical method that measures voltage in the ground to produce images that depict the resistivity properties of the subsurface. This approach can be useful for detecting vertical and horizontal changes in sediment layers or changes in groundwater quality because of differences in the material's ability to conduct electricity. Electrical resistivity measurements of the underlying materials are performed by injecting a specified current into the ground. The resulting measured voltage is used to calculate the ground's resistance to current flow by Ohm's Law, R = V/I, where R = resistance, V = voltage, and I = current. Resistance varies with the distance between and orientation of the dipoles so it is normalized with the addition of a geometric factor that converts the measurement to apparent resistivity (ohm-meters). The term apparent resistivity is used because it is a measure of the resistivity of a thickness of sediment that may have variable layers with different electrical properties, so it is in a sense averaging the electrical characteristics of a large volume of underlying sediments. Inverse modeling can be performed with RES2DINV (2-D) (www.geoelectrical.com) or RES3DINV (3-D) resistivity inversion software to estimate actual resistivity of subsurface layers from surveyed apparent resistivity data.

Electrical resistivity surveys can be performed at ground-level to determine the subsurface electrical resistivity at various depths (Loke, 2013). The transmitter emits and couples an AC current with the earth; the resulting voltage is collected by the receiver. The voltage and current data are used to calculate apparent electrical resistivity. The apparent resistivity measurements are processed using computer models in order to estimate the actual resistivity of the subsurface. The actual resistivity data may help with characterizing subsurface properties such as water table depth, changes is soil and sediment grain size/texture, and presence of contaminant plumes. Interpretation of the resistivity data (in units of ohm-m) is largely based on the inverse relationship between resistivity and conductivity (Table 1). Areas with high resistivity have low conductivity values and areas with low resistivity values have high conductivity values. Groundwater influenced by OWS wastewater may exhibit a lower level of resistivity compared to groundwater that has not been impacted by wastewater (Humphrey et al., 2010). The subsurface resistivity distribution is influenced by various geologic parameters including mineral and fluid content, porosity and degree of water saturation in the subsurface (Loke, 2013). For instance, soils that have high clay content are highly conductive, and are therefore characterized by low resistivity. More research is necessary to determine how effective the ER survey is in detecting changes in groundwater conductivity in the surficial aquifer in coastal plain environments. Electrical resistivity surveys have been used for hydrogeological, mining, geotechnical investigation, soil and agricultural studies, and recently, environmental surveys (Loke, 2013; Samouelian et al. 2005).

1.2.3. Ground Penetrating Radar

Ground penetrating (GPR) radar provides subsurface stratigraphic and water table information by transmitting electromagnetic (EM) waves at microwave frequencies into the sediment, and recording reflections as a function of two-way travel time. The EM wave propagates downward

at a velocity dictated by the permittivity of the sediment (i.e., the ability of the sediment to store and permit passage of an EM wave). Reflections are generated within the stratigraphic column where a permittivity contrast occurs across an interface, which is largely dictated by the porosity and degree of saturation of the sediment. Only a portion of the pulsed signal is reflected and the

Table 1. Typical ranges of electrical resistivity of earth materials and specific conductivity of groundwater (modified from Samouelian et al. 2005).

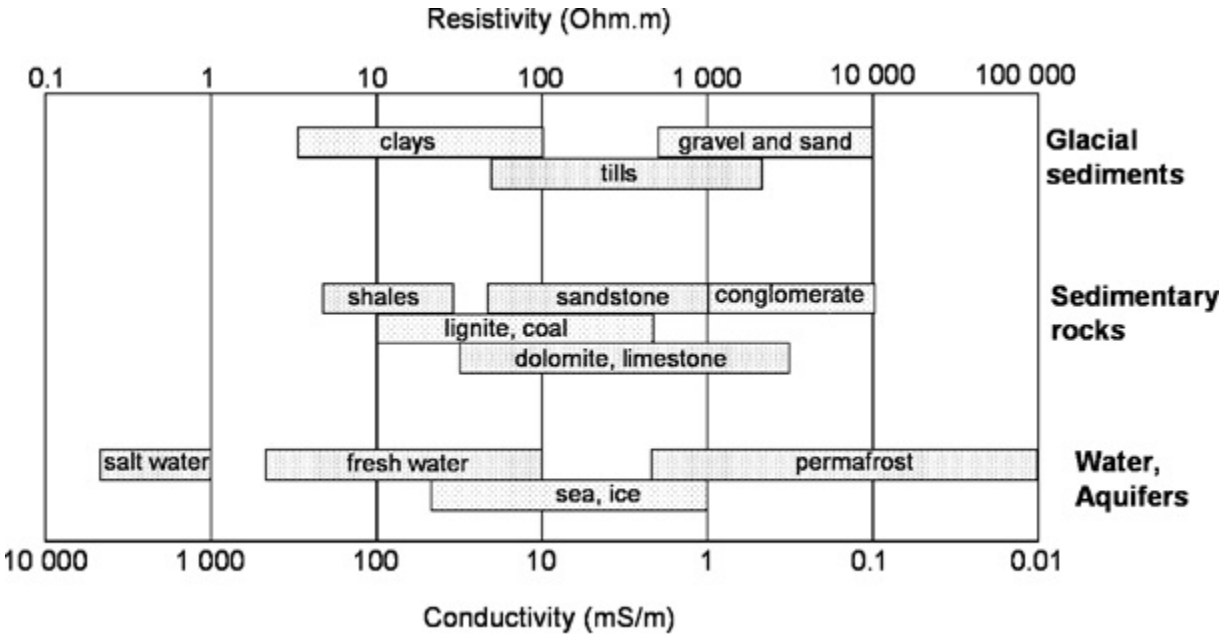

remaining part of the pulse travels across the interface to again be reflected back to the receiver from another interface boundary (Hyslip et al., 2003).The time it takes the pulse to travel through the layer and back is controlled by the thickness and properties of the material (Hyslip et al., 2003). The travel time between upper and lower boundaries of a layer can be used to calculate the layer thickness using a known velocity (Hyslip et al., 2003). Antennas are used to transmit and receive the radio pulse and are moved across an area with a continuous series of radar pulses, giving a profile of the subsurface. Permittivity (a.k.a. dielectric permittivity) can be expressed as $r = (c/v)^2$, where r is the dielectric constant, c = 0.3 m/ns, and v = electromagnetic velocity of the sediment. Amplitude and attenuation of the signal are also a function of the conductivity and magnetic permeability of the sediments (Baker et al. 2007), which varies greatly in response to the ionic concentrations within pore water, or the presence of clays. GPR that has been applied to investigating the subsurface for various applications such as detecting underground storage tanks, buried drums, and debris (Hyslip et al., 2003). The conductivity of a material controls how deep the pulse will penetrate and influences how quickly the pulse of radio energy decays in amplitude (attenuates) with distance.

1.2.4 Geophysical Research

GPR was used in Sao Paulo, Brazil to determine the lateral extent of a landfill plume and ER surveys were used to establish the vertical dimensions of the plume (Porsani et al. 2004). Geoelectrical surveys have also been used to successfully detect and define light non-aqueous phase liquid groundwater plumes (LNAPL) at the former Wurtsmith Air Force Base near

Oscoda, Michigan (Bermejo et al., 1997). The LNAPL plumes were confirmed by extensive subsurface soil and fluid sampling within and outside the plume boundaries. The LNAPL plumes had electrical conductivity readings 2.5 to 3.3 times above background concentrations and were successfully outlined with the geophysical tools.

Electrical resistivity mapping was successful in detecting sewage pit pollution plumes in a bedrock environment (Adepelumi et al., 2001). Fifty stations were utilized to collect electrical resistivity measurements, and twenty pits were dug to collect water quality samples for comparison to the geophysical data. The spatial distribution of the waste effluent constituents was determined using geophysical techniques coupled with water quality analysis, and a waste effluent flow path between the disposal ponds and the groundwater was located. The study successfully coupled the direct current ER geophysical method with water quality analysis and supported the reliability of geophysical techniques applied in a crystalline bedrock environment.

Lee et al. (2006) conducted a study directly focused on detecting malfunctioning septic systems in glacial till and found that electromagnetic induction (EMI) could help identify the location of septic system components, failed septic systems, and associated effluent plumes. Expansion of the research conducted by Lee et al. (2006) with EMI indicates a potential for a broader spectrum of environments and settings in which geophysical techniques are applied when delineating OWS plumes.

Research by Humphrey et al (2010) showed that groundwater influenced by two OWS (at two different locations) installed in sandy, shallow (< 2 m to water table), coastal plain soils could be delineated via ER surveys. Groundwater within the ER predicted plume areas near the drainfield trenches had elevated nitrogen concentrations and electrical conductivity values (> 9 mg/L TDN and > 700 uS/cm) relative to groundwater up-gradient and outside the plume areas (< 2 mg/L TDN and < 200 uS/cm).

In a study of subsurface wastewater migration in the Canadian Rockies, Roy et al. (2009) used 2-D OhmMapper resistivity transects to help detect zones of elevated groundwater conductivity associated with wastewater. The resistivity data indicated a potential zone of wastewater affected groundwater between a drainfield and a lake. However, groundwater specific conductivity data were not collected to verify resistivity interpretations. They concluded that the OhmMapper surveys could provide a promising technique to map wastewater plumes but these techniques need to be tested in a variety of hydrogeological settings.

Prior studies have shown that geophysical surveys may be useful techniques for detecting groundwater contamination. However, more research is needed to determine the effectiveness of geophysical techniques in delineating plumes from OWS installed in different soil types and geologic settings.

The objectives of this study were: 1) evaluate the effectiveness of the geophysical tools in delineating OWS contaminant plumes and 2) assess the fate and transport of OWS derived nutrients (nitrogen and phosphorus) in the Coastal Plain surficial aquifer.

2. Methods

2.1 Site Selection

Four sites that utilized OWS were evaluated in this study. The sites included J.W. Smith Elementary School (JWS) in Cove City, NC, West Craven High School (WCH) in Vanceboro, NC, a private residence (Site 100) in the Eastern Pines area of Pitt County, NC and an environmental education center "A Time for Science" (ATFS) in Ayden, NC (Figure 3). All sites excluding ATFS had pre-existing groundwater monitoring networks. The sites were chosen because they had different soil types, various depths to water, different OWS technologies, and because property owners were cooperative.

2.2 Groundwater Monitoring Network

Piezometers were installed using hand augers (Figure 4a) and a geoprobe. The piezometers were constructed using either 3.1 cm or 5.05 cm diameter PVC with 0.9 m screen intervals (Figure 4b). Sand was used to fill the annular space between the piezometer screen and borehole. Above the screen, the annular space was sealed with a mixture of sand, bentonite, and native soil. Piezometers were encased in valve boxes that extended flush with the ground surface in locations where property owners mowed the lawns. Piezometers installed in the floodplain and near the creek at JWS, extended approximately 1 m above the surface.

Piezometer networks were already in place by the start of this project at JWS (20), WCH (28), and Site 100 (15). However, additional piezometers were installed at WCH and JWS to better evaluate the extent of OWS plumes at the sites. The piezometer network at ATFS was installed before wastewater from the center was discharged to the subsurface. For ATFS, three piezometers were initially installed and surveyed, and with depth to water information, the 3-pt contouring method (Heath, 1998) was used to determine groundwater flow direction. The rest of the monitoring network (17 total piezometers) was installed based on the calculated groundwater flow direction. Site maps with piezometer and OWS component locations were produced using a *Trimble* GPS and *ArcGIS* software.

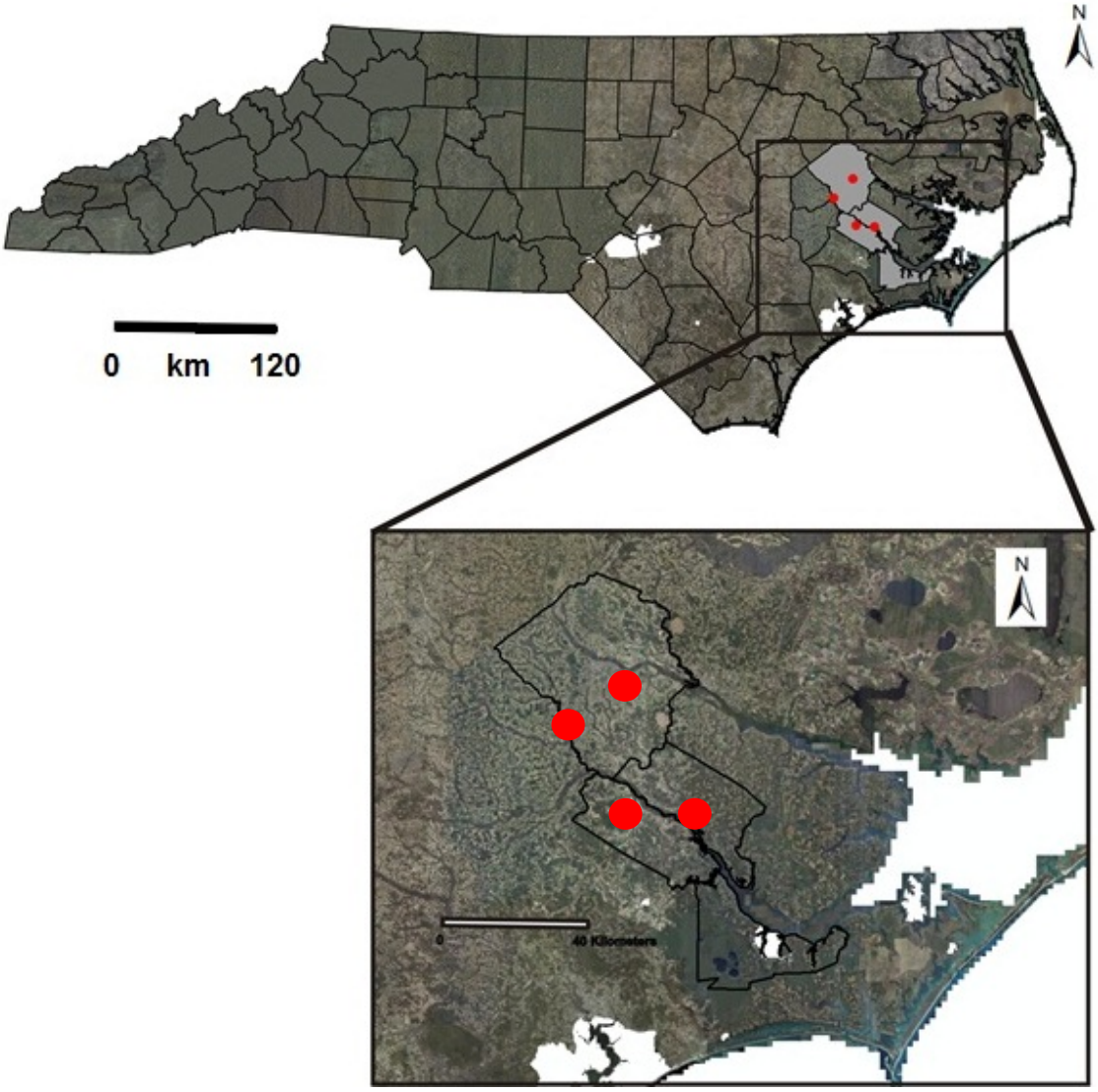

Figure 3. Research sites (red circles) located in Eastern Pines (Site 100), Ayden (ATFS), Cove City (JWS) and Vanceboro (WCH), NC.

Figure 4. Boreholes created with hand augers (top) and piezometer construction with well screen, solid pipe, primer and glue (bottom)

2.3 Electrical Resistivity Surveys

A capacitively coupled resistivity mapper (Ohm Mapper, © Geometrics, Inc.) was used to measure electrical resistivity of the subsurface up-gradient, down-gradient, and within the boundaries of the drainage fields and to construct a resistivity profile at each site. The dipole-dipole array is the electrode configuration used by the OhmMapper. This array is more sensitive to horizontal changes in resistivity than to vertical changes. Capacitive coupling does not require direct ground contact and has the advantage of being able to collect data in built areas that normal galvanic resistivity methods may have difficulty (Loke 2013).A rectangular grid with 2-4 m line spacing was used for intensive 3-D surveys (Figure 5a). Dipole length ranged from 5-10m and rope spacing (a surrogate for depth of investigation) for each 2-D and 3-D survey was typically 2.5,5,10, and 20 m (four passes were performed along each survey line). Typical surveys imaged up to approximately 6-7 m depth. Apparent resistivity data collected from the surveys was inversely modeled using Res2Dinv and Res3Dinv (© Geotomo Software) to estimate actual resistivity of the subsurface sediments and to aid with the interpretation of the data.

2.4 Ground Penetrating Radar Surveys

A Geophysical Survey Systems Inc. (GSSI), SIR-2000 system was used with a 200 MHz antenna to image the stratigraphy GPR data were collected in continuous monostatic mode, using a calibrated survey wheel at a scan rate of 20 scans/m, and a sampling rate of 1023 samples/scan, with a sampling window of 300 ns. A grid pattern with 2 m line spacing surrounding the targeted monitoring sites was used to characterize subsurface stratigraphy in 3-D. Data were processed at the ECU Department of Geological Sciences, using Radan v.6 software (copyright GSSI), which allows for 2-D and 3-D visualization. Geophysical surveys including ER and GPR were conducted three times during the study in summer (July or September 2012), fall (November 2012), and in early spring (March or April 2013).

2.5 Environmental Readings and Sample Collection

Depth to groundwater was measured at each piezometer using a *Solinst* Temperature, Water Level, and Conductivity meter (Figure 5b). Piezometers were purged using a disposable bailer and allowed to recharge for sample collection and environmental readings. Wastewater effluent samples were collected from either the outlet compartment of the septic tank (Site 100, ATFS, and WCH) or from a distribution box (JWS). Surface water samples were collected from a spring at JWS, and from a location in the adjacent creek 5 m upstream and 5 m downstream of where overland flow from the spring discharged into the creek. Groundwater, wastewater, and surface water pH, temperature, specific conductance (µS/cm), and dissolved oxygen (mg/L) were measured in the field using a *YSI-556 Multi-Probe Meter*. Groundwater, and wastewater samples were collected using bailers and poured into separate, labeled, Nalgene sample bottles, and then placed in an ice-filled cooler for storage until transported to the laboratory. Surface water samples were collected by hand with sample bottles, labeled, and stored in the cooler. Samples were collected three times for nutrient analysis during the study to coincide with geophysical surveys. Environmental readings were performed during the sampling events, and on two additional months.

Figure 5 (a) Geophysical survey grid for Site 100 with blue flags marking the transect. (b) Environmental readings performed at WCH using a bailer and field meters.

2.6 Water Sample Analysis

Total dissolved nitrogen (TDN) included NO_3-N + NO_2-N + dissolved Kjeldahl nitrogen. Kjeldahl nitrogen was the sum of NH_4/NH_3 and organic nitrogen. Ammonia was quantified using the phenol-hypochlorite method and SmartChem 200 method 210-201B (Westco Scientific Instruments Inc.). Kjeldahl nitrogen was analyzed using SmartChem method 390-200E (Westco Scientific Instruments Inc.). Nitrate/nitrite were quantified using the SmartChem 200 method 375-100E-1 (Westco Scientific Instruments Inc.). Total dissolved nitrogen concentration was determined by combining the individual nitrogen species. Dissolved orthophosphate (soluble reactive phosphorus, PO_4) analysis was conducted via the SmartChem 200 Method 410-3651. Chloride was measured by SmartChem 200 Method 231N-0406C. All laboratory analyses were conducted in the East Carolina University Central Environmental Research Laboratory (CEL).

2.7 Assessment of Geophysical Delineation of OWS Plumes

The 2-D geophysical profiles and 3-D volumes produced from the survey data were analyzed to determine if areas of relatively low resistivity could be detected within the drainfield area and down-gradient from the OWS, thus potentially indicating the OWS "plume". Piezometers within the low resistivity areas were listed as plume, and other piezometers were listed as background or non-plume. Groundwater specific conductance readings for plume piezometers were compared to non-plume piezometers to determine if there was a statistically significant ($p < 0.05$) difference using Mann Whitney non-parametric tests with Minitab 16. The electrical resistivity of soil/water at the screen interval of each piezometer was compared to the specific conductance of groundwater measured for each piezometer to determine if there was a relationship between conductance measured via field meter and resistance measured via ER mapper. The 2-D and 3-D surveys produced from GPR were evaluated to determine if signal attenuation was observed beneath the OWS drainfield and down-gradient from the OWS systems. The survey images were compared to OWS permit information (Appendix 2) to determine if the OWS components including the drainfield trenches could be detected.

2.8 On-site Wastewater System Nutrient Fate and Transport

Water quality data (TDN, PO_4, and SC) were displayed on boxplots, tables, and/or maps to show the spatial variability of the groundwater characteristics. Septic effluent concentrations of TDN and PO_4 were compared to groundwater concentrations beneath the drainfield trenches, up-gradient from the OWS, and down-gradient from the OWS. Groundwater data from piezometers within the drainfield areas were deemed "drainfield piezometers", piezometers up-gradient from the drainfields were deemed "background piezometers", and piezometer down-gradient and within the groundwater flow-path of the OWS were deemed "down-gradient piezometers". "Plume core" indicates the piezometers within the drainfield, and down-gradient from OWS with the highest concentration of nutrients. TDN and PO_4 treatment efficiencies for the OWS were calculated using equation 1. Treatment efficiencies from tank to groundwater beneath the drainfied, and from tank to down-gradient piezometers and surface waters were calculated.

$$TE = \frac{Tank - Groundwater}{Tank} X\ 100\% \qquad \text{Equation (1)}$$

Where TE is nutrient treatment efficiency, tank is tank nutrient concentration, and groundwater is groundwater nutrient concentrations for piezometers of interest.

2.9 On-site Wastewater System Treatment Processes

Chloride has been used as a conservative tracer by researchers because it moves freely in most aquifers, and is not subject to potential loss via transformations to gaseous phases like other ions such as NO_3 (denitrification), NH_4 (anammox), or loss via adsorption or mineral precipitation like PO_4 (Harman et al., 1996; Desimone and Howes, 2006). OWS effluent typically contains elevated concentrations of TDN, Cl, and PO_4 relative to non-saline groundwater. Evaluating the ratios of TDN/Cl and PO_4/Cl in OWS effluent and groundwater within the plume will help determine if nutrient reduction processes such as denitrification, anammox, adsorption or mineral precipitation have occurred (Harman et al., 1996; Desimone and Howes, 2006). The TDN/Cl and PO_4/Cl ratios decrease from tank to groundwater beneath and down-gradient from the OWS if the mass of TDN and PO_4 has been reduced. If concentration reductions along the groundwater

flow-path from the OWS were because of dilution alone, the ratios remain constant from the source. These analyses were conducted by using the mean Cl, TDN, and PO_4 data for tanks, drainfield piezometers, down-gradient piezometers at each site. The concentration reductions were compared to nutrient/Cl ratios to gain a better understanding of potential mass reduction processes.

3. Results and Discussion

3.1 On-site Wastewater System Characteristics

The OWS at WCH had the largest design flow (73,827 L/d), septic tank storage capacity (73,827 L), and dispersal field area (1115 m^2) (Table 2) of the 4 study sites. WCH utilized a low pressure pipe (LPP) system, which uses pressure dispersal of effluent to dual alternating fields (one field dosed, then the next). JWS had the second largest OWS with septic tank storage capacity of 37,800 L and 892 m^2 of drainfield trench area (Table 2). JWS uses a pump to distribution box(es) system with dual alternating drainfields. The OWSs at AFTS and Site 100 were smaller, gravity flow systems, both with 3,780 L septic tanks and effluent distribution boxes. The dispersal field area for Site 100 (155 m^2) was larger than the ATFS dispersal field because of differences in soil type and permeability, and thus a lower wastewater loading rate was assigned to Site 100 (Table 2).

Table 2. Onsite wastewater system characteristics for the 4 research sites.

Site	Install Date	Septic Tank Capacity (L)	Max Design Flow (L/d)	Distribution Device	Dispersal Area (m^2)	Vertical Separation (m)	Soil Series
Site 100	1998/2004	3780	1360	D-box	155	< 0.1 m	Goldsboro and Lynchburg
JWS	1987	37,800	37,800	D-box (2)	892	> 3 m	Autryville
WCHS	1999	73,827	73,827	LPP (2)	1115	> 1 m	Tarboro
ATFS	2012	3780	1512	D-box	59	> 3 m	Wagram

3.2 Geophysical Surveys at West Craven High

Figure 6 depicts groundwater specific conductivity data and a map view of 3-D resistivity survey data collected at West Craven High School on 11/14/2012. The resistivity data shown represents values for a 1.3 m depth. There is a large contrast in resistivity values at this site. Higher values are shown in red and lower values in green. Generally, the groundwater specific conductivity values suggest that wastewater affected groundwater is more common in the western section of the survey area, and corresponds with lower resistivity values. At the southern and eastern edges of the survey area, higher resistivity values and lower groundwater conductivity values suggest the effects of wastewater are limited in those areas and the wastewater plume is generally migrating to the north. The presence of an inactive drainfield to the north of piezometer 25 may also have an influence on resistivity values at this shallow depth, even if wastewater is not actively cycling through that portion of the system. Overall, the conductivity and resistivity data at this site suggest that wastewater affects the shallow groundwater system and the plume is

vertically stratified and moving to the north. More nested piezometers to the north of the 3-D survey area; particularly near piezometer 21 and the service road would help to verify the plume movement. At the beginning of this study, the resistivity transect near piezometer 25 suggested that the shallow piezometer at that location was not deep enough to characterize the lower resistivity zone located at approximately 4-6 m deep (Figure 7). After installing deeper piezometers at that location, the groundwater samples showed that there is a deeper zone of groundwater with elevated specific conductivity. This revealed that the resistivity patterns can help to detect vertical stratification in groundwater quality (assuming that the geological substrate is relatively constant with depth).

Six 2-dimensional transects were collected at WCH on 11/14/2012 (Appendix 2). Figure 7, Transect 1 (T1) shows the piezometers adjacent to the survey line and the associated groundwater specific conductivity values for the sampling date. The electrical resistivity survey began at the southern end of the site and proceeded north towards the drainage ditch at the northern end of the site and extended for 300 m. Along the transect, the drainfield was first encountered near piezometer 8 at the 80 m mark. Near this piezometer location, the resistivity showed a large decrease, and groundwater conductivity increased relative to piezometer 7. This pattern suggests that the resistivity responded to the change in groundwater conductivity associated with wastewater inputs. Resistivity measurements through the active drainfield area were consistently below 200 ohm-m. At piezometer 25, which was nested at 3 depths, the data suggest that wastewater affected groundwater is present at approximately 4 m depth. The shallower piezometers, 25 s and 25 m, revealed lower groundwater conductivity and higher resistivity values than those measured adjacent to the deepest piezometer in this nest. The groundwater conductivity and resistivity values at piezometers 21 and 22, outside of the drainfield and closer north towards the ditch, suggest that at shallow depths of 1-2 m, there is no indication of wastewater migration. However, in the deeper piezometer in the 22 nest, there is higher conductivity groundwater and lower resistivity, suggesting the possibility that diluted wastewater could be present at depths > 3m and could potentially be discharging to the ditch.

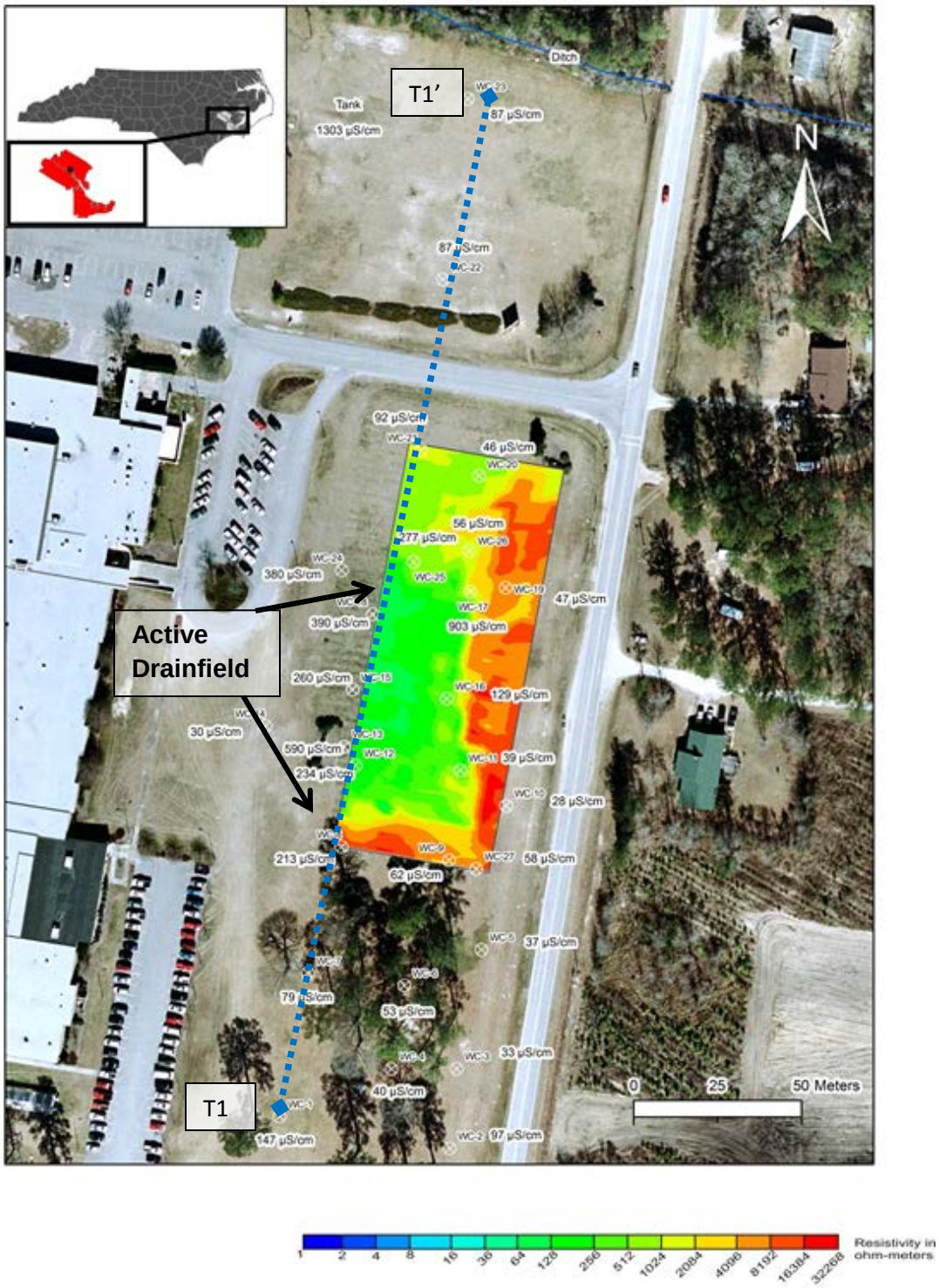

Figure 6. Plan-view electrical resistivity map at WCH (1.3 m depth). Survey completed November 2012. Areas shaded in light green indicate low resistivity values indicative of wastewater influence near the active drainfield. Specific conductivity of groundwater labeled next to piezometers. Blue line indicates a transect that started south of the field and ended north of the field.

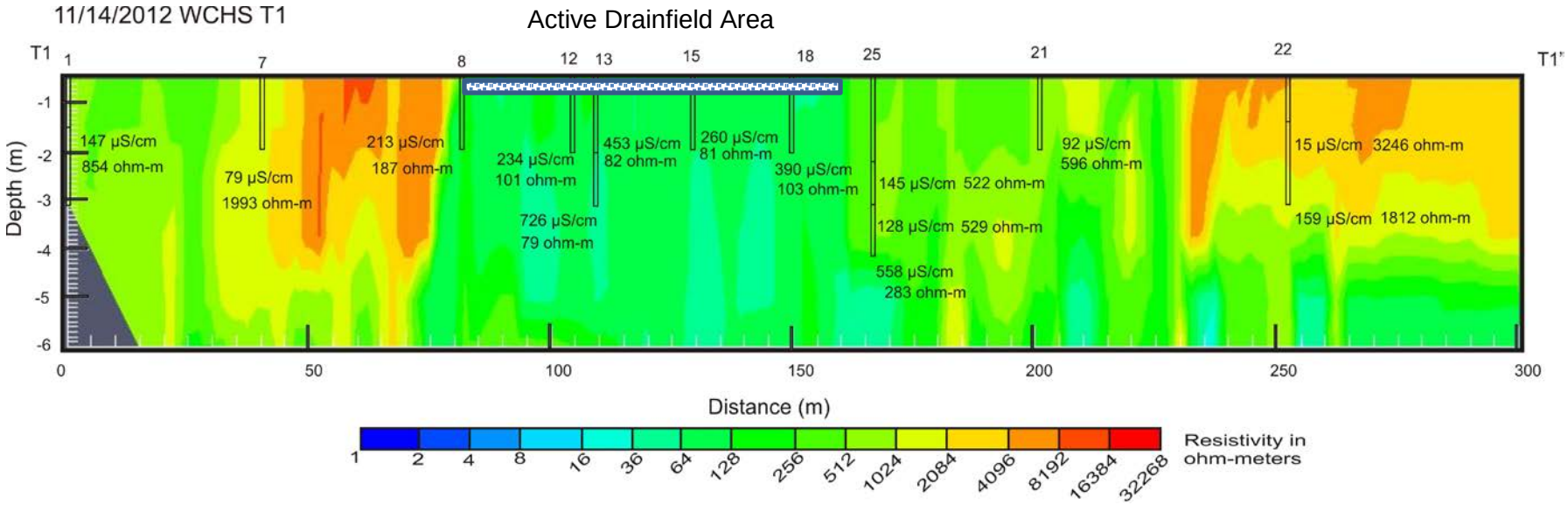

Figure 7. Profile-view of an electrical resistivity survey conducted along a transect of piezometers at WCH as shown in aerial view in Figure 6. The active drainfield is located between piezometers 8 and 18. Areas shaded in green and blue have low resistivity values, indicative of wastewater influence. Specific conductivity (µS/cm) and resistivity (ohm-m) are labeled near the screen section of each piezometer.

A GPR survey was conducted at WCH on November 14, 2012. Figure 8 shows a plan-view image of the survey data. The survey shows the effluent conveyance pipes in the drainfield trenches (expresssed as red lines indicating high amplitude reflections) for the active and de-actived drainfields. The surrounding blue shades indicate low amplitude data, likely due to high conductivity associated with wastewater. A transect at the site in profile view also shows the drainfield trenches, and significant attenuation of the radar signal beneath the active drainfield (Figure 9). The signal likely attenuated because of the influence of the wastewater infiltrating the soil and thus increasing the specific conductance of soil and groundwater beneath the active drainfield, which is consistent with the Ohm-mapper data. At this site, GPR was successful in detecting active and de-activated OWS drainfield trenches. However, the GPR signal was attenuated due to the influence of the wastewater, thus affecting the ability of investigators to determine the full vertical extent of the plume.

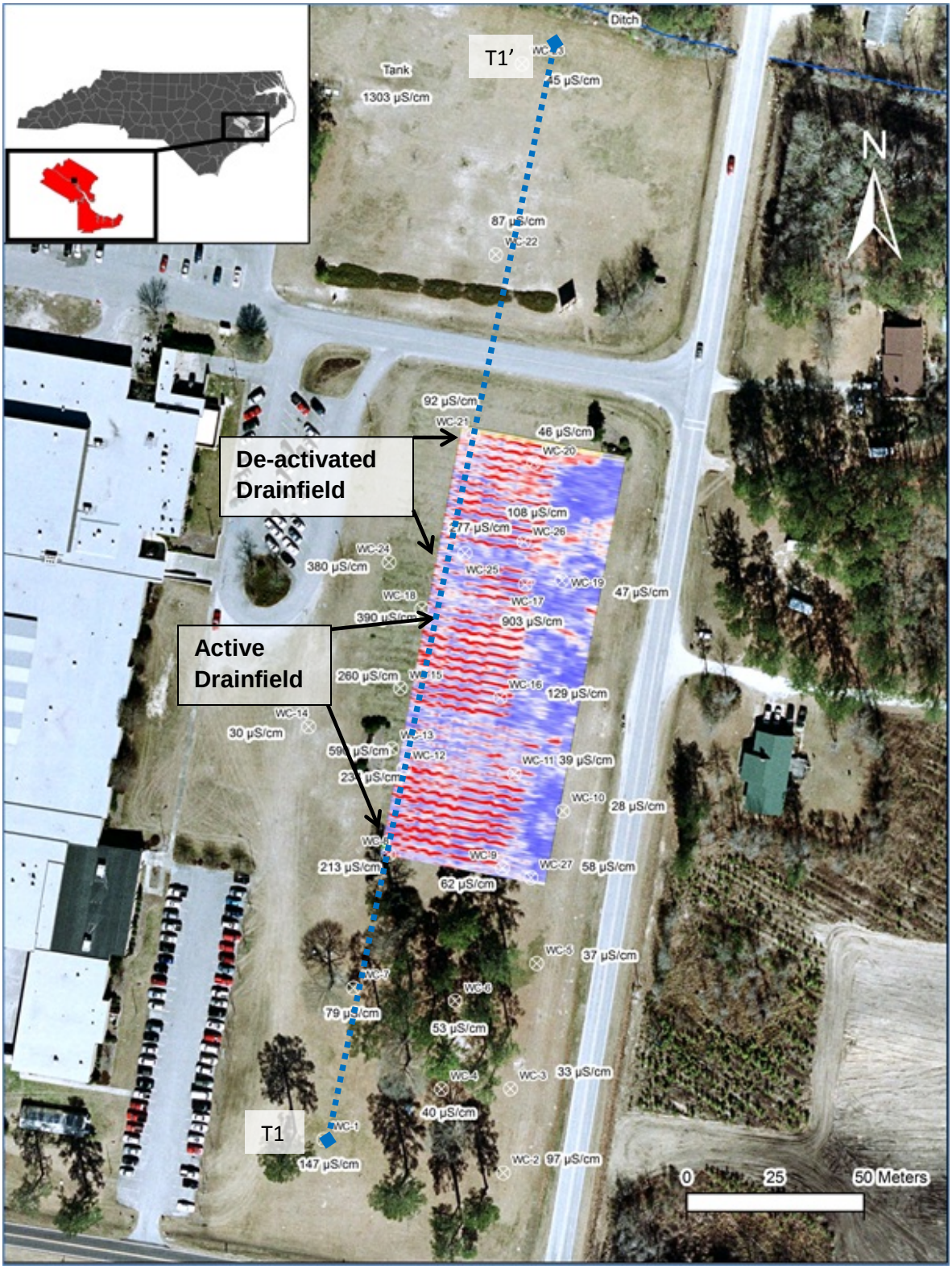

Figure 8. Ground penetrating radar survey of WCH (1.3 m depth) conducted on November 14, 2012. Red lines are high-amplitude reflections, and indicate the conveyance pipes in the drainfield trenches. Specific conductivity values are listed beside the piezometers. Blue dashed line shows the transect (T1) path.

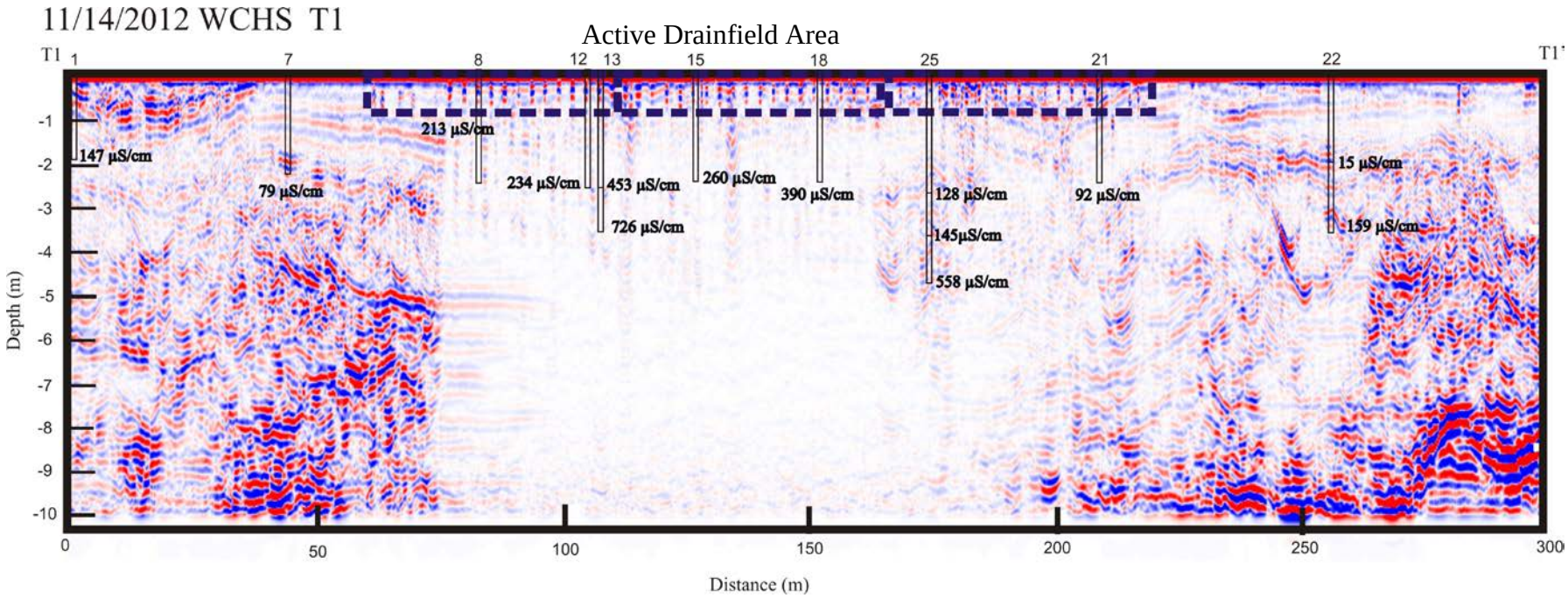

Figure 9. Profile-view GPR transect at WCH showing significant signal attenuation beneath the active OWS drainfield trenches (shown in black, dashed line), indicative of wastewater influence on the electrical properties of soil and water.

3.3 Geophysical Surveys at JWS

Figure 10 depicts the groundwater conductivity data and a map view of 3-D resistivity survey data collected at JW Smith School on 11/19/2012. The resistivity data shown represents values for 4 m depth. There is a large contrast in resistivity values, higher values are in red and lower values in green. Generally, the elevated groundwater specific conductivity values suggest that wastewater-affected groundwater is more common in the center of the drainfield, and corresponds with lower resistivity values.

At the western and northeastern edges of the survey area, higher resistivity values and lower groundwater conductivity values suggest the effects of wastewater are relatively lower in those areas and the wastewater plume is generally migrating to the north. The specific conductivity and resistivity values from this view and the transect (Figure 11) suggest that the groundwater to the south and west of the drainfield is minimally affected by wastewater disposal. However, there is an interesting specific conductivity pattern revealed to the north of the drainfield and 3D survey area. A spring that is present approximately 30 m to the north of the drainfield had elevated specific conductivity values (394 µS/cm) and piezometers adjacent to the spring also suggested that wastewater affected groundwater is migrating to this discharge area. These water quality data are in general agreement with the resistivity data which suggests a plume that is oriented approximately NW-SE. Overall, the conductivity and resistivity data at this site suggest that wastewater affects the shallow groundwater system and the plume is vertically stratified and moving to the north. Obstructions in the forested riparian buffer zone prevented geophysical transects through that portion of the site. If we could be granted permission to remove some of the vegetation transects could be conducted in the riparian zone and this information could help further enhance the delineation of the zone with wastewater-affected groundwater. It is possible that there is also a component of groundwater flow that migrates to the northeast as the groundwater gets closer to the stream, if there are permeable alluvium deposits in the floodplain. The riparian buffer at this site appears to remove nitrogen from wastewater-affected groundwater. However, this benefit is short-circuited when groundwater discharge at the spring becomes surface water flow and has a direct surface flowpath to the stream, bypassing the riparian sediments where denitrification would be likely. Future work at this site should compare how well the riparian sediments remove nitrogen in contrast to the spring/surface flowpath to the stream. This work can help quantify the effectiveness of riparian buffers to attenuate nitrogen from OWS sites.

At JWS, six 2-dimensional transects were surveyed on 11/19/2012 (Appendix 2). Transect 1 (T1) shows the piezometers adjacent to the survey line and the associated groundwater specific conductivity values for the sampling date (Figure 11). The electrical resistivity survey began at the southern end of the site and proceeded north towards the stream at the northern end of the site and extended for 175 m. Along the transect, the drainfield was first encountered at approximately 90 m near piezometer 4. Resistivity values tended to be greater than 500 ohm-m for the depths of approximately 2-6 m and groundwater specific conductivity values were less than 200uS/cm, prior to reaching the drainfield area. After encountering the drainfield, the resistivity values were generally less than 500 ohm-m at the 2-6 m depth range and groundwater conductivity values were approximately 500-600 µS/cm (piezometers 6, 10, and 13). This pattern suggests that the resistivity responded to the change in groundwater conductivity associated with wastewater inputs. Similar to the WCH site, resistivity measurements through the active

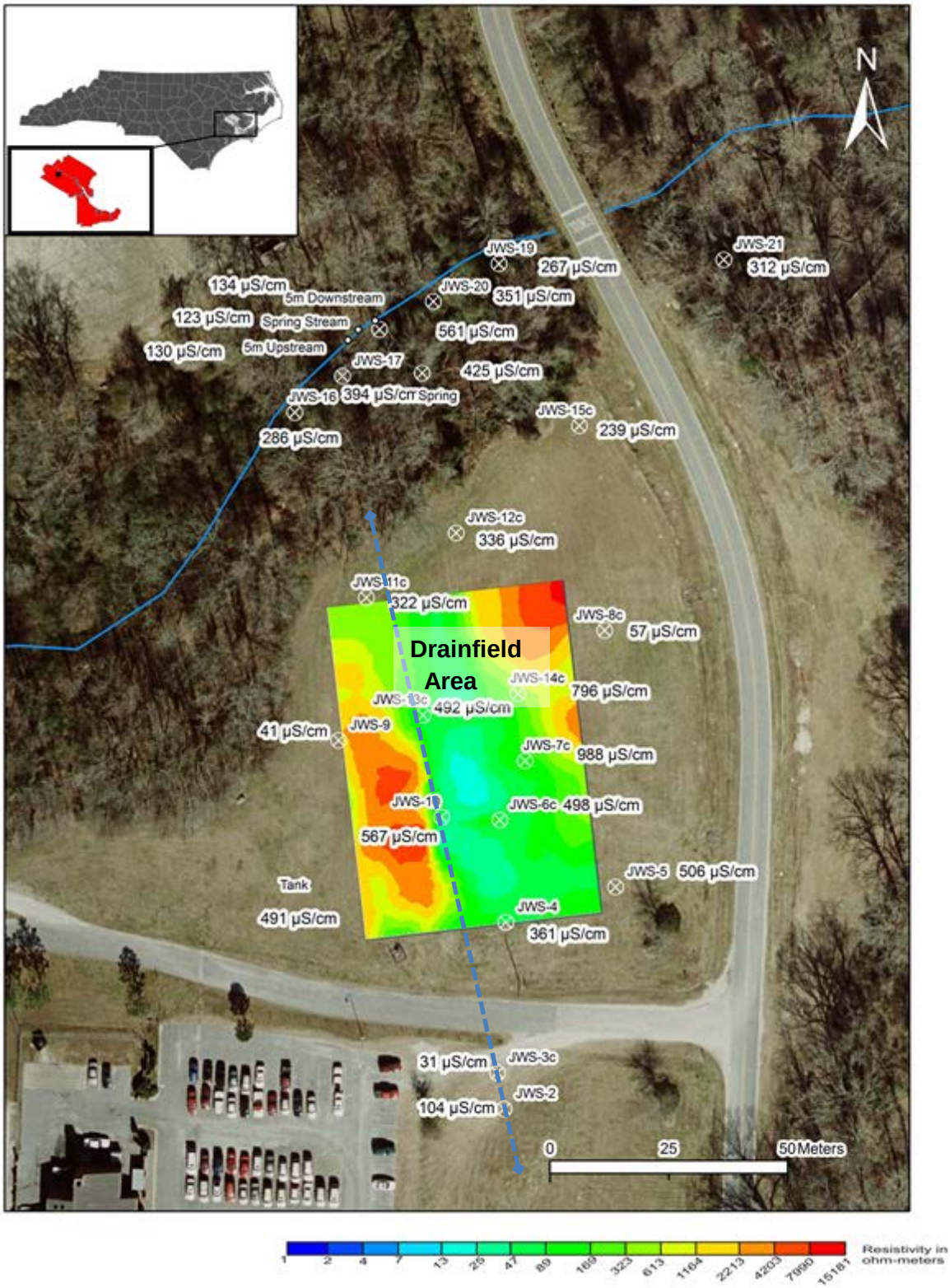

Figure 10. Plan-view map of electrical resistivity survey (4 m depth) conducted in November 2012 at JWS. Areas shaded light green indicate low resistivity values indicative of wastewater influence. The low resistivity material is oriented northwest towards a spring in the forested buffer. Blue line indicates the location of a transect (T1) for profile-view.

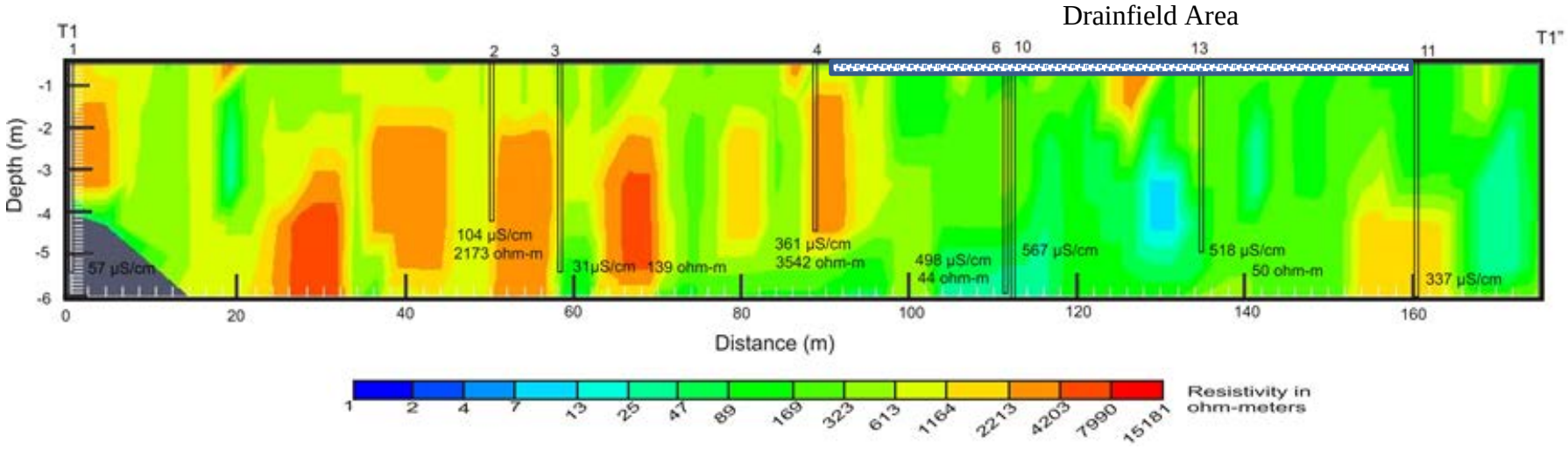

Figure 11. Profile-view of an electrical resistivity survey conducted along a transect (T1) of piezometers at JWS as shown in Figure 12. The drainfield is located between piezometers 4 and 11. Areas shaded in green and blue have low resistivity values, indicative of wastewater influence. Specific conductivity (µS/cm) and resistivity (ohm-m) are labeled near the screen section of each piezometer.

drainfield area were consistently below 200 ohm-m at depths underlying the drainfield trenches. The transect suggests that the higher conductivity groundwater underneath the drainfield is present at depths of 3 m or greater. This site had the deepest groundwater table of all sites, so it would be expected to see the effects of wastewater inputs at greater depths.

A GPR survey was conducted at JWS on November 19, 2012. Figure 12 shows a plan-view image of the survey data. The survey shows the effluent conveyance pipes in the drainfield trenches (expressed as red lines indicating high amplitude reflections) for the dual drainfields. The surrounding blue shades indicate low amplitude data, likely due to high conductivity associated with wastewater. A transect at the site in profile view also shows the drainfield trenches, and some attentuation of the radar signal beneath the drainfield (Figure 13). The signal is likely attenuated because of the influence of the wastewater inflrating the soil and thus increasing the specific conductance of soil and groundwater beneath the active drainfield. At this site, ground penetrating radar was also successful in detecting the drainfield trenches.

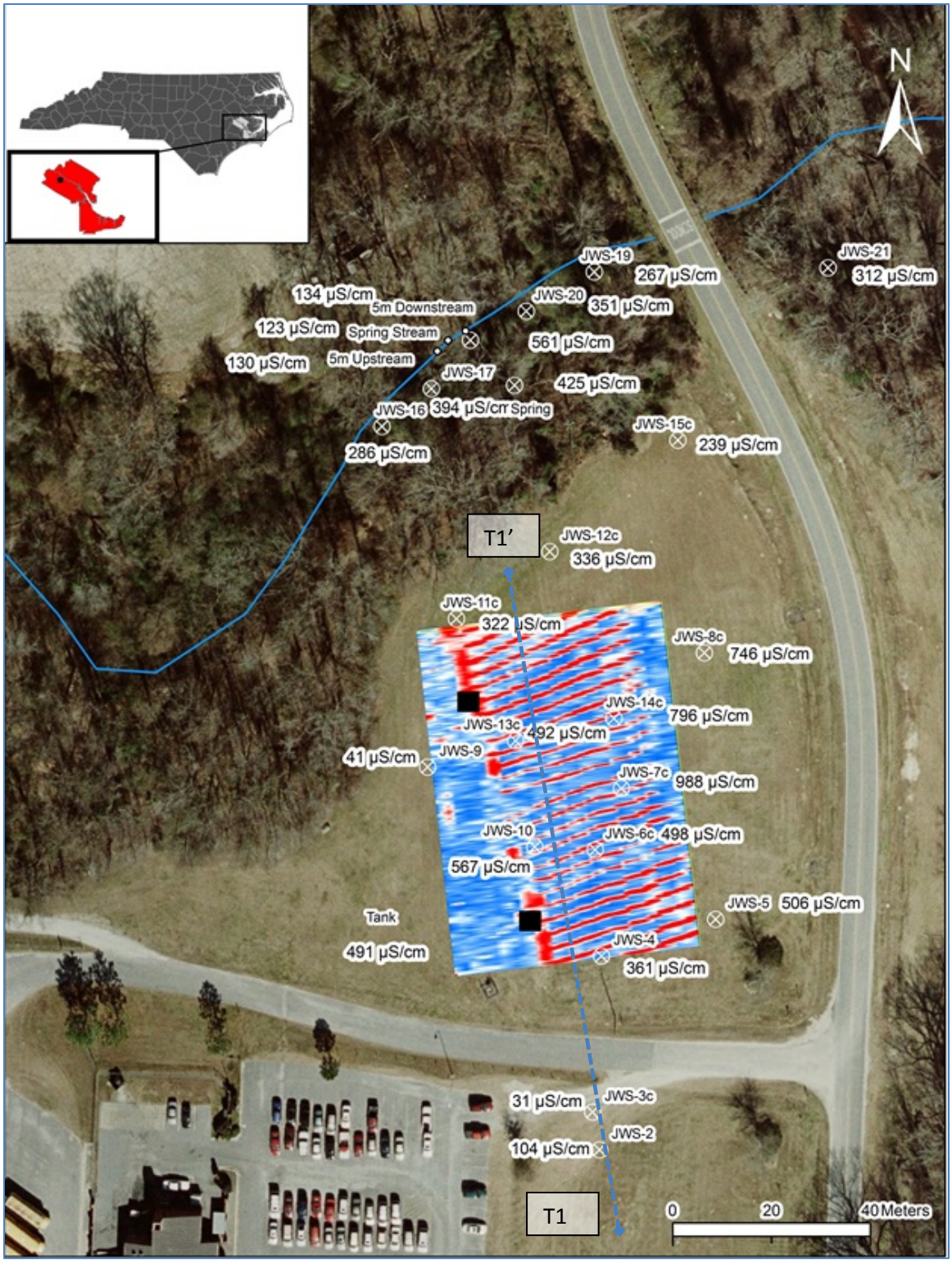

Figure 12. Ground penetrating radar survey at JWS (1.3 m depth). Red lines indicate effluent conveyance pipes in the drainfield trenches extending to the north east from the distribution boxes. Transect 1 (T1) locations shown by dashed blue line.

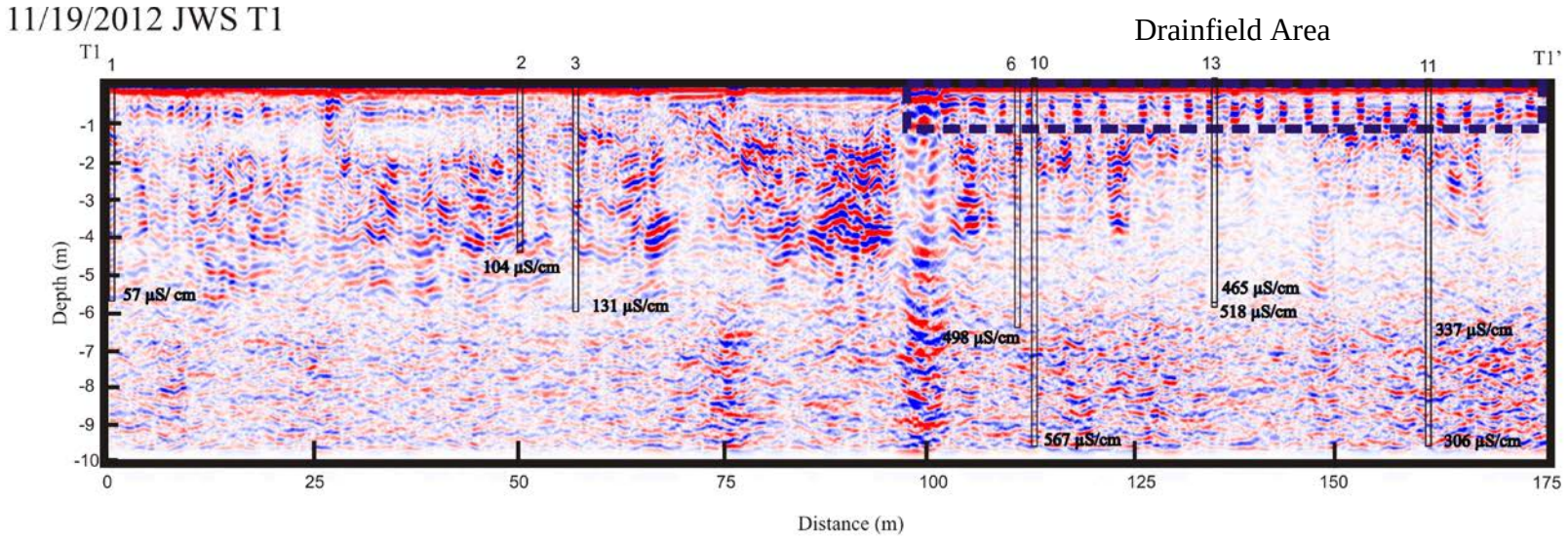

Figure 13. Profile-view ground penetrating radar transect (T1) at JWS showing the drainfield trenches, and some signal attenuation beneath the drainfield area indicating wastewater influences on soil and water.

3.3 Geophysical Surveys at ATFS

Six geophysical survey transects were conducted at ATFS on three dates (3/23/12, 9/4/12, and 4/17/13) (Figure 14). Figure 15 shows electrical resistivity surveys (Transect 3) collected on 3/23/2012 (before OWS system use); 9/4/2012; and 4/17/2013 (after OWS system use began).

The ATFS site was unique because it served as a science education center and had sporadic use from school groups around the county. When groups were present and used the lavatory facilities in the building there was the possibility for wastewater inputs to the drainfield, but during non-use periods wastewater discharge would cease. We performed background surveys in March 2012, prior to system use. In figure 15, the resistivity and groundwater conductivity data for transect 3 are presented, this transect was performed directly over the drainfield and piezometers 2 and 3 were located in the drainfield. For the 3 survey dates, there was a general pattern of resistivity declines with increased depth. This is likely related to vertical changes in sediment properties in the surficial aquifer, since the patterns extend away from the drainfield.

Underneath the drainfield, although the differences were subtle, it appears that for the dates following system initiation (9/4/12 and 4/17/13) the specific conductivity of groundwater did increase in the drainfield once the site was commissioned for use (Figure 15). On the first survey date (prior to OWS use) groundwater specific conductivity was approximately 65 uS/cm in both drainfield piezometers, but during the later dates when the OWS was operational the groundwater conductivity ranged between 100 and 284 uS/cm. Prior to system use, the resistivity value adjacent to the drainfield piezometer screens was 352-819 ohm-m. After system use began the range of resistivity values measured in the drainfield was 131-615 ohm-m (Figure 15). These data suggest that there has been a slight increase in median groundwater conductivity beneath the drainfield and a slight decrease in median resistivity. However the resistivity data was much more variable and there is overlap between the before and after point values. Close study of transect 1 does show that for the area directly under the drainfield there has been a general decline in resistivity when comparing the date prior to system use (3/23/12) with the dates surveyed after the system was in use. The same color scale was used for all dates and it is evident that the zone in red (highest resistivity values> 2000 ohm-m) has shrunk since the system began disposing wastewater (Figure 15). This site exhibited the lowest specific conductivity values in the drainfield groundwater, so it is expected that the resistivity contrasts will be more subtle than those observed at the previously mentioned school sites. It is likely that with greater use of the OWS at this site there will be increases in the groundwater conductivity underlying the drainfield over time. Future work could continue to monitor this site to better understand the rates of wastewater plume expansion and migration in the surficial aquifer.

Figure 14. Site map of ATFS showing the location of several transects at the site (black, blue and green lines). The green line (T3) indicates a south-north transect across the drainfield. The blue line (T1) indicates an east-west transect across the drainfield area (red rectangle).

GPR surveys conducted at ATFS on September 4, 2012 and November 30, 2012 are shown in Figure 16. Transects at the site in profile view show the 3 drainfield trenches but the influence of wastewater on subsurface properties could not be identified via this method (Figure 16). The wastewater loading rates to the subsurface at ATFS may not be great enough to change the conductive properties of the subsoil to the point where differences are captured using GPR.

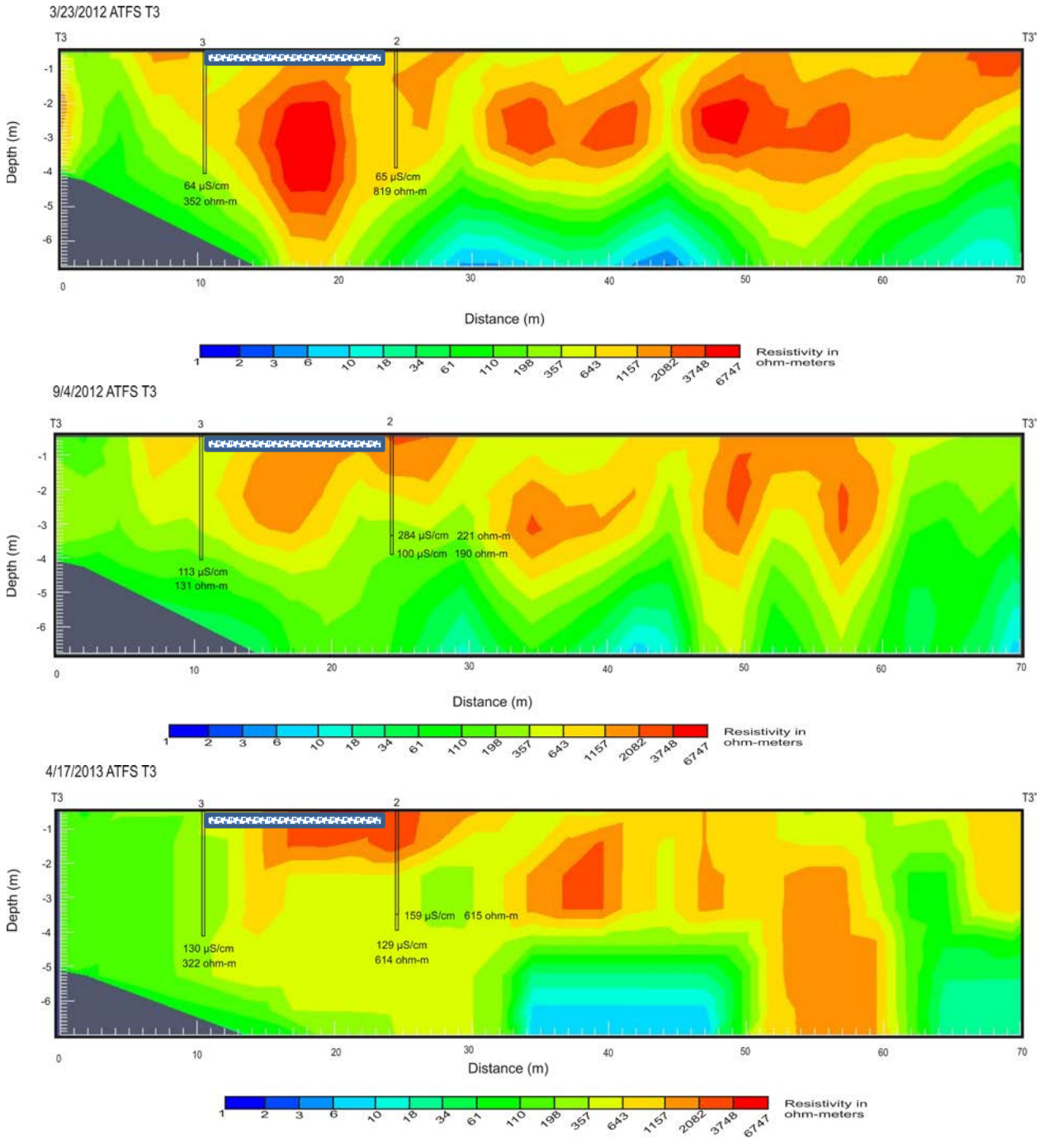

Figure 15. Electrical resistivity transects (T3) conducted at ATFS before (top image) and after (bottom two) the on-site wastewater system was used. Wastewater discharge to the subsurface was not continuous, but event driven. Drainfield area between peiozometers 2 and 3.

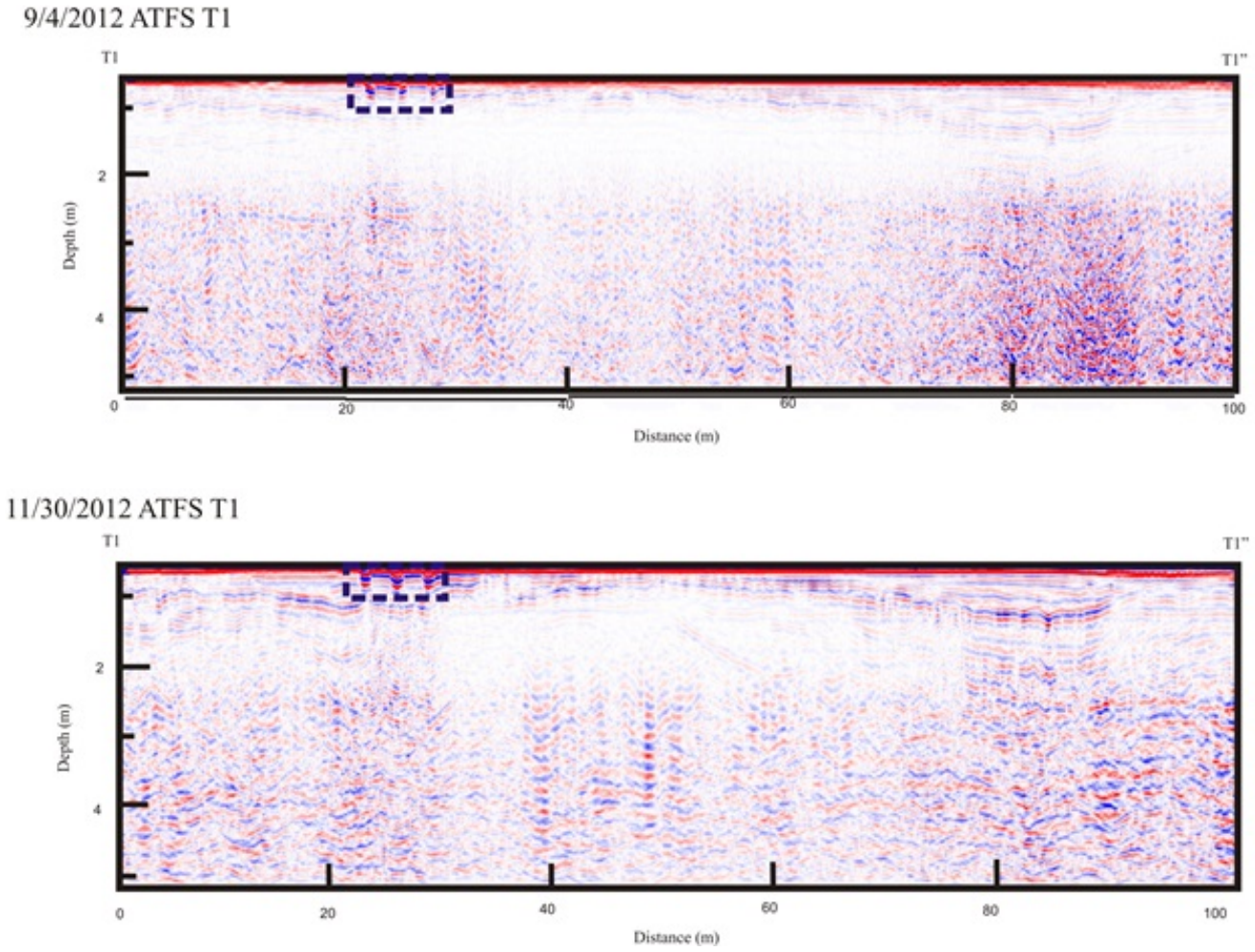

Figure 16. Profile-view ground penetrating radar data for September and November 2012, with signal reflections indicating the effluent conveyance pipes in the three drainfield trenches (boxed area).

3.4 Geophysical Surveys at Site 100 (Residential Site)

At the residential site (Site 100), the water table in the drainfield was the shallowest of all sites. This site had more clay-rich soils (Goldsboro series) than the other sites and was the closest to a stream (Table 2). The range of resistivity values across this site was the lowest, from approximately 3000 ohm-m to 10 ohm-m. The upper limit of resistivity values at the other sites was generally over 10,000 ohm-m because they had more sandy sediments. The narrow range of resistivity values observed in the drainfield at this site (Figures 17 and 18) may reflect the smaller change between drainfield and background groundwater conductivity at this site (see Figure 20). In the riparian zone, the transect 1, showed a slight decline in resistivity adjacent to piezometer nest 108, corresponding with elevated groundwater conductivity values. During the course of the study, as indicated in the average specific conductivity map, groundwater conductivity was consistently elevated at piezometer 108, suggesting that this is near the core of the wastewater plume. Wastewater-affected groundwater may discharge into the stream in this area. To the east of piezometer 109 along the same transect (T1) there was a low resistivity zone that could indicate a neighboring wastewater plume, geological heterogeneity, or disturbance due to the installation of a subsurface drain that outlets to the stream. Floodplain settings are known to have complex sediment assemblages related to stream migration, aggradation, and degradation processes over time. Because Site 100 is located directly adjacent to a stream, the presence of finer grained alluvial sediments may result in lower resistivity background conditions and a smaller contrast between resistivity in wastewater-affected areas and background areas, thus making interpretation more challenging, when compared to surficial aquifer settings with coarser-grained sand deposits. Also, based on this site's location and hydraulic head patterns, it is generally in a groundwater discharge area near a stream valley, where groundwater flow from up-gradient areas may dilute wastewater. The other three sites were generally located in recharge areas.

Ground penetrating radar surveys were successful in locating the OWS drainfield trenches, a curtain drain up-gradient and down-gradient of the active drainfield, and a few of the original OWS trenches upgradient from the OWS (Figure 19).

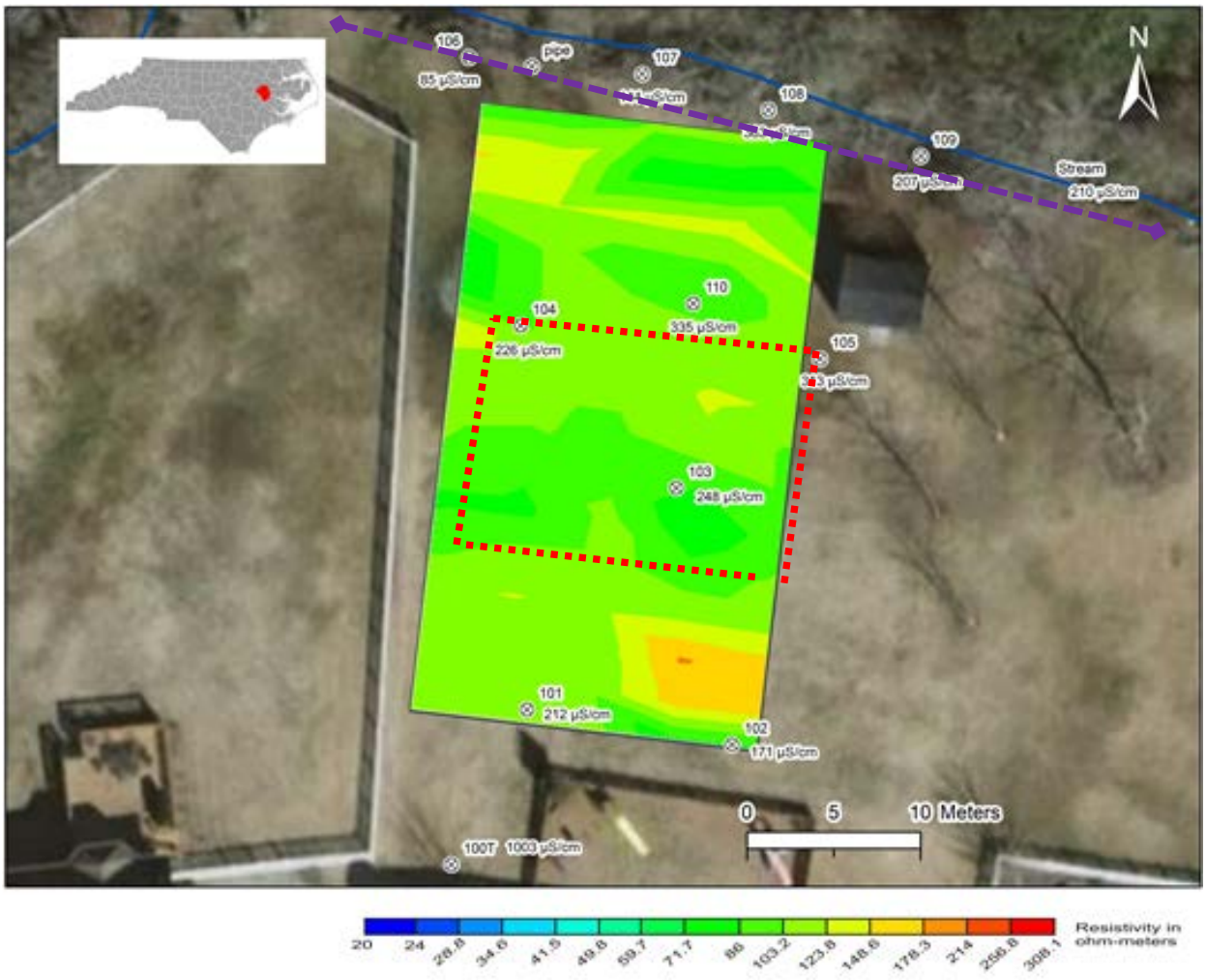

Figure 17. Plan-view map of an electrical resistivity survey (0.5 m depth) conducted in July 2012 at Site 100 (residential site). Areas shaded dark green indicate low resistivity values indicative of wastewater influence. The low resistivity material is oriented north east towards an adjacent stream. The purple line shows a transect (T1) adjacent to the creek. The red box shows the drainfield area.

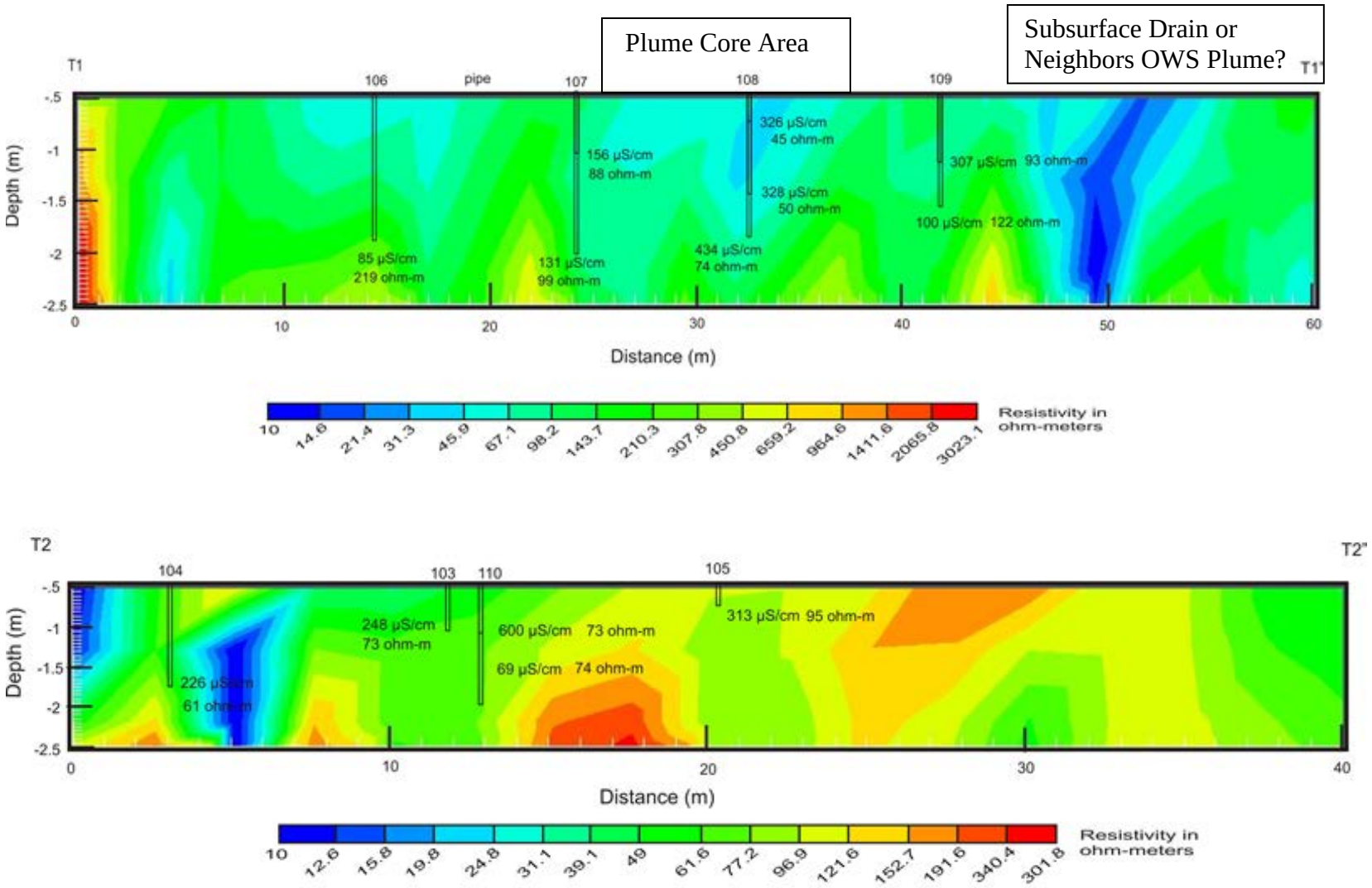

Figure 18. Site 100 transects adjacent to the creek (top) and across the drainfield (bottom). The lowest resistivity values and highest groundwater specific conductivity values were observed near piezometer 108 adjacent to the creek.

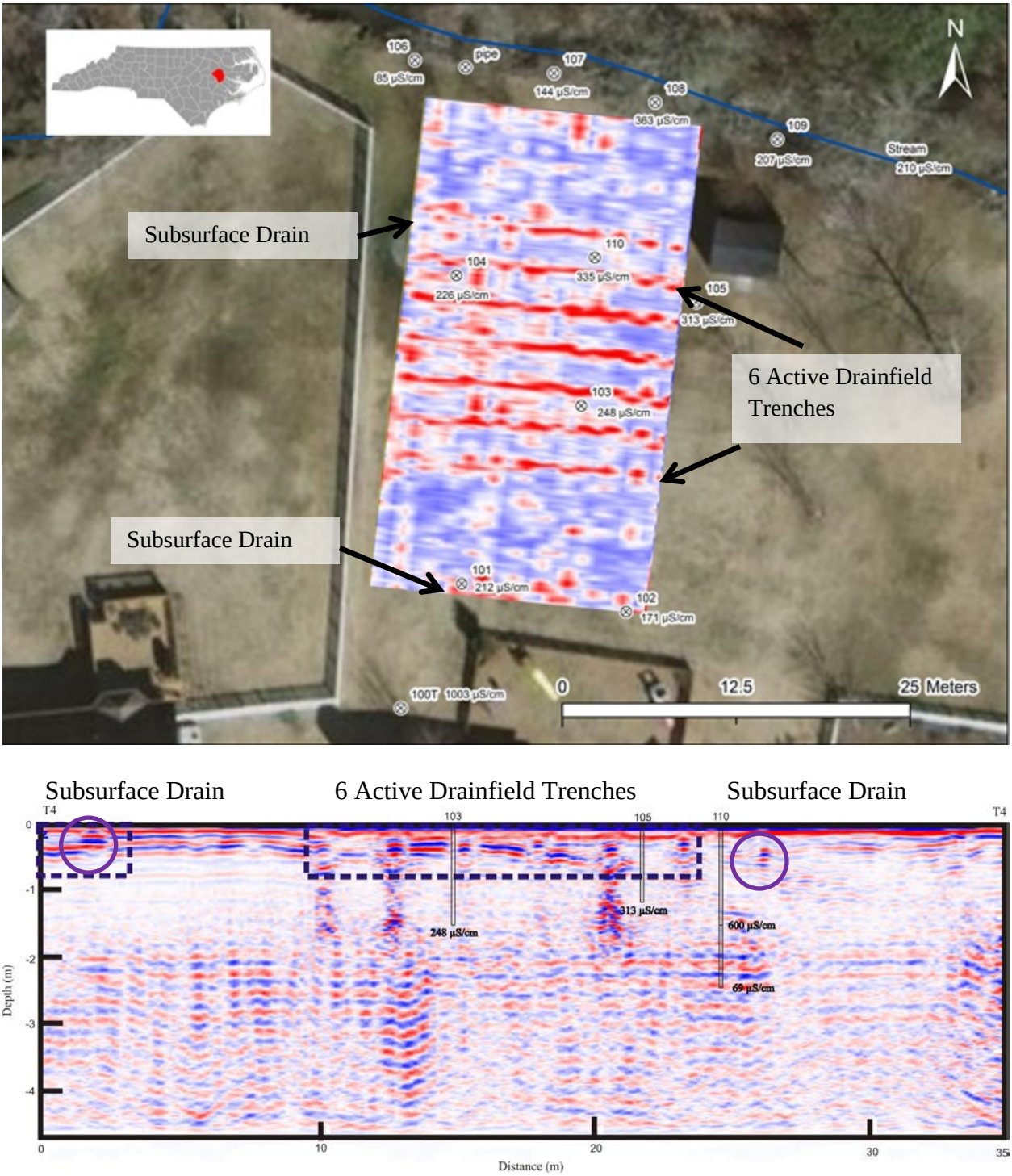

Figure 19. GPR 3-D (0.9 m depth) and transect conducted at Site 100 in July 2012. The red lines in the upper image indicate pipes in the drainfield trenches and subsurface drain tile up and down-gradient from the OWS. The lower image shows reflections where the pipes in the drainfield trenches and drains (purple circles) alter the signal.

3.5 Groundwater Specific Conductivity and Electrical Resistivity

For the transects shown in Figures 7-18, the resistivity data at the piezometer screens was compared with groundwater conductivity in the drainfield and background wells (Figure 20). Across the four sites there was a general inverse relationship between groundwater conductivity and resistivity. In general, resistivity fell below 250 ohm-m when groundwater conductivity was greater than 200 µS/cm. For the dates shown in the figures above, for 14 of 18 data points (78%) when resistivity was below 250 ohm-m groundwater specific conductivity was elevated above 200 µS/cm. These data suggest that in the vicinity of on-site wastewater treatment systems, surficial aquifer resistivity values below approximately 250 ohm-m may indicate the presence of wastewater-affected groundwater. However, it is important to mention that groundwater conductivity can vary in the surficial aquifer due to the presence of clay minerals that may leach ions and therefore cause elevated groundwater conductivity unrelated to wastewater inputs.

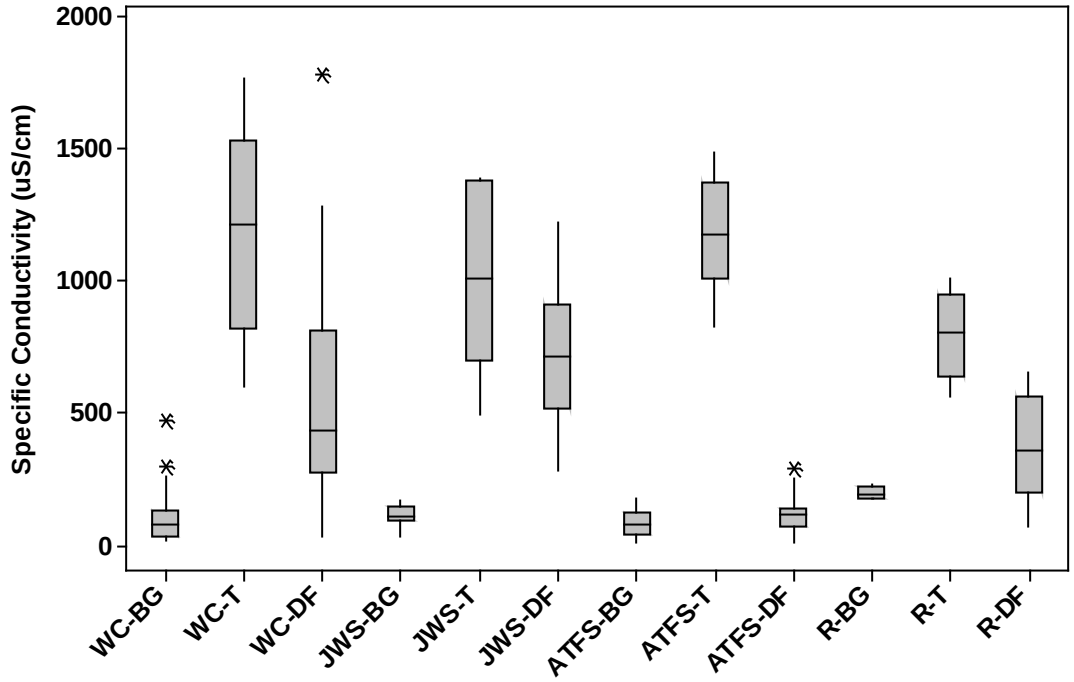

Figure 20. A comparison of specific conductivity of wastewater (T: Tank); background groundwater (BG); and drainfield (DF) during the study period. Specific piezometers used in this figure are: ATFS- DF (2,3), BG (1); Residential (R)-DF (110), BG(101); JWS-DF (6,7,10,13,14), BG (1,2,3); and WC-DF (11,12,13,15,16,17,18), BG(1).

Specific conductivity values of wastewater, background groundwater and drainfield groundwater are presented in Figure 20. Wastewater specific conductivity was highest at the West Craven High School site and lowest at the residential site. The residential site had the highest background specific conductivity in groundwater (192 µS/cm). Based on the groundwater specific conductivity data, the electrical resistivity contrasts between back ground and drainfield should be greatest at JWS and WC, therefore these sites should exhibit the greatest contrasts in electrical resistivity. The median drainfield groundwater conductivity was elevated above

background levels at all sites, although at ATFS this difference was small (35µS/cm). Even though tank wastewater had elevated conductivity, it appears that water use at the ATFS site may not have been great enough to result in large enough quantities of wastewater discharge to influence water quality extensively throughout the drainfield. These groundwater conductivity data suggest that wastewater inputs had the potential to affect subsurface electrical resistivity values at the school and residential sites, and to a lesser extent at the ATFS site. The median specific conductivity difference between background and drainfield groundwater was highest at JWS (605 uS/cm) then WC (353 µS/cm) at the residential site the difference was 166 uS/cm. At the ATFS site, there was minimal difference (35 µS/cm) between median background and drainfield groundwater conductivity. However, since there were several drainfield piezometers at the ATFS site it is instructive to look at the groundwater conductivity data for the individual background (piezometers 1s and 1d) and drainfield (piezometers 2s, 2d, and 3) piezometers (Appendix 2). These data show that over the course of the study, the wastewater inputs in the drainfield may have caused an increase in groundwater specific conductivity in piezometer 2s at this site. The other piezometers in the drainfield had similar groundwater specific conductivity as background groundwater. These data suggest that local resistivity contrasts at the ATFS site near piezometer 2s may indicate the influence of wastewater on groundwater quality.
A comparison of groundwater specific conductivity and resistivity in the drainfield and background piezometers was conducted for the geophysical survey dates shown in Figures 7-18 (3/23/12; 7/16/12; 9/14/12; 11/14/12; 11/19/12; and 4/17/13). The groundwater data revealed that median background conductivity (130 µS/cm) was lower than median drainfield conductivity (272 µS/cm) at the study sites (Figure 21a). The resistivity comparison for the same piezometers, showed that resistivity at background piezometer screens (865 ohm-m) was elevated relative to drainfield piezometers (168 ohm-m). These data suggest that the influence of wastewater on groundwater conductivity may be detected in areas near drainfields where the resistivity is less than approximately 250 ohm-m.

The formation factor (F) can be used to quantify the relationship between the pore-water resistivity (ρ_w) and bulk resistivity (ρ_b) (Archie, 1942), based on the equation: $F= \rho_b/\rho_w$. F is related to porosity based on the following equation (Winsauer et al. 1952): $F=\alpha\phi^{-m}$, where α is a constant and for sand should be approximately 1, ϕ is porosity and for sand is approximately 0.4, m is the cementation constant and for sand should be approximately 1.3 (Urish 1983). Based on these assumptions, the formation factor (F) should be approximately 3.29 for a sandy aquifer. This value can then be used to estimate the pore water resistivity by: $\rho_w = \rho_b/F$ (Urish, 1983). The calculated pore water resistivity (ρ_w) I ohm-m can be converted to uS/cm by the following conversion factor: 10,000/(ρ_w (ohm-m). This process can allow for the direct comparison between calculated pore water resistivity values and measured groundwater specific conductivity values.

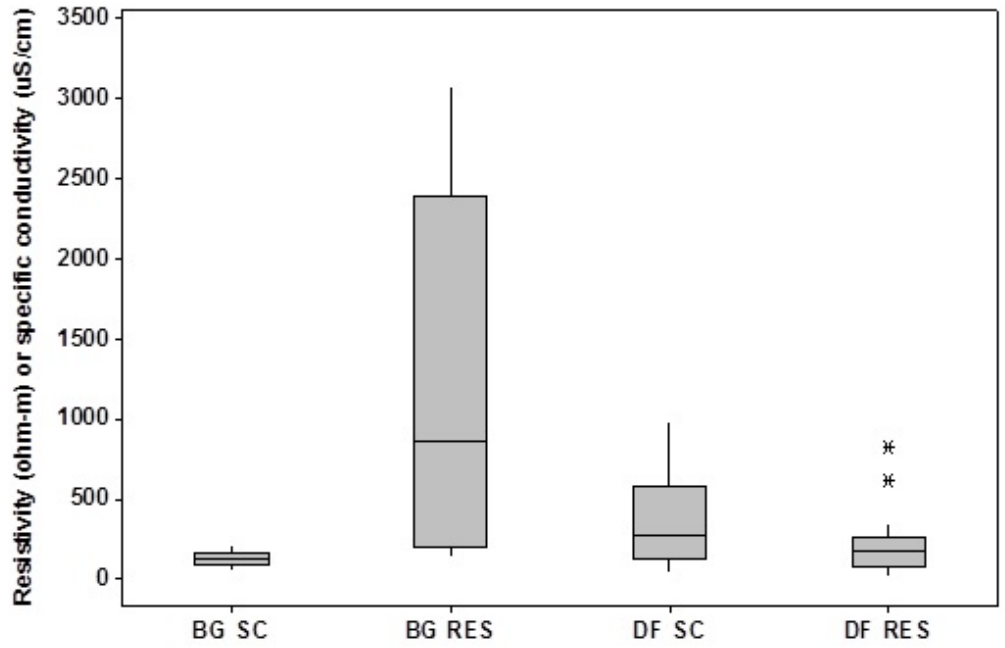

Figure 21a. A summary of pooled groundwater conductivity and resistivity data for the geophysical survey dates. The background and drainfield data are presented to show the potential contrasts in resistivity and groundwater conductivity values in areas affected by wastewater.

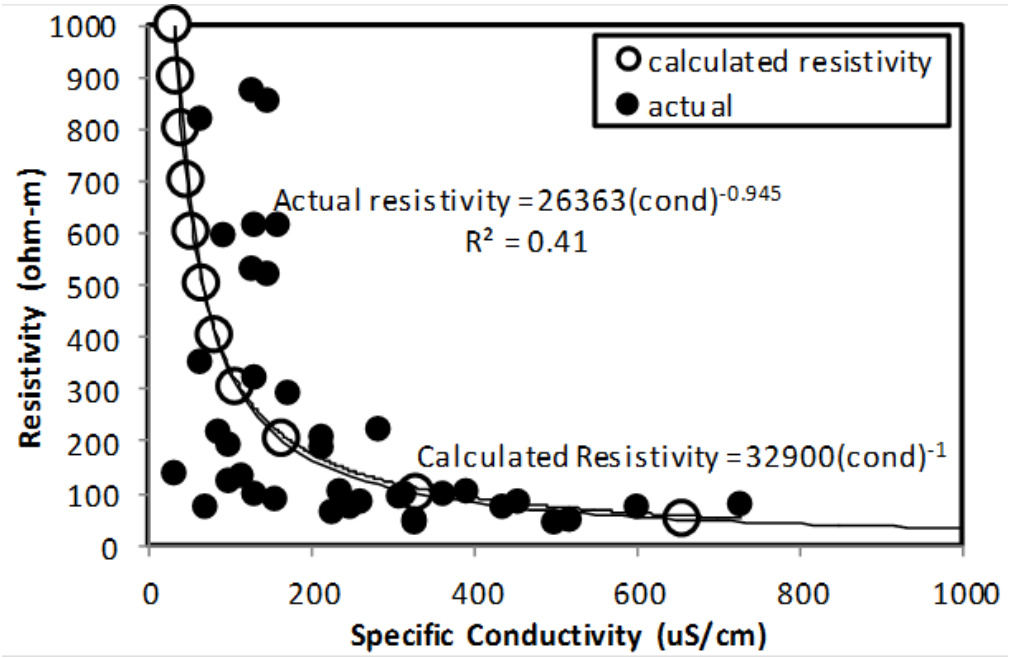

Figure 21b. The predicted relationship between bulk resistivity (calculated resistivity) and pore water conductivity, compared to the range of measured values at the four sites for the transects shown in figures 7-18. The theoretical value assumes a formation factor for sandy aquifers of 3.29 at each site, however this likely varies based on differences in surficial aquifer properties within and across sites.

In the Figure 21 b. above, the measured groundwater conductivity at the drainfield and background piezometers were plotted against the respective resistivity values estimated at the piezometers screen. Although there was some scatter, there was a general inverse relationship. This pattern was similar to the theoretical relationship between bulk resistivity and groundwater specific conductivity using the equation $\rho_{w} = \rho_{b}/(3.29)$ as described in the preceding paragraph. Future work will aim to better estimate individual site formation factors, it is likely that if individual formation factors are estimated for each site the fit would likely improve. Based on the median differences in resistivity between the drainfield (168 ohm-m) and the background piezometers (865 ohm-m), the equation predicted that for this range of approximately 700 ohm-m, the median difference in groundwater conductivity between the drainfield and background piezometers should be approximately 158 µS/cm. The measured (actual) difference between the median drainfield (272 µS/cm) and background specific conductivity (130 µS/cm) was 142 µS/cm. These comparisons show that the range of groundwater conductivity changes that are observed across these sites are sufficient to explain some of the observed changes in resistivity adjacent to drainfields.

3.6 Fate and Transport of On-site Wastewater System Derived Nutrients

3.6.1 West Craven High

There was a 72% reduction in the mean TDN concentration from the tank (80.83 ± 25.86 mg/L) to all drainfield piezometers (22.26 ± 25.49 mg/L), but only a 25% reduction to drainfield plume core piezometers (60.33 ± 30.08 mg/L) (Figure 23). Groundwater 10 m down-gradient from the OWS at piezometer 25 had TDN concentrations of 16.27 ± 10.26 mg/L (79% reduction from source concentrations). However, groundwater beneath the drainfield trenches and 10 m down-gradient from the OWS had significantly (both $p < 0.01$) higher TDN concentrations than background (1.57 ± 1.62 mg/L). Also, when evaluating the TDN/Cl ratio for groundwater 10 m from the OWS, there was only 10% change from the tank ratio, indicating that reductions in the mass of nitrogen were minimal (Table 3). No reductions in the mean mass of nitrogen were observed from the tank to groundwater beneath the drainfield during the study at WCH.

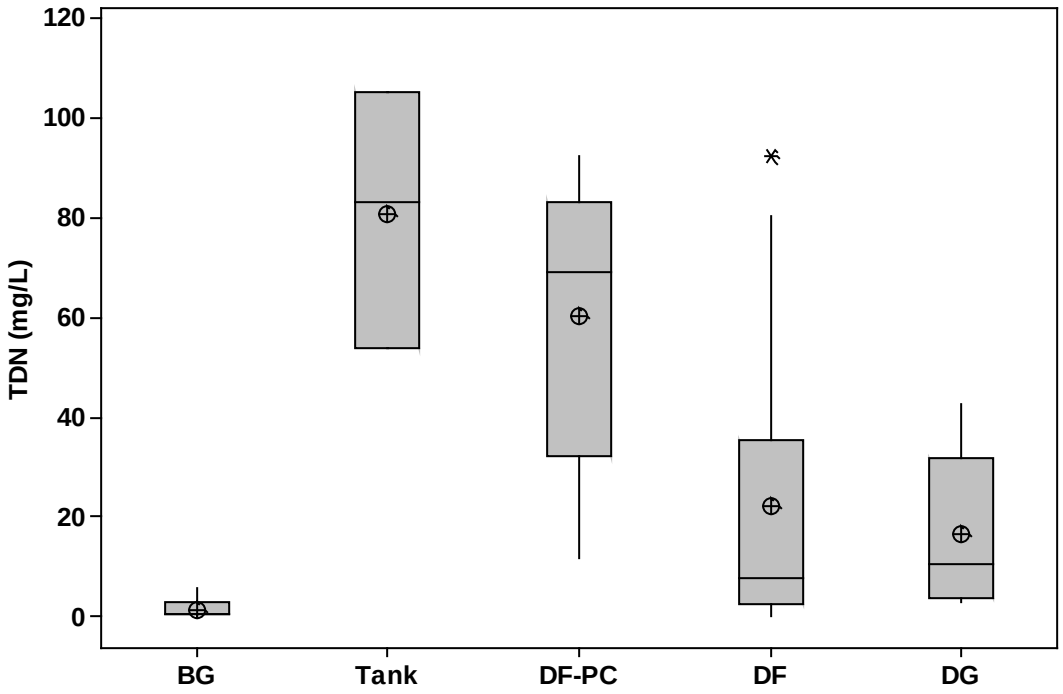

Figure 22. Mean total dissolved nitrogen (TDN) concentrations at WCH for background groundwater (BG); drainfield (DF), drainfield plume core (DF-PC) and down-gradient (DG) piezometers.

Table 3. Total dissolved nitrogen and chloride ratios for sampling locations at WCH. Negative values indicate increases in groundwater TDN relative to Cl, in comparison to tank ratios.

Parameter	Tank	Drainfield	Drainfield Plume Core	Downgradient	Background
TDN/Cl	80.83 / 106.57	22.26 / 25.82	60.33 / 64.33	16.64 / 24.3	1.57 / 8.03
TDN/Cl	0.758	0.862	0.938	0.685	0.196
Reduction	N/A	-14%	-24%	10%	

Mean PO_4 concentration reduction from the tank (8.86 ± 2.55 mg/L) to drainfield piezometers (0.06 ± 0.10 mg/L) was 99%, and from tank to drainfield plume core piezometers (0.24 ± 0.09 mg/L) was 97% at WCH (Figure 23). Piezometers down-gradient and within the flow path of the OWS had mean PO_4 concentrations of 0.26 ± 0.21 mg/L, which was 97% lower than tank effluent, but also significantly ($p = 0.0013$) higher than background groundwater PO_4 (0.04 ± 0.08 mg/L) (Figure 23). The PO_4/Cl ratios indicate an 87% or more reduction in the mass of PO_4 between the septic tank, drainfield piezometers, and groundwater 10 down-gradient from the OWS (Table 4). Therefore, the OWS at WCH was much more efficient at reducing PO_4 transport than TDN transport.

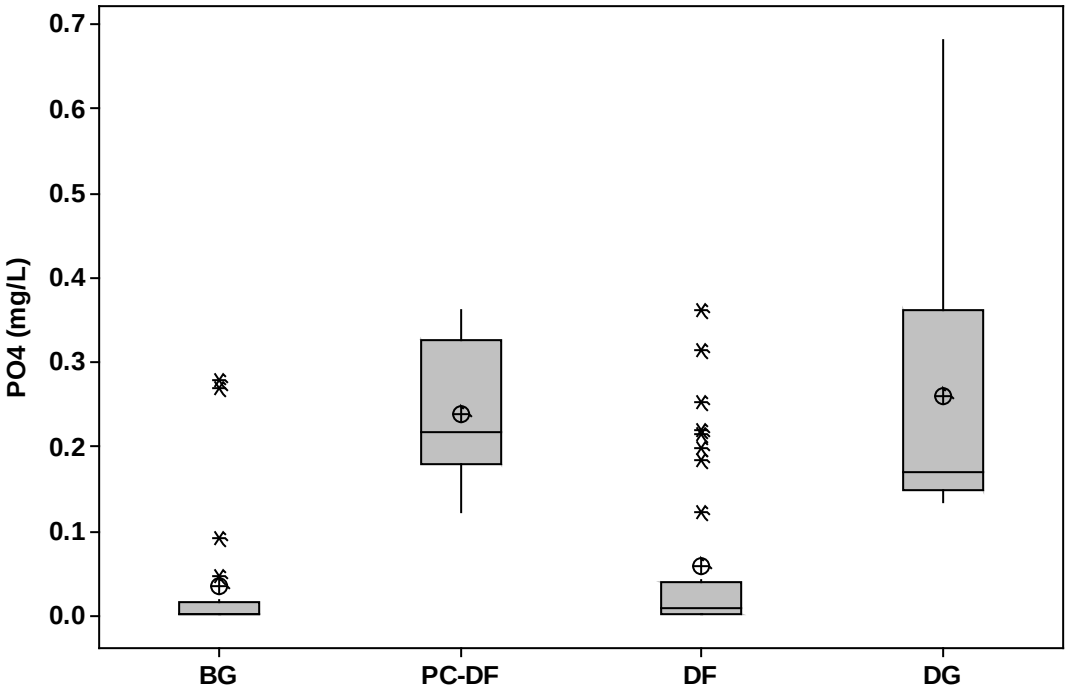

Figure 23. Mean PO_4 concentrations for background groundwater (BG); drainfield (DF); drainfield plume core (DF-PC); and down-gradient (DG) piezometers. Mean septic effluent PO_4 was (8.86 ± 2.55 mg/L).

Table 4. Mean PO_4 and chloride ratios for selected sampling locations at WCH.

Parameter	Tank	Drainfield	Drainfield Plume Core	Downgradient	Background
PO_4/Cl	8.86 / 106.57	0.06 / 25.82	0.24 / 64.33	0.26 / 24.3	0.04 / 8.03
PO_4/Cl	0.083	0.002	0.004	0.011	0.005
Reduction	N/A	98%	95%	87%	

Groundwater TDN species beneath the drainfield trenches and down-gradient from the OWS at WCH was predominately NO_3 (> 90%) (Appendix 2). Mean groundwater dissolved oxygen concentration in the drainfield area was 5.28 mg/L, thus indicating aerobic conditions necessary for nitrification (Table 5). Prior studies have shown that OWS plumes enriched in NO_3 can extend for great distances (> 30 m) in some aquifers (Robertson et al., 1991; Harman et al., 1996). Groundwater specific conductance and pH were elevated in the drainfield area and down-gradient from the OWS, relative to background conditions, indicating that wastewater was also influencing the chemical properties of groundwater. Groundwater pH values near the OWS were slightly acidic, and aerobic conditions were present, therefore, it is possible that PO_4 was removed via precipitation of the minerals variscite ($AlPO_4.2H_2O$), strengite ($FePO_4.\ 2H_2O$), and/or through adsorption (Robertson et al., 1998).

Table 5. Mean and standard deviation environmental readings data including depth to water (DTW), specific conductance (SC), dissolved oxygen (DO), pH, and temperature at WCH.

Location	DTW (m)	SC (µS/cm)	DO (mg/L)	pH	Temp (C°)
Background	1.08 ± 0.28	81 ± 79	3.73 ± 1.95	5.46 ± 0.76	17.07 ± 4.50
Tank		1181 ± 422	1.31 ± 0.31	7.10 ± 0.39	18.45 ± 5.80
Drainfield	1.59 ± 0.17	388 ± 313	5.28 ± 2.36	6.36 ± 0.49	17.44 ± 4.33
Downgradient	1.28 ± 0.16	206 ± 240	3.37 ± 1.90	6.21 ± 0.46	17.45 ± 4.38

3.6.2 JWS Nutrient Transport

TDN concentrations at JWS were reduced an average of 51% from septic tank (41.87 ± 19.62 mg/L) to groundwater beneath the OWS (20.44 ± 16.67 mg/L), but plume core TDN concentrations (40.10 ± 8.99 mg/L) were only 4% lower than septic effluent (Figure 24). The mean effluent TDN concentration was reduced by 98% from the tank to piezometers more than 15 down-gradient in the riparian buffer (0.96 ± 0.72 mg/L) (Figure 24). However, groundwater from a piezometer near a spring (Spring-Piez: piezometer 18) was still enriched with TDN (7.96 ± 0.92 mg/L). A spring (Spring 1) within the flow-path of the OWS had TDN concentrations of 11.83 ± 3.64 mg/L (Figure 24). The overland flow from the spring and additional groundwater inputs 10 m from Spring 1 (and towards the creek) also contained elevated TDN concentrations (10.05 ± 5.02 mg/L) (Spring 2). Surface water 5 m upstream of where the spring overland flow discharged into the stream had lower mean TDN (2.04 ± 0.47 mg/L) relative to the spring/stream interface (5.17 ± 4.21 mg/L) and 5 m downstream of the interface (2.56 ± 0.42 mg/L). Background groundwater TDN was 1.50 ± 0.97 mg/L. Therefore, the OWS at JWS was influencing groundwater and surface water TDN concentrations. TDN and Cl ratios indicate less than 25% reduction in TDN mass from the tank to groundwater beneath the drainfield (Table 6). However, there was significant reduction of TDN mass (90%) in groundwater that flowed through the forested riparian buffer (Table 6). Groundwater that discharged at the spring showed less than 27% mass reduction of TDN (Table 6). This indicates that forested riparian buffers can greatly reduce TDN groundwater loads to surface waters if they are not by-passed via short circuit discharges such as springs.

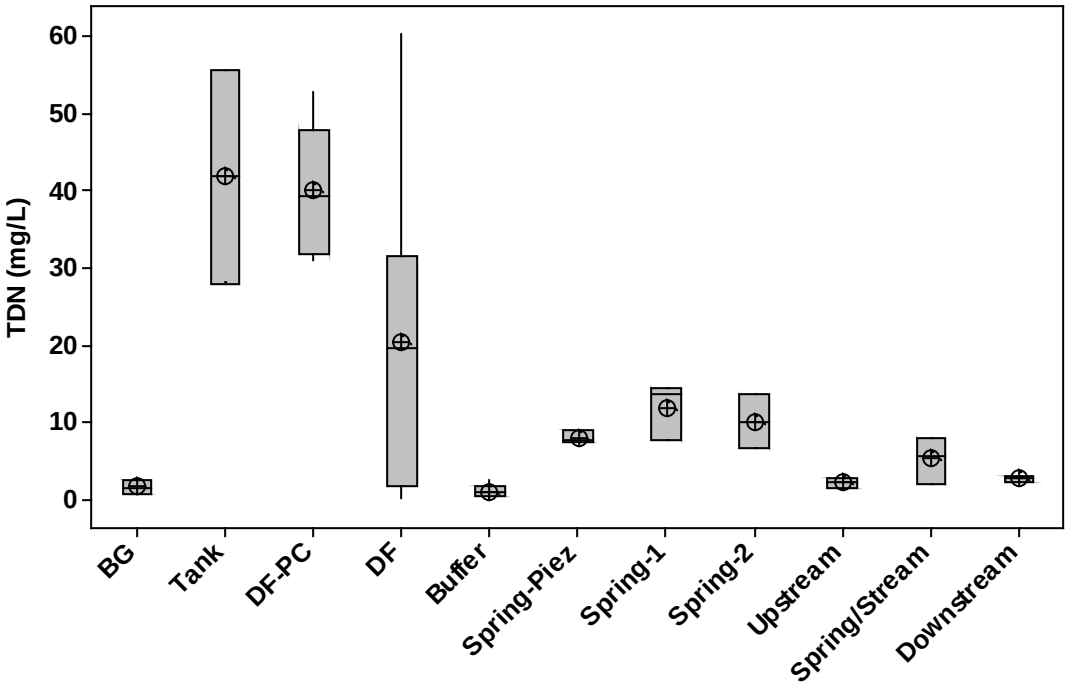

Figure 24. Total dissolved nitrogen (TDN) concentrations for select locations at JWS including background piezometers (BG); drainfield (DF); drainfield plume core (DF-PC); a spring piezometer (Spring-Piez).

Table 6. Mean total dissolved nitrogen (TDN) and chloride ratios for select locations at JWS.

Parameter	Tank	Drainfield	Drainfield Plume Core	Buffer	Spring-Piez	Spring 1	Spring 2	BG
TDN/Cl	41.87 / 80.5	20.44 / 51.7	40.10 / 67.3	0.96 / 18.6	7.96 / 32.7	11.83 / 30.9	10.05 / 22.4	1.50/4.4
TDN/Cl	0.52	0.395	0.596	0.052	0.243	0.383	0.449	0.341
Reduction	N/A	24%	-15%	90%	53%	26%	14%	

Tank PO_4 (7.55 ± 5.31 mg/L) concentrations at JWS were reduced by an average of 95% before reaching groundwater beneath the OWS (0.37 ± 0.51 mg/L) (Figure 25). Plume core PO_4 concentrations (0.92 ± 0.97 mg/L) were 88% lower than tank effluent. Buffer piezometer (0.08 ± 0.09 mg/L) and spring piezometer (0.04 ± 0.06 mg/L) PO_4 concentrations were 99% lower than septic effluent. Mean PO_4 concentrations for Spring 1 (0.22 ± 0.01 mg/L) were 97% lower, and Spring 2 PO_4 concentrations (0.16 ± 0.03 mg/L) were 98% lower respectively, than septic effluent, but still elevated relative to background groundwater (0.02 ± 0.01 mg/L) (Figure 25). The spring and stream interface had slightly elevated PO_4 concentration (0.13 ± 0.07 mg/L), but

upstream (0.08 ± 0.04 mg/L) and down-stream (0.07 ± 0.02 mg/L) PO_4 concentrations were similar. Mean PO_4/Cl ratios also indicate significant reduction (>84%) in the mass of PO_4 before discharge to groundwater beneath the OWS, and more than 92% mass reduction before reaching the springs in the buffer area (Table 7).

There was a thick vadose zone at JWS (> 4 m) near the drainfield area, thus enabling aerobic treatment of the wastewater (Table 8). While elevated NO_3 concentrations were present in groundwater beneath the OWS, and NO_3 was discharged to the stream via overland from the spring, there was also significant removal of nitrogen mass (90%) possibly via denitrification in the buffer area away from the springs.

PO_4 reduction was also significant at JWS in the unsaturated zone (>84%) possibly via mineral precipitation or adsorption. With mean groundwater pH values typically between 6 and 7, and aerobic conditions (Table 8), precipitation of strengite or variscite may occur at this site (Robertson et al., 1998). Groundwater specific conductance beneath the drainfield (640 ± 237 µS/cm) and within the flow-path of the OWS (all > 370 µS/cm) was elevated relative to background groundwater (103 ± 20 µS/cm), and the stream (147 ± 11 µS/cm) (Table 8). Surface water upstream from where the overland flow from the spring enters the stream had lower specific conductivity (147 ± 11 µS/cm) than down-stream (164 ± 375 µS/cm), indicating the OWS was influencing surface water specific conductance.

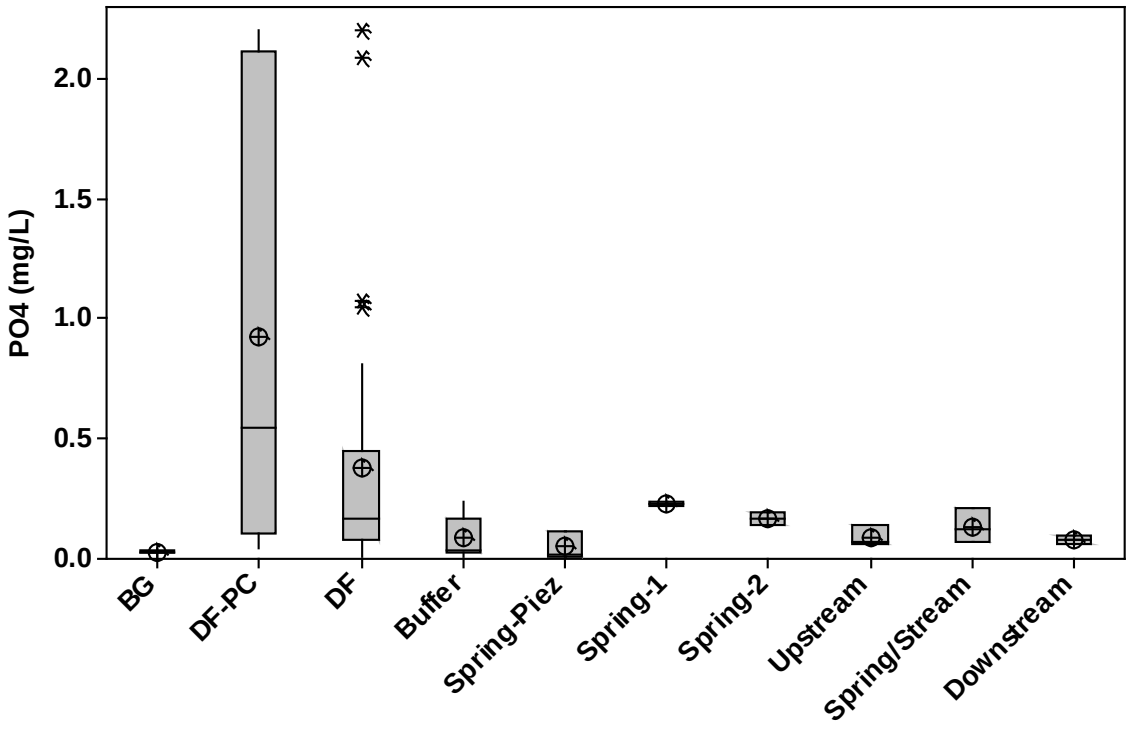

Figure 25. Mean PO_4 concentrations for background groundwater (BG); drainfield (DF) and drainfield plume core piezometers (DF-PC) and other labeled locations at JWS.

Table 7. Mean PO_4 and chloride ratios for selected sampling locations at JWS.

Parameter	Tank	Drainfield	Drainfield Plume Core	Buffer	Spring-Piezometer	Spring 1	Spring 2	Background
PO_4/Cl	7.55 / 80.5	0.37 / 51.7	0.92 / 67.3	0.08 / 18.6	0.04 / 32.7	0.22 / 30.9	0.16 / 22.4	0.02 / 4.4
PO_4/Cl	0.094	0.007	0.014	0.004	0.001	0.007	0.007	0.005
Reduction	N/A	93%	85%	96%	99%	93%	93%	

Table 8. Mean and standard deviation environmental readings data including depth to water (DTW), specific conductance (SC), dissolved oxygen (DO), pH, and temperature at JWS.

Location	DTW (m)	Temp (C°)	SC (µS/cm)	DO (mg/L)	pH
Background	3.98 ± 0.25	18.57 ± 2.72	103 ± 20	5.93 ± 1.72	5.72 ± 0.74
Tank	----------	19.25 ± 5.09	1063 ± 375	1.53 ± 0.73	7.17 ± 0.35
Drainfield	5.61 ± 1.32	19.15 ± 4.32	640 ± 237	5.62 ± 2.52	6.67 ± 0.63
Buffer	----------	14.78 ± 4.38	373 ± 80	2.74 ± 0.84	6.91 ± 0.22
Spring-Piezometer	----------	15.5 ± 3.58	469 ± 72	5.36 ± 2.08	7.03 ± 0.14
Spring 1	----------	18 ± 1.48	659 ± 72	5.84 ± 0.86	6.84 ± 0.29
Upstream	----------	14.48 ± 4.08	147 ± 11	10.65 ± 1.31	7.22 ± 0.23
Spring/Stream	----------	16.57 ± 2.43	385 ± 28	9.28 ± 0.72	7.13 ± 0.04
Downstream	----------	14.59 ± 5.09	164 ± 12	11.15 ± 0.73	7.3 ± 0.35

3.6.3 Site 100 On-site System Nutrient Transport

There was an 83% reduction in mean TDN concentration from tank (55.44 ± 9.13 mg/L) to drainfield piezometers (9.18 ± 7.70 mg/L) at Site 100 (Figure 26). The drainfield plume core had a mean TDN concentration of 20.53 ± 5.57 mg/L, and was 63% lower than the mean tank TDN concentrations (figure 26). The near stream plume core TDN concentration was 12.63 ± 1.49 mg/L, or 77% lower than effluent concentrations (Figure 26). The mean TDN concentration of all piezometers within the OWS flow path was 7.30 ± 3.43 mg/L, and was elevated relative to background groundwater TDN (4.74 ± 0.70 mg/L). Stream TDN concentrations were 1.84 ± 0.14 mg/L. The TDN/Cl ratios suggest there was less than a 45% reduction in TDN mass between the tank and groundwater beneath the trenches and less than 55% reduction in TDN mass from tank to near stream (Table 9).

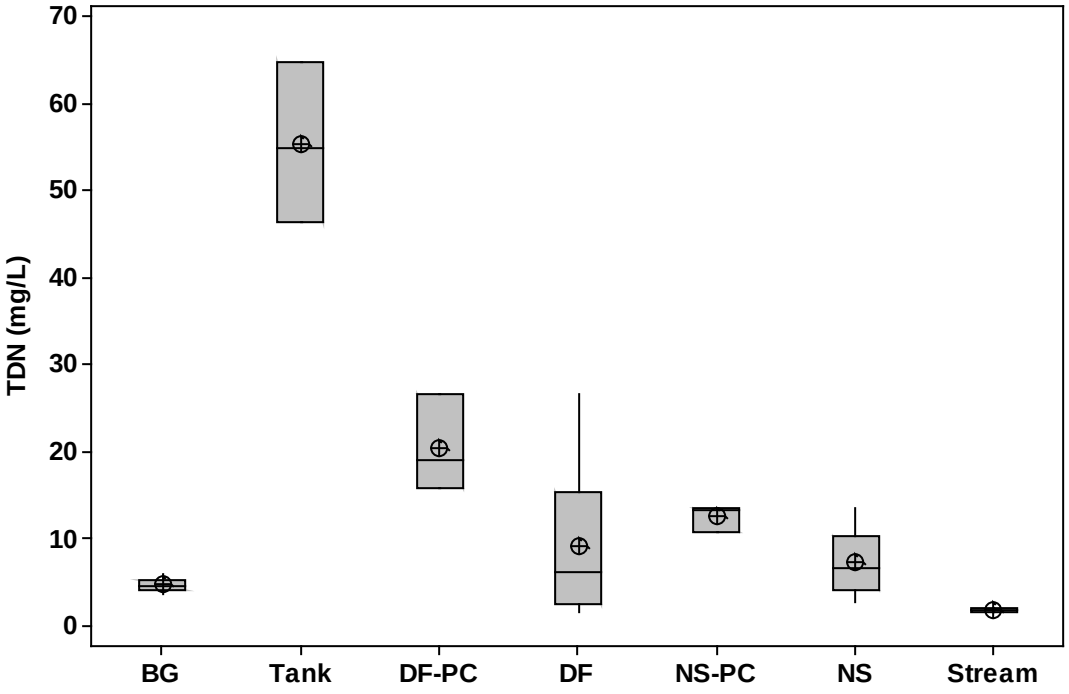

Figure 26. Mean total dissolved nitrogen (TDN) concentrations for select locations at Site 100 including background piezometers (BG); drainfield (DF); drainfield plume core (DF-PC); near stream (NS) and near stream plume core (NS-PC).

Table 9. Mean total dissolved nitrogen (TDN) and chloride ratios for select locations at Site 100.

Parameter	Tank	Drainfield	Drainfield Plume Core	Near Stream	Near Stream Plume Core	Background
TDN/Cl	55.44 / 62.8	9.18 / 18.1	20.53 / 36.9	7.30 / 14.9	12.63 / 30.8	4.74 / 10.3
TDN/Cl	0.882	0.507	0.556	0.490	0.410	0.460
Reduction	N/A	43%	37%	44%	54%	

Site 100 PO_4 concentration was reduced by 98% from tank (5.77 ± 2.08 mg/L) to groundwater beneath the drainfield (0.12 ± 0.30 mg/L) (Figure 27). The plume core TDN concentrations near the drainfield were 0.43 ± 0.61 mg/L, or 93% lower than septic effluent concentrations. Near-stream mean PO_4 concentrations were 0.19 ± 0.39 mg/L, or 97% lower than septic effluent. Plume core PO_4 concentrations near the stream (0.71 ± 0.81 mg/L) were 88% lower than septic effluent, but higher than background groundwater concentrations (0.21 ± 0.49 mg/L). Stream PO_4 concentrations were 0.01 ± 0.005 mg/L. The PO_4/Cl ratios also indicate a significant reduction (75% or more) in the mass of PO_4 from tank to stream edge, possibly because of

adsorption, mineral precipitation or plant uptake (Table 10). Site 100 had less than 0.1 m separation from the drainfield trenches to groundwater, and the lowest mean dissolved oxygen concentrations near the drainfield area (2.13 ± 0.93 mg/L) of the study sites (Table 11). Given these conditions, adsorption may be the most important PO_4 removal mechanism at Site 100 (Harman et al.,1996). Groundwater specific conductivity and pH near the drainfield trenches (280 ± 170 µS/cm; 6.59 ± 0.66) were elevated relative to background groundwater (181 ± 63 µS/cm; 5.87 ± 1.58) (Table 11). The OWS at Site 100 was influencing the chemical properties of groundwater.

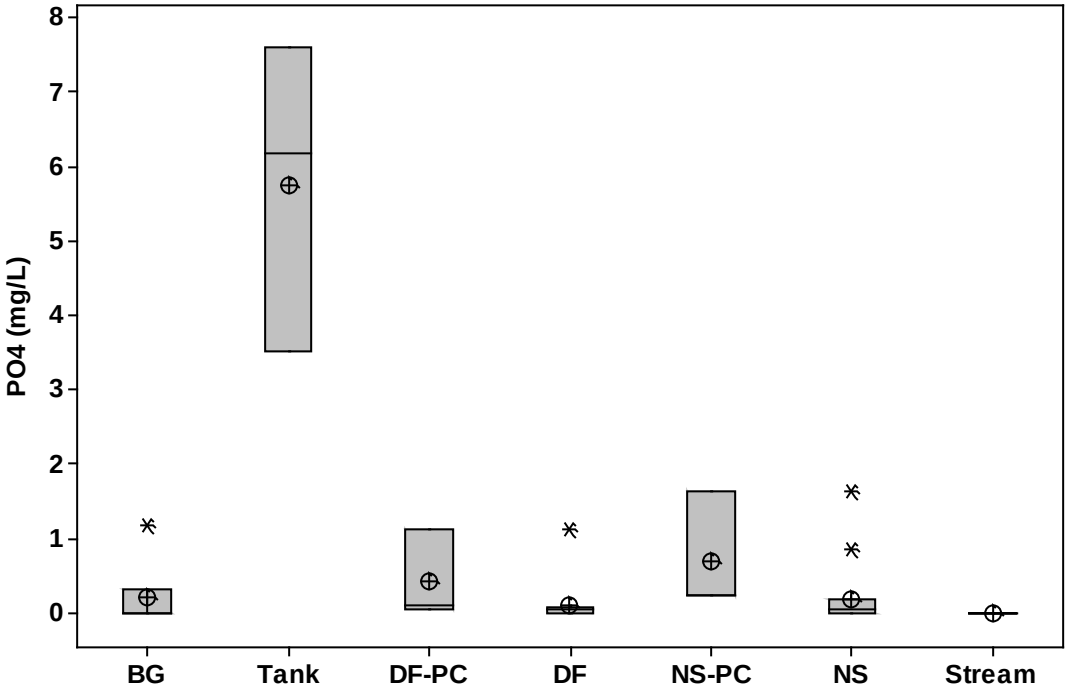

Figure 27. Mean PO_4 concentrations for select locations at Site 100 including background piezometers (BG); drainfield (DF); drainfield plume core (DF-PC); near stream (NS) and near stream plume core (NS-PC).

Table 10. Mean PO_4 and chloride ratios for selected sampling locations at Site 100.

Parameter	Tank	Drainfield	Drainfield Plume Core	Near Stream	Near Stream Plume Core	Background
PO_4/Cl	5.77 / 62.8	0.12 / 18.1	0.43 / 36.9	0.19 / 14.9	0.71 / 30.8	0.21 / 10.3
PO_4/Cl	0.092	0.007	0.012	0.013	0.023	0.020
Reduction	N/A	92%	87%	86%	75%	

Table 11. Mean and standard deviation environmental readings data including depth to water (DTW), specific conductance (SC), dissolved oxygen (DO), pH, and temperature at Site 100.

Location	DTW (m)	SC (uS/cm)	pH	DO (mg/L)	Temp (C°)
BG	0.8 ± 0.13	181 ± 63	5.87 ± 1.58	3.19 ± 0.67	19.58 ± 4.95
Tank		858 ± 222	6.42 ± 0.23	0.96 ± 0.68	22.0 ± 5.73
DF	0.46 ± 0.19	280 ± 167	6.59 ± 0.66	2.13 ± 0.93	19.17 ± 6.09
NS	1.15 ± 0.13	191 ± 109	6.02 ± 0.27	1.89 ± 0.87	17.21 ± 4.21

3.6.4 ATFS On-site System Nutrient Transport

ATFS septic effluent TDN concentrations were 68.48 ± 8.43 mg/L (Figure 28). Groundwater beneath the drainfield had mean TDN concentrations 4.49 ± 2.34 mg/L, and mean drainfield plume core TDN concentration of 6.01 ± 1.66 mg/L. Therefore, TDN was reduced by an average of 93% beneath the drainfield, and 91% in the most concentrated portion of the OWS plume. Piezometers down-gradient and within the flow path of the OWS plume had mean TDN concentrations of 4.6 ± 2.22 mg/L, while piezometers outside the flow path had TDN concentrations of 2.92 ± 1.76 mg/L. Background groundwater TDN was 1.83 ± 1.51 mg/L. The TDN/Cl ratios indicated between a 51 and 60% possible mass reduction in TDN beneath and adjacent to the OWS (Table 12). Overall, there was not much difference in groundwater TDN concentrations, most likely because of low flows and wastewater loading rates to the subsurface.

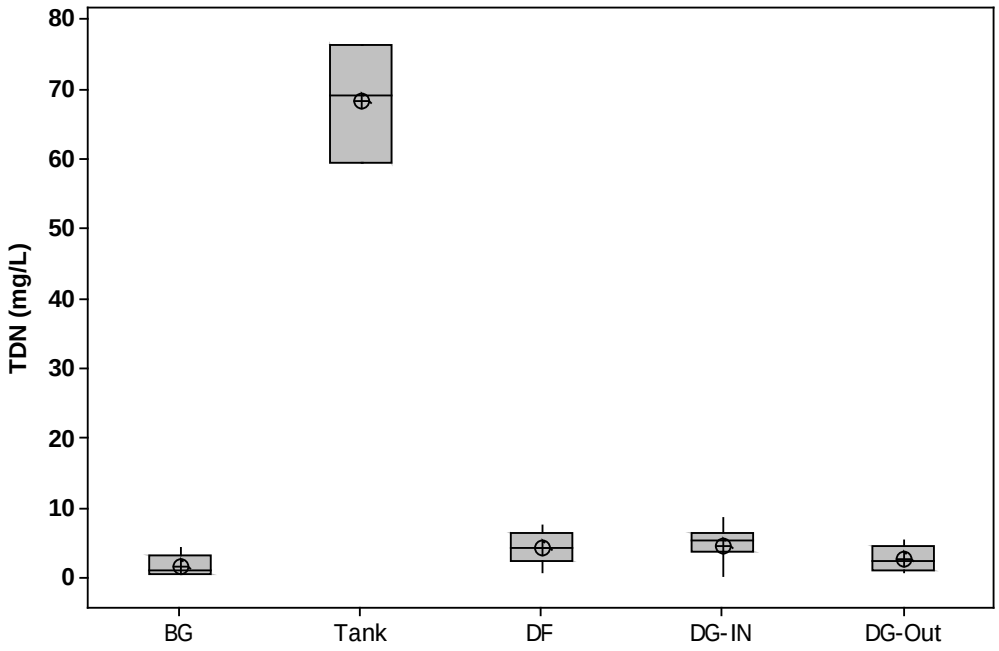

Figure 28. Mean total dissolved nitrogen (TDN) concentrations for select locations at ATFS including background piezometers (BG); drainfield (DF); piezometer down-gradient within the plume flow path (DG-IN) and down-gradient outside the flow path (DG-Out).

Table 12. Mean total dissolved nitrogen (TDN) and chloride ratios for select locations at ATFS.

Parameter	Tank	Drainfield	Drainfield Plume Core	Downgradient	Background
TDN/Cl	68.48 / 81.5	4.49 / 10.8	6.01 / 17.1	4.66 / 13.6	1.83 / 10.0
TDN/Cl	0.841	0.414	0.351	0.339	0.183
Reduction	N/A	51%	58%	60%	

ATFS septic effluent PO_4 concentrations were 5.99 ± 1.70 mg/L (Figure 29). Groundwater beneath the drainfield had mean PO_4 concentrations of 0.37 ± 0.71 mg/L and plume core PO_4 concentrations of 0.70 ± 1.08 mg/L, for a reduction percentage of more than 88%. The mean background groundwater PO_4 concentration at ATFS was 0.91 ± 0.91 mg/L (Figure 29). Excluding an outlier (4.95 mg/L), the background groundwater PO_4 concentration was 0.20 ± 0.27 mg/L. The PO_4/Cl ratios show more than a 45% reduction in the mass of PO_4 near the drainifield, and more than 99% reduction in down-gradient from the OWS (Table 13). With limited wastewater generation, and a thick unsaturated zone (Table 13), significant PO_4 transport was not expected at ATFS. Mean groundwater specific conductivity beneath the drainfield trenches (136 ± 72 µS/cm) was slightly elevated relative to background groundwater (83 ± 47 µS/cm), but other environmental readings were similar (Table 14).

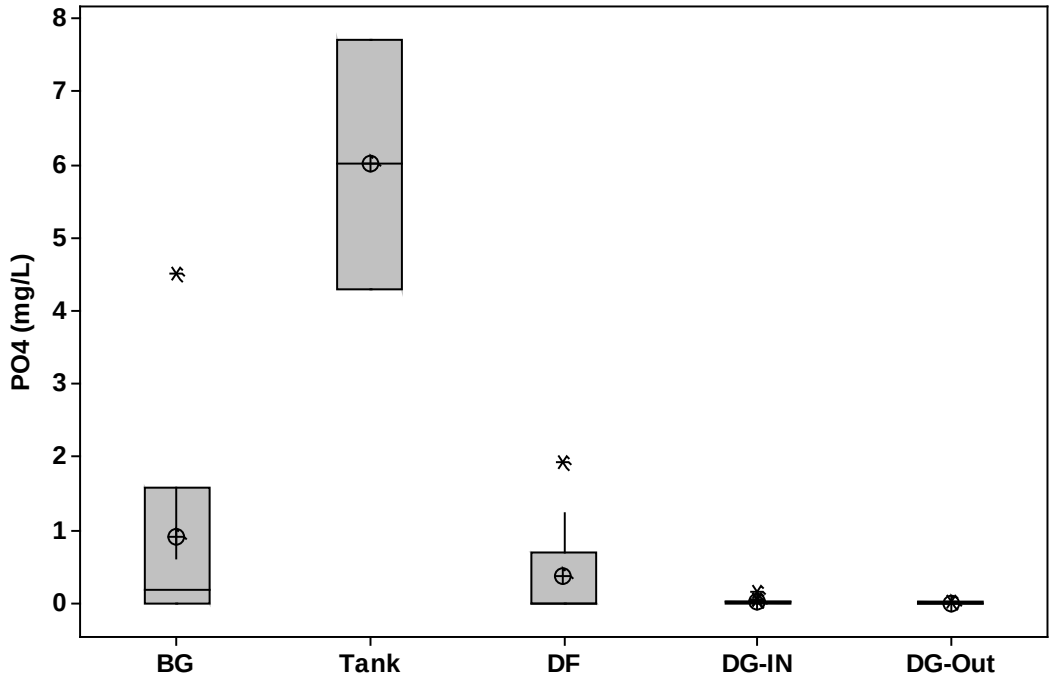

Figure 29. Mean PO_4 concentrations for select locations at ATFS including background piezometers (BG); drainfield (DF); piezometer down-gradient within the plume flow path (DG-IN) and down-gradient outside the flow path (DG-Out).

Table 13. Mean PO_4 and chloride ratios for selected sampling locations at ATFS.

Parameter	Tank	Drainfield	Drainfield Plume Core	Downgradient	Background
PO_4/Cl	5.99 / 81.5	0.37 / 10.8	0.70 / 17.1	0.02 / 13.6	0.20 / 10.0
PO_4/Cl	0.074	0.034	0.041	0.001	0.02
Reduction	N/A	54%	45%	99%	

Table 14. Mean and standard deviation environmental readings data including depth to water (DTW), specific conductance (SC), dissolved oxygen (DO), pH, and temperature at ATFS.

Location	DTW (m)	Temp (^{0}C)	pH	SC (µS/cm)	DO (mg/L)
BG	2.75 ± 0.84	17.94 ± 4.17	5.61 ± 0.56	83 ± 47	4.73 ± 2.28
DF	3.20 ± 0.31	18.01 ± 3.55	5.43 ± 0.51	136 ± 72	4.91 ± 1.95
Tank		18.03 ± 8.17	7.09 ± 0.22	1115 ± 196	1.92 ± 0.2

4. Summaries

4.1 Geophysical Survey Summary

ER surveys were most effective at detection and delineation of OWS plumes at WCH and JWS. These two sites had sandy soils and background groundwater had low specific conductance. Groundwater influenced by OWS had much higher specific conductance, and lower resistivity than background groundwater, allowing for accurate determinations of plumes at these sites. The ER surveys at Site 100 were also effective at enabling researchers to locate the plume core areas such as near piezometer nest 108 at the creek. However, background groundwater specific conductance was elevated, and there was not as much of a contrast in specific conductance of groundwater or electrical resistivity of soil and water near the drainfield area in relation to other areas. Therefore, plume characterization at Site 100 using ER was not as effective as at JWS or WCH. For ATFS, some minor differences were shown in groundwater specific conductance and electrical resistance after the initiation of the new OWS. However, because of the sporadic generation and subsurface discharge of wastewater, differences in specific conductance and electrical resistance were not significant enough to really proclaim that the plume was identified.

GPR surveys were effective at every site in showing the location of drainfield trenches, and drain tile. For JWS and WCH, the GPR signal appeared to attenuate beneath the drainfield trenches, indicating the influence of wastewater on subsurface electrical conductance. The same trend also occurred at Site 100, but to a lesser extent. GPR surveys at ATFS did not reveal any noticeable differences in signal attenuation that could be confidently attributed to wastewater discharges.

4.2 Onsite Wastewater System Nutrient Concentration Reduction Summary

Mean TDN reduction from tank to groundwater beneath the drainfield was highest for Site 100 (63% plume core; 83% all drainfield); followed by WCH (25% plume core; 72% all drainfield), and JWS (4% plume core; 51% all drainfield). NH_4 was the dominant nitrogen species in

groundwater beneath the drarinfield trenches (65%) and down-gradient from the OWS near the stream (81%) at Site 100, with NO_3 comprising less than 10 % of groundwater TDN within the plume area (Appendix 2). This indicates that nitrification was inhibited at Site 100. The mean separation from OWS trench to water table for Site 100 was < 0.1 m (Table 2). Nitrification requires aerobic conditions. Prior studies have shown that OWS with limited separation from drainfield trenches to water table may discharge significant NH_4 to groundwater (Carlile et al., 1981; Humphrey et al., 2010). Therefore, nitrification rates may have been limited by the small vadoze zone at Site 100. The dominant groundwater N species at JWS, WCH and ATFS were NO_3 (all > 90%) (Appendix 2). Each of these sites had separation distances to groundwater of more than 1 m (Tables 2), which is double the NC Division of Environmental Health required minimum distance for sandy soils (0.45 m). Therefore nitrification was not inhibited at JWS, WCH, and AFTS, and elevated NO_3 concentrations were observed in groundwater beneath and down-gradient from the systems.

With respect to TND fate and transport away from the OWS, the JWS site performed the best. Mean TDN concentrations were reduced by the highest percentage at JWS when groundwater flowed through the riparian buffer system (TDN: 0.96 ± 0.72 mg/L; 98% reduction), however groundwater discharging at the spring had higher TDN values (11.83 ± 3.64 mg/L) and thus the reduction efficiency (72%) was lower. TDN concentrations at WCH were reduced by 79% from tank to groundwater 10 m down-gradient from the OWS drainfield. TDN concentrations for Site 100 were reduced by 77% from the tank to near stream 15 m from the OWS.

Vadose treatment for PO_4 was highest for WCH (97% for all drainfield; 99% for plume core) followed by Site 100 (98% drainfield; 93% plume core), and JWS (95% for all drainfield; 88% plume core). ATFS treatement efficiency was (94% drainfield, and 88% plume core).

The mean PO_4 treatment efficiency was highest at JWS for groundwater that flowed through the buffer (99%), followed by JWS groundwater that discharged to the spring (97%), WCH groundwater 10 m from the OWS (97%), and at Site 100 (88%) reduction adjacent to the creek, 15 m from the OWS.

4.3 Onsite Wastewater System Nutrient Mass Reduction Summary

The TDN/Cl values indicate that Site 100 was most effective at reducing TDN from tank to groundwater beneath the drainfield trenches (37% reduction). AFTS values indicated a 51% reduction, but the wastewater generation at the sites was not comparable to the others, and thus efficiencies may be skewed by the low loading rates. Nitrogen was not reduced in the vadoze zones beneath the OWS at JWS and WCH, bases on TDN/Cl data. However there was a 10% reduction in groundwater TDN between the WCH drainfield and piezometers 10 m down-gradient from the OWS. The TDN reduction at JWS between the tank and buffer piezometers indicated a 90% TDN reduction. For groundwater samples collected from the piezometers adjacent to Spring 1, there was a 53% TDN reduction. However, for Spring 1, only a 26% TDN reduction from source concentrations was observed due to mass reduction mechanisms. At Site 100, there was a 44% TDN reduction at the edge of the stream.

PO_4 reduction from tank to groundwater beneath drainfield was greatest for WCH (98%) and JWS (93%). Site 100 reduced PO_4 by an average of 86% from tank to all near stream

piezometers, and by 75% for plume core piezometers. There was an 87% PO_4 reduction from tank to piezometers 10 m down-gradient from WCH. The greatest PO_4 reductions were observed at JWS, where there was a 93% or greater reduction from source to all buffer piezometers and the spring. While ATFS ratios indicated a 99% reduction from source to down-gradient piezometers, again the wastewater loading rates to soil were not comparable to the other sites.

Overall, OWS were more efficient are reducing PO_4 concentrations relative to TDN. The OWS that was most effective at reducing nutrient transport was JWS, where groundwater was flowing through a forested buffer. However, elevated TDN and PO_4 was discharged via a spring and spring overland flow to an adjacent creek.

5. Conclusions

Based on wastewater and groundwater conductivity patterns at four field sites, it was that groundwater beneath the drainfields typically had elevated specific conductivity. At each site, there were locations adjacent to the drainfield where the resistivity values declined, corresponding with increased groundwater specific conductivity values. Since wastewater inputs were greatest at the school sites (WCHS and JWS), the increases in groundwater conductivity in the drainfields tended to be highest at those sites. Generally, the resistivity patterns at the school sites showed an inverse relationship with groundwater conductivity values. Although subtle resistivity declines were evident at ATFS and the residential site, the resistivity patterns generally showed less variability and appeared to be less affected by wastewater inputs than those patterns observed at the school sites. Overall, the data suggest that in sandy surficial aquifers, resistivity values below approximately 250 ohm-m may indicate zones of high conductivity groundwater (> 200 uS/cm). If these zones are adjacent to on-site wastewater treatment systems, it may be assumed that they are zones of wastewater-affected groundwater. It is important to mention that sediment heterogeneity in the surficial aquifer can also cause changes in resistivity, therefore it is important to collect sediment and groundwater quality data to verify the reasons for resistivity changes. The geophysical techniques presented in this report can be paired with water quality and hydrogeological data to better delineate wastewater systems that may affect surface water quality in nearby streams, lakes, wetlands, and estuaries.

Geophysical surveys including GPR and ER, can be applicable for detecting OWS components including distribution boxes and drainfield trenches, and for delineating groundwater influenced by OWS in some geologic settings. Permits for OWS often include sketches of the property and general location of the OWS components (Appendix 2). However, if the permits are not drawn to scale, if the OWS was not installed in an area different than what is shown on the permit, or if the permit is lost/missing, then locating OWS components can very difficult. GPR was very useful in detecting drainfield trenches lined with gravel and polystyrene-aggregate material, and for detecting subsurface drain tile. Because GPR data is shown in real-time, OWS components can be flagged in the field upon detection. GPR can be very helpful in locating abandoned OWS, OWS that are installed relatively deep, and OWS that use gravel-less trench media.

ER surveys can be applicable for identifying wastewater plumes in locations that have relatively low background groundwater specific conductance and soil/sediment layers that do not have very different electrical resistance. The use of ER surveys can help reduce the number of piezometers and monitoring wells needed to assess fate and transport of OWS and other contaminants.

The OWSs evaluated in the study were more effective at reducing the concentration and mass of PO_4 relative to TDN. Treatment efficiencies were variable and were potentially influenced by factors such as wastewater loading rate, thickness of the vadose zone beneath the OWS drainfield trenches, speciation of nitrogen, soil type, and presence of riparian vegetation within the flow-path of the OWS. The OWS most effective at reducing TDN and PO_4 was at JWS, where groundwater flowed through the vegetated riparian buffer. Much lower nutrient reductions (higher nutrient concentrations) were observed at JWS where groundwater discharged to a spring.

6. Recommendations

Future work will aim to:

- Compare how well the riparian sediments remove nitrogen in contrast to the spring/surface flowpath to the stream at the JWS site. This work can help quantify the effectiveness of riparian buffers to attenuate N from OWTS sites.
- It is likely that with greater use of the OWTS at the ATFS site there will be increases in the groundwater conductivity underlying the drainfield over time. Future work could continue to monitor this site to better understand the rates of wastewater plume expansion and migration in the surficial aquifer.
- Ongoing geological site characterization work will help better isolate the influence of pore water resistivity on bulk resistivity. Future work will aim to better estimate individual site formation factors, it is likely that if individual formation factors are estimated for each site the relationship between pore water resitivity and bulk resistivity could be used to predict groundwater conductivity values.
- OWS nutrient concentration reduction efficiencies were calculated for these sites and the nutrient/chloride ratios helped provide some evidence of treatment mechanisms that reduce mass loads. More work to quantify the actual processes responsible for the reduction in mass of nitrogen and phosphorus would be beneficial.

References

Adepelumi, A.A., Ako, B.D., and Ajayi, T.R. 2001. "Groundwater contamination in the basement-complex area of IIE-Ife, southwestern Nigeria: A case study using the electrical-resistivity geophysical method". *Hydrogeology Journal* 9:611-622.

Aravena, R., M.L. Evans, and J.A. Cherry. 1993. Stable isotopes of oxygen and nitrogen in source identification of nitrate from septic systems. Ground Water. 31 (2) 180-186.

Archie, G.E. 1942. The electrical resistivity log as an aid in determining some reservoir characteristics. Trans. Am. Inst. Metall. Engrs. 146:54-62.

Baker GS, Jordan TE, and Pardy, J (2007) An introduction to ground penetrating radar (GPR), in Baker, GS and Jol, HM (eds.) Stratigraphic Analyses Using GPR. The Geological Society of America Special Paper 432, 181 pp.

Bermejo, J.L., Sauck, W.A., and Atekwana, E.A. 1997. "Geophysical discovery of a new LNAPL plume at the former Wurtsmith AFB, Oscoda, Michigan". *Ground Water Monitoring and Remediation* 17 (4): 131-137.

Cahoon, L.B., Hales, J.C., Carey, E.S., Loucaides, S., Rowland, K.R., and Nearhoof, J.E. 2006. Shellfishing closures in southwest Brunswick County, North Carolina: Septic tanks vs. stormwater runoff as fecal coliform sources. Journal of Coastal Research. 22 (2) 319-327.

Carlile, B.L., Cogger, C.G., Sobsey, M.D., Scandura, J., and Steinbeck, S.J. 1981. Movement and Fate of Septic Tank Effluent in Soils of the North Carolina Coastal Plain. Report for the Coastal Plains Regional Commission through the Division of Health Services on NC Department of Health.

Cogger, C. G., Hajjar, L.M., Moe, C.L, and Sobsey, M.D. 1988. Septic System Performance on a Coastal Barrier Island. *Journal of Environmental Quality.* 17 (3) 401-408.

Corbett, D.R., Dillon, K., Burnett, W., and Schaefer, G. 2002. The spatial variability of nitrogen and phosphorus concentration in a sand aquifer influenced by onsite sewage treatment and disposal systems: a case study on St. George Island, Florida. Environmental Pollution. 117 (2) 337-345.

Desimone, L.A. and Howes, B.L. 2006. Denitrification and Nitrogen Transport in a Coastal Aquifer Receiving Wastewater Discharge. Environ. Sci. Techno. 30, 1152-1162.

Fear, J., Gallow, T., Hall, N., Loftin, J., and Paerl, H. 2004. Predicting benthic microalgal oxygen and nutrient flux responses to a nutrient reduction management strategy for the eutrophic Neuse River Estuary, North Carolina, USA. Estuarine, Coastal and Shelf Science 61, 491-506.

Harman, J., Robertson, W.D., Cherry, J.A., and Zanini, L. 1996. Impacts on a sand aquifer from an old septic system: Nitrate and Phosphate. Ground Water. 34 (6) 1105-1114.

Heath, R.C. 1998. “Basic Ground-Water Hydrology”. US Department of Interior, US Geologic Survey. Water –Supply Paper 2220.

Humphrey, C.P. and O’Driscoll, M.A. 2011. Biogeochemistry of Groundwater Beneath On-site Wastewater Systems in a Coastal Watershed. *Universal Journal of Environmental Research and Technology*, 1(3) 320-328.

Humphrey, C.P., O’Driscoll, M.A., and Armstrong, M.C. 2012. Onsite Wastewater System Nitrogen Loading to Groundwater in the Newport River Watershed, North Carolina. *Environment and Natural Resources Research*, 2 (4), 70-79

Humphrey, C.P., O’Driscoll, M.A., Deal, N., Lindbo, D., Zarate-Bermudez, M., and Thieme, **S**. (in press). On-site Wastewater System Nitrogen Contributions to Groundwater in Coastal North Carolina. *Journal of Environmental Health*.

Humphrey, C., Deal, N., O’Driscoll, M., and Lindbo, D. 2010. Characterization of on-site wastewater nitrogen plumes in shallow coastal aquifers, North Carolina. Proceedings of the World Environmental and Water Resources Congress, May 16-20, Providence, RI.

Humphrey, C. P., O'Driscoll, M. A., & Zarate, M. A. 2011. Evaluation of On-site Wastewater System E. coli Contributions to Shallow Groundwater in Coastal North Carolina. *Journal of Water Science and Technology 63 (4), 789-795*.

Humphrey, C., O’Driscoll, M., and Zarate, M. 2010**.** Controls on groundwater nitrogen contributions from on-site wastewater systems in coastal North Carolina. Water Science and Technology. 62 (6) 1448-55.

Hoover, M.T. 2004. Soil Facts: Septic Systems and Their Maintenance, AG-439-13. North Carolina Cooperative Extension Service.

Hyslip, J., Smith, S., Olhoeft, G., and Selig, E. 2003. “Assessment of Railway Track Substructure Condition Using Ground Penetrating Radar.” *Proc. of the 2003 Annual Conference of AREMA*, Chicago, October.

Lee, B.D., Jenkinson, B.J., Doolittle, J.A., Taylor, R.S., and Tuttle, J.W. 2006. “Electrical conductivity of a failed septic system soils adsorption field”. *Vadose Zone Journal* 5 (2): 757-763.

Loke, M.H. 2013. Electrical imaging surveys for environmental and engineering studies: A practical guide to 2-D and 3-D surveys. Accessed on 7/3/2013 at www.geotomosoft.com

North Carolina Department of Environment and Natural Resources. 2003. Nutrient Sensitive Waters Management Strategy. Website: http://h2o.enr.state.nc.us/nps/neuse.htm

North Carolina National Estuarine Research Reserve. 2003. Workshop Proceedings. “Addressing Microbial Pollution in Coastal Waters”. Duke University Marine Laboratory, Beaufort, NC.

Porsani, J.L., W. M. Filhob, V.R. Elisa, F. Shimelesa, J.C. Douradob, and H.P. Mourab.Baker, 2004. The use of GPR and VES in delineating a contamination plume in a landfill site: a case study in SE Brazil . Journal of Applied Geophysics 55 (3-4): 199-209.

Ptacek, C.J. 1998. Geochemistry of a septic system plume in a coastal barrier bar, Point Pelee, Ontario, Canada. Contaminant Hydrology 33, 293-312.

Robertson, W.D., Cherry, J.A., and Sudicky, E.A. 1991. Groundwater Contamination From 2 Small Septic Systems on Sand Aquifers. Ground Water 29 (1) 82-92.

Robertson, W.D., Schiff, S.L., and C.J. Ptacek. 1998. Review of Phosphate Mobility and Persistence in 10 Septic System Plumes. *Groundwater* 36 (6) 1000-1010.

Roy, J.W., Robillard, J.M., Watson, S.B., and Hayashi, M. 2009. Non-intrusive characterization methods for wastewater-affected groundwater plumes discharging to an alpine lake. Environmental Monitoring and Assessment 149: 201-211.

Samouëlian, A., Cousin,I., Tabbagh, A., Bruand, A., and Richard, G. 2005. Electrical resistivity survey in soil science: a review. Soil and Tillage Research 83(2): 173-193.

Scandura, J.E. and M.D. Sobsey. 1997. Viral and Bacterial Contamination of Groundwater from On-Site Sewage Treatment Systems. Water Science Technology. 35 (11-12) 141- 146.

United States Environmental Protection Agency. 2002. On-site Wastewater Treatment Systems Manual.EPA/625/R-00/008.

Urish, D.W. 1983. The practical application of surface electrical resistivity to detection of ground-water pollution. Ground Water 21(2): 144-152.

Westco Scientific Instruments, Incorporated.. 2011. Smartchem 200 Discrete Chemistry Analyzer. 117 Old State Road, Brookfield, Connecticut 06804.

Appendix 1. Alphabetical list of commonly used abbreviations

ATFS: *A Time for Science*, an environmental education center in Ayden, NC that uses an onsite wastewater system and was one of the volunteered research sites for this study

CEL: Central Environmental Research Laboratory at East Carolina University, the laboratory samples were analyzed for nutrients during this study

ER: electrical resistivity, measured in ohm-m, is the resistance to conduct electrical current. ER surveys can provide information on subsurface characteristics such as changes in soil texture and moisture content

GPR: ground penetrating radar, a technology that transmits electromagnetic waves at microwave frequencies into the sediment, and records reflections as a function of two-way travel time. Used for determining subsurface properties

JWS: James Smith School, an elementary school in Cove City, NC that uses an onsite wastewater system and was one of the volunteered research sites for this study

NC: North Carolina, location of the study

OWS: onsite wastewater system (septic system) used to treat and disperse wastewater and include a septic tank, effluent distribution mechanism, drainfield trenches, and soil.

TDN: total dissolved nitrogen, the sum of dissolved organic and inorganic nitrogen species including NH4, NO3, NO2.

TE: treatment efficiency, the percentage reduction in nitrogen or phosphorus from source concentrations

Appendix 2. List of presentations and publications

Humphrey, C. P. & O'Driscoll, M. A. (2012). Controls on Phosphorus Transport from Onsite Wastewater Treatment Systems to Groundwater and Adjacent Surface Water in Coastal North Carolina. *Geologic Society of America,* Charlotte, NC.

Smith, M., O'Driscoll, M., Mallinson, D., & Humphrey, C. (2012). Evaluation of Geophysical Techniques for Delineating On-site Wastewater Treatment System Effluent Plumes. *NC On-site Water Protetction Conference* Hickory, NC.

Hardison, S. E., Humphrey, C. P., O'Driscoll, M. A., & Mallinson, D. (2012). Geophysical Delineation and Groundwater Characterization of a Contaminant Plume from a Residential On-site Wastewater System in Pitt County, North Carolina. *Geologic Society of America*, Charlotte, NC.

Smith, M. J., O'Driscoll, M. A., Mallinson, D. J., & Humphrey, C. P. (2012). Geophysical and Water Quality Characterization of On-site Wastewater Treatment System Effluent Plumes at Two Schools in The North Carolina Coastal Plain. *Geologic Society of America*, Charlotte, NC.

Two Geology graduate students (Matt Smith and Sarah Hardison) are currently writing their theses with geophysical and water quality data collected from the sites in this study. Upon completion, project investigators will forward copies of the two theses to WRRI and any other publications related this project.

Appendix 2. Environmental Readings

JWS Environmental Readings (Average)

Well ID	Location	DTW (ft)	Temp (°C)	Spec Cond (µ/cm)	DO (mg/L)	pH
1	Background	12.03	18.17	104	5.18	6.59
2	Background	13.36	18.83	110	7.09	5.35
3	Background	13.75	18.72	95	5.51	5.24
4	Drainfield	13.13	18.64	580	6.12	5.99
5	Drainfield	13.04	18.48	590	5.83	5.95
6	Drainfield	15.75	18.86	721	4.15	6.00
7	Drainfield	19.92	19.28	1083	4.48	6.87
8	Drainfield	19.94	18.62	858	6.07	7.23
9	Outside Flow Path	17.15	19.47	52	8.74	6.71
10	Drainfield	12.98	18.74	776	7.26	6.56
11d	Drainfield	22.73	19.89	372	3.68	7.29
11s	Drainfield	22.56	19.56	381	6.59	7.35
12d	Drainfield	25.22	19.13	490	2.87	7.38
12s	Drainfield	23.07	20.85	402	5.70	7.20
13d	Drainfield	15.65	18.78	539	6.47	6.06
13s	Drainfield	15.07	19.56	603	7.44	6.08
14	Drainfield	20.08	18.57	931	6.41	6.71
15	Outside Flow Path	23.39	19.23	255	3.87	7.69
16	Buffer	2.82	16.29	348	3.05	7.12
17	Buffer	2.81	15.52	446	2.86	6.83
18	Spring-piezometer	4.04	15.55	659	5.36	7.03
19	Buffer	5.93	12.68	293	2.64	6.77
20	Buffer	3.13	14.65	406	2.43	6.91
Sping1	Spring		18.00	469	5.84	6.84
Sping2	Spring		20.00	507	8.60	7.20
5m upstream	Stream		14.48	147	10.65	7.22
spring/stream	Stream		16.57	385	9.28	7.13
5m downstream	Stream		14.59	164	11.15	7.30
TANK	Tank		19.25	1063	1.53	7.17

Appendix 2. Environmental Readings

ATFS Environmental Readings (Average)

Sample Point	Location	DTW (ft)	SC (μS/cm)	DO (mg/L)	pH	Temp (^{0}C)
1s	Background	8.98	18.07	5.33	112	4.73
1d	Background	9.08	17.81	5.89	88	3.53
2s	Drainfield	10.16	18.1	5.41	142	5.38
2d	Drainfield	10.04	17.85	5.15	110	5.44
3	Drainfield	11.3	17.83	5.47	123	5.11
4	Downgradient-In	11.58	17.93	5.45	116	3.8
5	Downgradient-In	10.87	17.36	4.99	134	5.59
6	Downgradient-In	6.12	16.98	4.81	142	3.84
7	Downgradient-In	5.7	17.11	5.06	143	2.86
8	Downgradient-Out	5.99	17.34	4.55	135	3.4
9	Downgradient-Out	4.51	16.57	4.84	69	4.13
10	Downgradient-Out	6.95	15.92	4.79	116	3.14
11s	Downgradient-In	2.75	15.53	4.65	120	5.24
11d	Downgradient-In	3.11	15.79	4.71	124	4.37
12sb	Downgradient-In	5.23	15.61	4.75	119	5.1
12da	Downgradient-In	7.48	16.5	4.93	137	3.54
13	Downgradient-In	4.9	15.6	4.76	121	4.72
TANK			18.03	7.09	1115	1.92

Appendix 2. Environmental Readings

WCH Environmental Readings (Average)

Sample Point	Location	DTW (ft)	SC (µS/cm)	DO (mg/L)	pH	Temp (^{0}C)
WC-1d-c	Background	2.99	201	3.24	4.92	17.13
WC-1s	Background	3.07	160	3.41	4.99	17.04
WC2-c	Background	2.84	98	2.87	5.21	17.25
WC3-c	Background	3.72	31	3.26	5.39	16.84
WC-4-c	Background	3.27	31	3.65	5.51	16.8
WC-5d-c	Background	3.41	47	3.76	5.14	17.28
WC-5s-c	Background	3.84	44	4.3	5.8	19.12
WC-6	Background	3.86	61	3.92	5.41	16.64
WC-7	Background	4.98	56	5.26	6.68	16.44
WC-8	Drainfield	5.51	171	6.42	5.8	17.27
WC-9	Drainfield	5.45	67	5.76	5.96	16.84
WC-10-c	Not in plume	4.81	38	5.55	5.96	17.72
WC-11	Drainfield	5.74	42	5.52	6.3	17.22
WC-12	Drainfield	5.57	380	5.24	6.62	17.65
WC-13d-c	Drainfield	5.35	953	4.42	6.37	17.63
WC-13s	Drainfield	5.4	650	5.03	6.43	17.46
WC-14	Outside	4.11	42	4.76	5.77	17.35
WC-15	Drainfield	4.98	353	5.41	6.76	17.59
WC-16	Drainfield	5.07	212	5.45	6.25	17.57
WC-17	Drainfield	4.96	761	5.24	6.48	17.34
WC-18	Drainfield	4.67	315	4.11	6.3	17.67
WC-19	Not in plume	4.2	49	6.39	6.67	17.4
WC-20	Not in plume	4.36	47	5.53	6.11	17.47
WC-21	Not in plume	4.28	108	3.63	6.5	17.22
WC-22d-c	Not in plume	3.7	124	4.15	6.47	17.75
WC-22s	Not in plume	3.58	35	4.97	6.6	17.38
WC-23	Not in plume	2.25	52	3.82	6.24	17.59
WC-24d	Drainfield	4.94	436	4.5	6.68	17.79
WC-24s	Drainfield	4.78	255	5.18	6.59	17.46
WC-27s	Downgradient	4.1	25	4.6	5.92	16.87
WC-27m	Downgradient	3.98	81	3.8	5.99	17.06
WC-27d	Downgradient	4.16	340	3.53	5.85	17.41
WC-26d	Not in plume	4.47	100	4	6.42	17.82
WC-26s	Not in plume	4.42	39	5.18	6.52	17.77
WC-25d	Downgradient	4.3	542	3.01	6.45	17.71
WC-25m	Downgradient	4.35	110	3.2	6.37	17.62
WC-25s	Downgradient	4.41	167	2.78	6.54	17.53
Ditch			127	5.57	6.3	16.54
Tank			1181	1.31	7.1	18.45

Appendix 2. Environmental Readings

Site 100 Environmental Readings (Average)

Sample Point	Location	DTW	Temp (C°)	SC (µS/cm)	pH	DO (mg/L
101	Background	2.84	18.73	179.40	5.85	2.96
102	Background	2.39	20.59	182.00	5.88	2.68
103	Drainfield	1.59	20.11	179.67	6.40	1.83
104	Drainfield	0.82	19.96	280.67	6.62	2.27
105	Drainfield	1.54	19.14	277.60	6.83	2.16
106	Outside Plume	2.42	16.68	82.33	6.17	1.84
107s	Near Stream	3.63	17.58	131.17	5.79	1.70
107d	Near Stream	3.61	17.53	78.67	5.89	1.75
108s	Near Stream	3.30	22.90	326.00	6.05	1.85
108m	Near Stream	4.32	16.94	223.67	6.25	2.35
108d	Near Stream	4.18	16.89	309.00	5.83	1.49
109s	Near Stream	3.60	16.64	216.33	6.05	1.49
109d	Near Stream	3.34	16.72	167.33	6.33	1.44
110s	Drainfield	1.62	18.25	471.50	6.51	1.81
110d	Drainfield	1.71	18.70	191.17	6.63	1.73
Tank			21.99	857.50	6.42	0.93
Pipe			12.12	196.00	5.71	6.45
Stream			15.44	169.50	6.31	7.22

Appendix 2. Nutrient data

Site 100 Nutrient Data

Day	Month	Year	Sample	NH4 (mg/L)	NO3+NO2 (mg/L)	DKN (mg/L)	Cl (mg/L)	PO4 (mg/L)	TDN (mg/L)
13	July	2012	101	0.28	2.96	0.81	6.42	0.00	3.77
13	July	2012	101	0.29	2.96	0.84	6.82	0.00	3.80
27	March	2013	101	0.63	3.70	0.20	10.58	0.00	4.33
16	November	2012	101	0.13	4.41	0.39	12.39	0.02	4.79
13	July	2012	102	0.85	2.89	1.77	6.57	1.20	4.65
27	March	2013	102	0.60	4.40	0.60	13.55	0.00	5.00
16	November	2012	102	0.12	5.45	0.43	11.95	0.02	5.88
13	July	2012	103	2.08	0.00	5.62	2.72	0.00	5.62
13	July	2012	103	2.32	0.00	5.66	3.16	0.00	5.66
27	March	2013	103	5.33	0.00	5.81	12.96	0.09	5.81
16	November	2012	103	4.70	5.11	6.67	9.51	0.06	11.79
13	July	2012	104	0.22	0.00	6.71	6.24	0.06	6.71
27	March	2013	104	10.62	0.03	10.62	24.73	0.06	10.65
16	November	2012	104	0.41	0.15	1.82	30.92	0.06	1.97
13	July	2012	105	0.09	0.00	1.67	2.05	0.09	1.67
27	March	2013	105	0.88	0.36	1.15	14.79	0.10	1.51
13	July	2012	106	2.26	0.03	2.62	9.43	0.00	2.65
27	March	2013	106	2.25	0.00	2.25	12.65	0.00	2.25
16	November	2012	106	3.26	0.02	3.57	12.17	0.03	3.59
16	November	2012	106	3.24	0.02	3.54	11.56	0.06	3.56
13	July	2012	Tank	35.02	0.00	64.78	36.95	3.52	64.78
27	March	2013	Tank	46.54	0.00	46.54	74.85	7.61	46.54
16	November	2012	Tank	54.99	0.01	54.99	76.71	6.18	55.00
13	July	2012	stream	0.40	0.56	1.13	22.05	0.00	1.70
27	March	2013	stream	1.33	0.63	1.33	17.73	0.00	1.97
16	November	2012	stream	1.04	0.58	1.28	21.97	0.01	1.86

Appendix 2. Nutrient Data

Site 100 Nutrient Data

Day	Month	Year	Sample	NH4 (mg/L)	NO3+NO2 (mg/L)	DKN (mg/L)	Cl (mg/L)	PO4 (mg/L)	TDN (mg/L)
17	September	2012	100 pipe	3.31	3.23	3.46	15.22	0.27	6.69
27	March	2013	100-pipe	0.63	3.30	0.63	11.87	0.00	3.93
13	July	2012	107d	1.28	0.00	3.91	2.99	0.87	3.91
27	March	2013	107d	3.30	0.00	3.30	7.23	0.24	3.30
16	November	2012	107d	6.36	0.01	6.81	9.49	0.07	6.82
13	July	2012	107s	5.69	0.01	10.51	5.07	0.07	10.52
27	March	2013	107s	7.08	0.00	7.08	5.93	0.19	7.08
16	November	2012	107s	8.70	0.04	10.08	9.69	0.09	10.12
13	July	2012	108d	5.14	4.45	7.11	44.94	0.00	11.56
27	March	2013	108d	13.26	0.00	13.29	24.91	0.00	13.29
16	November	2012	108d	8.60	0.46	8.60	22.48	0.00	9.06
13	July	2012	108m	11.51	2.11	11.56	11.98	0.14	13.67
27	March	2013	108m	3.77	0.19	3.77	10.37	0.02	3.96
16	November	2012	108m	10.62	0.30	10.62	15.45	0.00	10.92
13	July	2012	108s	0.57	1.15	3.20	38.90	0.15	4.35
27	March	2013	108s	1.65	2.94	1.65	8.04	0.00	4.59
13	July	2012	109d	0.52	0.19	2.57	2.96	1.65	2.76
27	March	2013	109d	5.85	0.06	6.56	15.48	0.06	6.62
16	November	2012	109d	7.37	0.02	7.64	13.08	0.25	7.66
13	July	2012	109s	5.86	0.09	5.86	13.77	0.00	5.95
27	March	2013	109s	2.14	0.70	2.62	14.64	0.01	3.32
16	November	2012	109s	5.02	0.01	6.52	20.72	0.00	6.53
13	July	2012	110d	0.40	0.00	3.01	3.72	1.14	3.01
27	March	2013	110d	2.36	0.00	2.83	7.53	0.06	2.83
16	November	2012	110d	15.28	0.02	15.28	27.12	0.01	15.30
13	July	2012	110s	26.66	0.00	26.66	43.55	0.00	26.66
27	March	2013	110s	14.63	0.00	15.77	32.14	0.00	15.77
16	November	2012	110s	19.12	0.03	19.12	35.10	0.00	19.15

Appendix 2. Nutrient Data

ATFS Nutrient Data

Day	Month	Year	Sample	NH4 (mg/L)	NO3+NO2 (mg/L)	DKN (mg/L)	Cl (mg/L)	PO4 (mg/L)	TDN (mg/L)
29	November	2012	ATFS-10	0.09	3.30	0.18	8.92	0.00	3.49
4	September	2012	ATFS-10	0.03	4.68	0.20	10.08	0.00	4.89
17	April	2013	ATFS-11d	1.25	5.19	1.25	7.69	0.05	6.43
29	November	2012	ATFS-11d	0.07	5.30	0.12	9.21	0.14	5.42
4	September	2012	ATFS-11d	0.03	5.18	0.15	9.23	0.04	5.34
17	April	2013	ATFS-11s	0.83	4.14	0.83	7.84	0.02	4.97
29	November	2012	ATFS-11s	0.06	6.04	0.11	8.09	0.02	6.15
4	September	2012	ATFS-11s	0.02	4.83	0.14	6.96	0.01	4.98
17	April	2013	ATFS-12d	0.75	4.69	0.75	8.73	0.02	5.44
17	April	2013	ATFS-12d	0.57	4.76	0.57	8.51	0.02	5.33
29	November	2012	ATFS-12d	0.51	3.26	0.51	10.25	0.01	3.78
4	September	2012	ATFS-12d	0.04	5.72	0.39	11.48	0.01	6.10
17	April	2013	ATFS-12s	1.01	5.55	1.01	7.36	0.00	6.56
29	November	2012	ATFS-12s	0.15	5.18	0.18	9.86	0.00	5.36
29	November	2012	ATFS-12s	0.45	5.22	0.45	9.61	0.00	5.67
4	September	2012	ATFS-12s	0.04	6.17	0.51	8.92	0.00	6.69
17	April	2013	ATFS-13	0.55	3.81	0.55	6.60	0.00	4.36
29	November	2012	ATFS-13	0.21	5.67	0.21	8.61	0.01	5.88
4	September	2012	ATFS-13	0.15	6.29	2.40	8.52	0.01	8.68
17	April	2013	ATFS-1d	0.24	0.04	0.94	2.03	0.34	0.98
29	November	2012	ATFS-1d	0.08	0.17	0.35	5.57	0.61	0.53
4	September	2012	ATFS-1d	0.03	0.00	1.65	16.58	4.49	1.65
17	April	2013	ATFS-1s	0.17	4.10	0.17	6.69	0.00	4.27
29	November	2012	ATFS-1s	0.20	2.62	0.40	9.80	0.00	3.02
4	September	2012	ATFS-1s	0.02	0.07	0.50	19.38	0.03	0.56
17	April	2013	ATFS-2d	0.23	3.85	0.23	7.63	0.00	4.07
29	November	2012	ATFS-2d	0.22	5.18	0.22	10.31	0.02	5.40
4	September	2012	ATFS-2d	0.05	0.27	0.54	6.42	1.22	0.81

Appendix 2. Nutrient Data

ATFS Nutrient Data

Day	Month	Year	Sample	NH4 (mg/L)	NO3+NO2 (mg/L)	DKN (mg/L)	Cl (mg/L)	PO4 (mg/L)
17	April	2013	ATFS-3	0.25	4.17	0.25	6.91	0.01
29	November	2012	ATFS-3	6.46	0.17	6.46	8.91	0.16
4	September	2012	ATFS-3	0.26	0.04	0.98	5.98	1.94
17	April	2013	ATFS-4	0.41	1.73	0.43	6.94	0.04
29	November	2012	ATFS-4	3.30	0.87	3.30	11.84	0.18
4	September	2012	ATFS-4	0.05	0.05	1.47	4.30	5.13
17	April	2013	ATFS-5	0.39	6.07	0.39	8.75	0.00
29	November	2012	ATFS-5	0.25	6.80	0.40	12.37	0.03
4	September	2012	ATFS-5	1.44	5.31	1.95	9.15	0.06
17	April	2013	ATFS-6	0.52	0.25	0.52	38.84	0.00
29	November	2012	ATFS-6	0.18	0.12	0.28	51.36	0.00
4	September	2012	ATFS-6	0.36	0.17	0.97	9.30	0.01
4	September	2012	ATFS-6	0.18	0.47	0.61	9.61	0.00
17	April	2013	ATFS-7	3.84	0.21	3.84	19.21	0.00
29	November	2012	ATFS-7	2.96	0.24	2.97	30.47	0.00
4	September	2012	ATFS-7	0.29	0.49	0.51	22.08	0.01
17	April	2013	ATFS-8	0.64	1.79	0.64	7.53	0.00
29	November	2012	ATFS-8	0.45	2.22	0.50	13.10	0.00
4	September	2012	ATFS-8	0.06	3.73	0.24	16.17	0.00
17	April	2013	ATFS-9	0.69	0.95	0.69	7.64	0.00
29	November	2012	ATFS-9	0.13	0.85	0.23	11.05	0.01
4	September	2012	ATFS-9	0.39	0.20	0.74	5.26	0.03
17	April	2013	ATFS-Tank	59.64	0.02	59.64	79.24	7.69
29	November	2012	ATFS-Tank	69.33	0.00	69.33	90.07	6.00
4	September	2012	ATFS-Tank	66.95	0.00	76.45	75.04	4.29

Appendix 2. Nutrient Data

JWS Nutrient Data

Day	Month	Year	Sample	NH4 (mg/L)	NO3+NO2 (mg/L)	DKN (mg/L)	Cl (mg/L)	PO4 (mg/L)	TDN (mg/L)
25	March	2013	Upstream	0.52	2.24	0.52	7.94	0.05	2.75
14	November	2012	Upstream	0.12	1.93	0.16	8.45	0.13	2.09
10	September	2012	upstream	0.02	1.01	0.26	9.84	0.06	1.27
25	March	2013	spring/stream	0.40	7.50	0.40	28.02	0.20	7.90
14	November	2012	spring/stream	0.11	1.85	0.11	8.76	0.06	1.95
10	September	2012	spring/stream	0.00	5.51	0.14	16.97	0.12	5.64
14	November	2012	JWS-1	0.18	0.31	0.70	2.71	0.59	1.00
14	November	2012	JWS-1	0.72	0.05	1.09	5.97	0.01	1.14
25	March	2013	JWS-10	0.35	44.25	0.35	87.30	0.50	44.60
14	November	2012	JWS-10	0.11	31.68	0.38	62.31	0.12	32.06
10	September	2012	JWS-10	0.00	30.35	0.55	40.45	2.20	30.90
25	March	2013	JWS-11d	0.09	0.44	0.09	7.74	0.46	0.54
14	November	2012	JWS-11d	0.46	0.38	0.46	8.02	1.07	0.84
10	September	2012	JWS-11d	0.28	0.59	0.56	11.16	0.81	1.14
25	March	2013	JWS-11s	0.38	0.04	0.38	5.91	0.16	0.04
14	November	2012	JWS-11s	0.14	1.25	0.36	7.84	0.26	1.61
10	September	2012	JWS-11s	0.09	0.14	0.29	8.18	0.30	0.43
25	March	2013	JWS-12	0.09	0.06	0.13	42.44	0.38	0.18
14	November	2012	JWS-12d	0.21	0.19	0.22	40.20	0.76	0.40
10	September	2012	JWS-12d	0.30	0.12	0.57	44.62	1.05	0.69
10	September	2012	JWS-12s	0.14	10.29	0.43	28.18	0.01	10.72
25	March	2013	JWS-13d	0.14	30.06	0.23	46.67	0.12	30.30
14	November	2012	JWS-13d	0.31	39.67	0.31	66.87	0.05	39.67
10	September	2012	JWS-13d	0.35	15.32	1.45	25.55	0.08	16.77
25	March	2013	JWS-13s	0.08	34.51	0.23	59.31	0.19	34.74
14	November	2012	JWS-13s	0.09	24.48	0.58	39.85	0.31	25.06
10	September	2012	JWS-13s	0.03	30.71	0.69	51.24	0.35	31.40

Appendix 2. Nutrient Data

JWS Nutrient Data

Day	Month	Year	Sample	NH4 (mg/L)	NO3+NO2 (mg/L)	DKN (mg/L)	Cl (mg/L)	PO4 (mg/L)	TDN (mg/L)
25	March	2013	JWS-14	0.09	29.47	0.17	77.61	0.14	29.64
14	November	2012	JWS-14	0.10	25.15	0.23	68.02	0.04	25.38
10	September	2012	JWS-14	0.02	25.42	0.32	71.86	0.09	25.74
25	March	2013	JWS-15	0.10	0.28	0.42	5.95	0.33	0.70
14	November	2012	JWS-15	0.77	0.35	1.05	4.22	0.00	1.40
10	September	2012	JWS-15	0.06	0.79	0.44	2.28	0.13	1.23
25	March	2013	JWS-16	0.15	0.10	0.15	7.25	0.23	0.10
14	November	2012	JWS-16	0.09	0.07	0.09	7.21	0.16	0.16
10	September	2012	JWS-16	0.04	0.03	0.19	6.02	0.03	0.22
25	March	2013	JWS-17	0.22	1.31	0.22	22.80	0.02	1.53
14	November	2012	JWS-17	0.42	0.00	0.59	32.67	0.01	0.59
10	September	2012	JWS-17	0.41	0.03	0.69	43.12	0.01	0.72
25	March	2013	JWS-18	0.25	7.00	0.25	26.94	0.00	7.25
14	November	2012	JWS-18	0.11	8.84	0.16	33.04	0.01	9.00
10	September	2012	JWS-18	0.00	7.32	0.30	38.06	0.11	7.62
25	March	2013	JWS-19	1.18	0.00	1.50	12.50	0.03	1.50
14	November	2012	JWS-19	1.80	0.00	2.28	11.54	0.00	2.28
25	March	2013	JWS-2	0.14	1.99	0.22	3.90	0.03	2.22
14	November	2012	JWS-2	0.33	2.28	0.36	4.30	0.00	2.64
10	September	2012	JWS-2	0.00	1.96	0.32	5.40	0.02	2.28
25	March	2013	JWS-20	0.40	0.03	0.56	18.23	0.16	0.59
14	November	2012	JWS-20	0.79	0.00	1.19	21.26	0.03	1.19
10	September	2012	JWS-20	1.09	0.09	1.57	22.25	0.19	1.67
14	November	2012	JWS-21	0.10	1.52	0.24	11.96	0.12	1.75
14	November	2012	JWS-3	0.17	0.42	0.20	2.53	0.04	0.62
10	September	2012	JWS-3	0.26	0.07	0.48	6.52	0.02	0.55
25	March	2013	JWS-3c	0.16	0.56	0.15	3.58	0.02	0.71

Appendix 2. Nutrient Data

JWS Nutrient Data

Day	Month	Year	Sample	NH4 (mg/L)	NO3+NO2 (mg/L)	DKN (mg/L)	Cl (mg/L)	PO4 (mg/L)	TDN (mg/L)
25	March	2013	JWS-4	0.12	35.43	0.42	70.69	0.58	35.85
14	November	2012	JWS-4	0.15	17.32	0.3	33.29	0.03	17.61
10	September	2012	JWS-4	0	14.23	0.35	24.3	2.08	14.58
25	March	2013	JWS-5	0.23	23.61	0.24	82.28	0.12	23.85
14	November	2012	JWS-5	0.11	21.42	0.32	62.19	0.18	21.74
10	September	2012	JWS-5	0.03	30.29	0.69	64.02	0.44	30.98
25	March	2013	Downstream	0.53	2.26	0.53	8.81	0.05	2.79
14	November	2012	Downstream	0.11	2.05	0.14	9.01	0.09	2.19
10	September	2012	Downstream	0.03	2.36	0.33	12.39	0.07	2.69
25	March	2013	JWS-6	0.31	52.48	0.31	85.19	0.16	52.79
14	November	2012	JWS-6	0.15	33.72	0.36	57.2	0.07	34.07
10	September	2012	JWS-6	0	45.72	0.46	71.56	0.15	46.19
25	March	2013	JWS-7	0.41	0.31	0.41	75.17	0.08	0.72
14	November	2012	JWS-7	0.19	5.83	0.39	88.22	0.07	6.22
14	November	2012	JWS-7	0.14	3.04	0.28	87.28	0.05	3.33
10	September	2012	JWS-7	0.14	59.51	0.87	70.62	0.44	60.38
25	March	2013	JWS-8	0.42	13.76	0.42	56.29	0	14.18
14	November	2012	JWS-8	0.07	14.23	0.37	63.77	0.03	14.6
10	September	2012	JWS-8	0	16.31	0.37	71.35	0.07	16.68
25	March	2013	JWS-9	0.55	0.16	0.55	2.07	0.07	0.71
14	November	2012	JWS-9	0.09	0.66	0.11	1.95	0.08	0.77
10	September	2012	JWS-9	0.01	0.26	0.14	1.65	0.06	0.39
25	March	2013	JWS-Sping2	0.39	6.5	0.39	6.1	0.14	6.5
10	September	2012	JWS-Sping2	0	13.43	0.17	38.71	0.18	13.6
25	March	2013	Spring1	0.33	7.64	0.33	26.01	0.23	7.64
14	November	2012	Spring1	0.09	7.56	0.09	28.26	0.21	7.65
10	September	2012	Sping1	0	13.28	0.17	38.3	0.22	13.45
10	September	2012	Spring1	0	14.25	0.13	40.41	0.22	14.38
25	March	2013	JWS-Tank	41.57	0.07	55.67	132.46	11.3	55.74
10	September	2012	JWS-Tank	27.97	0.03	27.97	28.5	3.79	28

Appendix 2. Nutrient Data

WCH Nutrient Data

Day	Month	Year	Sample	NH4 (mg/L)	NO3+NO2 (mg/L)	DKN (mg/L)	Cl (mg/L)	PO4 (mg/L)	TDN (mg/L)
10	April	2013	WC-10	0.14	0.16	0.14	1.29	0.00	0.31
7	September	2012	WC-10	0.08	0.16	0.50	1.06	0.02	0.66
10	April	2013	WC-11	0.17	0.88	0.17	2.64	0.01	1.05
14	November	2012	WC-11	0.54	0.16	0.74	2.14	0.00	0.90
7	September	2012	WC-11	0.04	0.01	0.36	1.80	0.00	0.37
10	April	2013	WC-12	0.14	34.50	0.22	42.67	0.00	34.72
14	November	2012	WC-12	0.08	4.89	0.37	10.93	0.01	5.26
7	September	2012	WC-12	0.08	7.78	0.70	8.43	0.01	8.48
10	April	2013	WC-13d	0.19	77.49	0.51	88.87	0.00	78.00
14	November	2012	WC-13d	0.13	59.37	0.78	67.61	0.01	60.16
7	September	2012	WC-13d	0.01	38.43	0.73	47.40	0.00	39.16
10	April	2013	WC-13s	0.37	50.20	0.44	63.32	0.02	50.64
14	November	2012	WC-13s	0.42	30.26	0.90	38.57	0.18	31.16
7	September	2012	WC-13s	0.03	5.32	0.59	13.43	0.01	5.91
10	April	2013	WC-14	0.81	0.07	0.81	1.31	0.01	0.89
14	November	2012	WC-14	0.09	0.15	0.30	1.51	0.04	0.45
7	September	2012	WC-14	0.24	0.08	0.57	1.42	0.05	0.65
10	April	2013	WC-15	1.16	49.47	1.16	54.34	0.32	50.63
14	November	2012	WC-15	0.05	6.73	0.59	8.43	0.36	7.32
7	September	2012	WC-15	0.03	1.38	0.44	6.35	0.12	1.82
10	April	2013	WC-16	1.32	43.64	1.32	48.03	0.01	44.96
14	November	2012	WC-16	0.14	4.12	0.42	8.21	0.02	4.54
7	September	2012	WC-16	0.05	0.20	0.24	2.18	0.00	0.44
10	April	2013	WC-17	1.41	90.84	1.41		0.01	92.24
14	November	2012	WC-17	0.13	80.09	0.35	109.34	0.25	80.44
7	September	2012	WC-17	0.02	11.60	0.37	8.43	0.04	11.96

Appendix 2. Nutrient Data

WCH Nutrient Data

Day	Month	Year	Sample	NH4 (mg/L)	NO3+NO2 (mg/L)	DKN (mg/L)	Cl (mg/L)	PO4 (mg/L)	TDN (mg/L)
10	April	2013	WC-18	1.24	31.97	1.24	47.43	0.20	33.22
14	November	2012	WC-18	0.18	28.47	0.54	32.97	0.22	29.01
7	September	2012	WC-18	0.02	2.77	0.60	4.29	0.22	3.37
10	April	2013	WC-19	0.59	1.56	0.59	2.25	0.01	2.15
14	November	2012	WC-19	0.47	0.10	0.47	3.29	0.01	0.57
7	September	2012	WC-19	0.04	0.12	0.37	4.03	0.08	0.49
10	April	2013	WC-1d	5.93	0.05	5.93	90.03	0.00	5.98
14	November	2012	WC-1d	4.22	0.00	4.22	38.97	0.00	4.22
10	April	2013	WC-1s	0.26	0.03	0.31	7.73	0.00	0.34
7	September	2012	WC-1s	0.04	0.00	0.74	16.29	0.00	0.74
7	September	2012	WC-1s	0.04	0.00	0.77	16.99	0.00	0.77
10	April	2013	WC-2	0.59	0.02	1.21	26.99	0.27	1.23
7	September	2012	WC-2	0.06	0.11	0.76	9.40	0.09	0.87
10	April	2013	WC-20	0.22	0.08	0.22	1.58	0.01	0.30
14	November	2012	WC-20	0.27	0.06	0.27	1.16	0.01	0.33
7	September	2012	WC-20	0.00	0.06	0.17	1.58	0.02	0.24
10	April	2013	WC-21	0.12	0.04	0.39	1.62	0.01	0.43
14	November	2012	WC-21	0.07	0.09	0.75	3.99	0.04	0.84
7	September	2012	WC-21	0.11	0.04	0.83	3.14	0.00	0.87
10	April	2013	WC-22d	0.11	0.43	0.11	1.38	0.00	0.54
14	November	2012	WC-22d	0.09	0.76	0.21	1.93	0.00	0.97
7	September	2012	WC-22d	0.94	0.94	1.16	1.94	0.04	2.10
10	April	2013	WC-22s	0.14	0.02	0.14	0.87	0.01	0.16
14	November	2012	WC-22s	0.22	0.01	0.36	2.12	0.00	0.37
7	September	2012	WC-22s	0.09	0.21	0.32	1.01	0.01	0.53

Appendix 2. Nutrient Data

WCH Nutrient Data

Day	Month	Year	Sample	NH4 (mg/L)	NO3+NO2 (mg/L)	DKN (mg/L)	Cl (mg/L)	PO4 (mg/L)	TDN (mg/L)
10	April	2013	WC-23	0.17	0.14	0.37	0.77	0.01	0.51
14	November	2012	WC-23	0.54	1.28	0.54	1.18	0.06	1.83
7	September	2012	WC-23	0.05	0.02	0.45	0.94	0.00	0.47
10	April	2013	WC-24d	0.25	35.48	0.32	46.75	0.00	35.80
14	November	2012	WC-24d	0.15	18.56	0.61	35.95	0.00	19.17
7	September	2012	WC-24d	0.05	5.44	0.45	23.12	0.00	5.89
10	April	2013	WC-24s	0.29	22.02	0.53	25.86	0.01	22.55
14	November	2012	WC-24s	0.08	5.24	0.53	9.01	0.01	5.77
7	September	2012	WC-24s	0.02	2.00	0.47	7.45	0.00	2.48
10	April	2013	WC-25d	0.38	27.70	0.51	35.32	0.02	28.21
14	November	2012	WC-25d	0.11	11.03	0.56	24.89	0.00	11.59
7	September	2012	WC-25d	0.06	9.53	0.51	23.85	0.00	10.04
10	April	2013	WC-25m	0.09	0.74	0.33	2.38	0.17	1.06
14	November	2012	WC-25m	0.06	1.13	0.43	3.99	0.26	1.56
7	September	2012	WC-25m	0.01	0.16	0.67	2.76	0.13	0.83
7	September	2012	WC-25m	0.03	0.13	0.84	2.27	0.13	0.96
10	April	2013	WC-25s	0.18	1.27	0.87	4.24	0.04	2.15
14	November	2012	WC-25s	0.75	0.44	1.44	4.65	0.05	1.88
7	September	2012	WC-25s	0.73	0.02	2.79	9.61	3.43	2.81
10	April	2013	WC-26d	0.68	2.11	0.68	5.15	0.00	2.79
14	November	2012	WC-26d	0.18	0.95	0.29	7.26	0.01	1.24
7	September	2012	WC-26d	0.36	0.01	0.30	11.21	0.00	0.31
10	April	2013	WC-26s	0.61	0.06	0.61	1.66	0.00	0.67
14	November	2012	WC-26s	0.18	0.19	0.18	2.46	0.00	0.37
7	September	2012	WC-26s	0.00	0.13	0.07	2.26	0.00	0.20
10	April	2013	WC-27d	0.91	41.85	0.91	48.02	0.17	42.76
14	November	2012	WC-27d	0.34	3.34	0.82	8.69	0.68	4.17
14	November	2012	WC-27d	0.36	3.32	0.81	9.42	0.68	4.12
7	September	2012	WC-27d	0.47	2.39	0.75	4.29	0.15	3.14

Appendix 2. Nutrient Data

WCH Nutrient Data

Day	Month	Year	Sample	NH4 (mg/L)	NO3+NO2 (mg/L)	DKN (mg/L)	Cl (mg/L)	PO4 (mg/L)	TDN (mg/L)
10	April	2013	WC-27m	0.79	0.75	0.79	4.82	0.00	1.54
14	November	2012	WC-27m	0.29	0.13	0.41	4.42	0.00	0.54
7	September	2012	WC-27m	0.06	0.12	0.60	1.83	0.29	0.72
10	April	2013	WC-27s	0.71	0.12	0.71	0.73	0.00	0.84
14	November	2012	WC-27s	0.13	0.11	0.26	1.88	0.00	0.37
7	September	2012	WC-27s	0.07	0.00	0.23	1.93	0.00	0.23
10	April	2013	WC-3	1.44	0.09	1.44	2.54	0.00	1.53
7	September	2012	WC-3	0.12	0.09	0.63	2.25	0.02	0.73
7	September	2012	WC-3	0.11	0.10	no sample	2.42	0.02	0.10
7	September	2012	WC-4	0.03	0.07	0.74	2.27	0.28	0.81
10	April	2013	WC-5d	2.93	0.18	2.93	3.58	0.00	3.11
10	April	2013	WC-5d	3.15	0.17	3.15	3.82	0.00	3.33
7	September	2012	WC-5d	0.06	0.06	0.38	2.62	0.00	0.43
14	November	2012	WC-5s	0.09	0.47	0.30	3.82	0.00	0.77
7	September	2012	WC-5s	0.03	0.22	0.40	3.70	0.00	0.62
10	April	2013	WC-6	3.37	0.01	3.37	7.31	0.02	3.38
14	November	2012	WC-6	0.17	0.10	0.19	6.49	0.00	0.29
7	September	2012	WC-6	0.13	0.05	0.52	3.21	0.05	0.58
10	April	2013	WC-7	3.02	0.14	3.02	2.08	0.00	3.16
14	November	2012	WC-7	0.35	0.03	0.35	1.95	0.01	0.38
7	September	2012	WC-7	0.03	0.01	0.42	4.11	0.01	0.43

Appendix 2. Nutrient Data

WCH Nutrient Data

Day	Month	Year	Sample	NH4 (mg/L)	NO3+NO2 (mg/L)	DKN (mg/L)	Cl (mg/L)	PO4 (mg/L)	TDN (mg/L)
10	April	2013	WC-8	1.77	3.98	1.77	6.53	0.00	5.75
14	November	2012	WC-8	0.83	20.32	0.83	20.15	0.00	21.16
7	September	2012	WC-8	0.03	2.88	0.36	4.88	0.01	3.24
10	April	2013	WC-9	0.07	2.14	0.22	2.81	0.01	2.37
14	November	2012	WC-9	0.32	0.63	0.32	1.77	0.04	0.96
7	September	2012	WC-9	0.03	0.28	0.36	1.44	0.01	0.64
10	April	2013	WC-ditch	0.09	0.31	0.54	5.64	0.00	0.85
10	April	2013	WC-Tank	51.82	0.04	53.79	98.11	7.66	53.83
14	November	2012	WC-Tank	75.23	0.03	83.24	121.95	11.80	83.27
7	September	2012	WC-Tank	101.84	0.00	105.38	99.65	7.13	105.38

Appendix 2. Geophysics Maps (Site 100 GPR transects with drainfield area in dashed box).

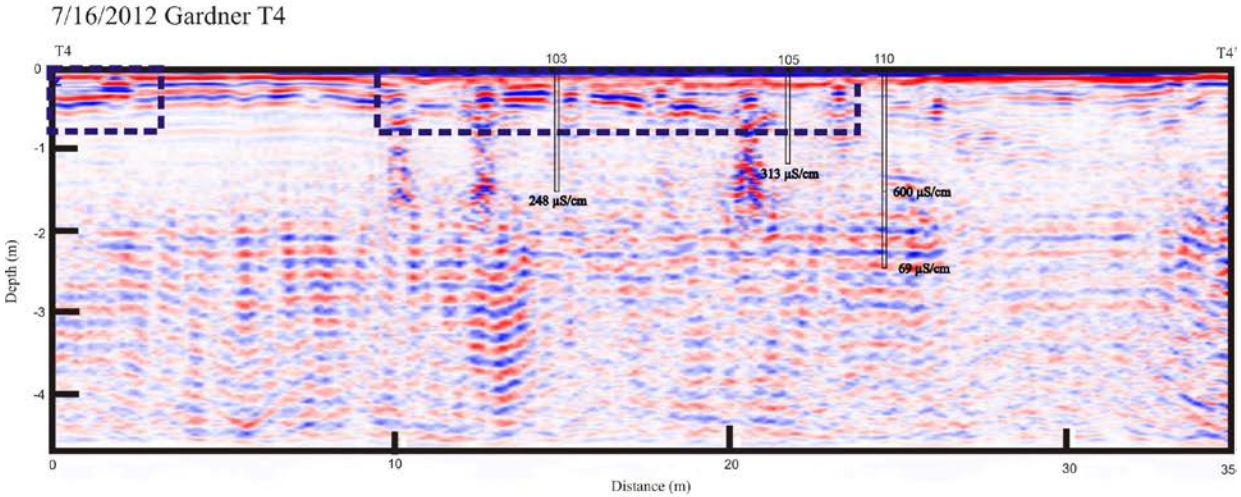

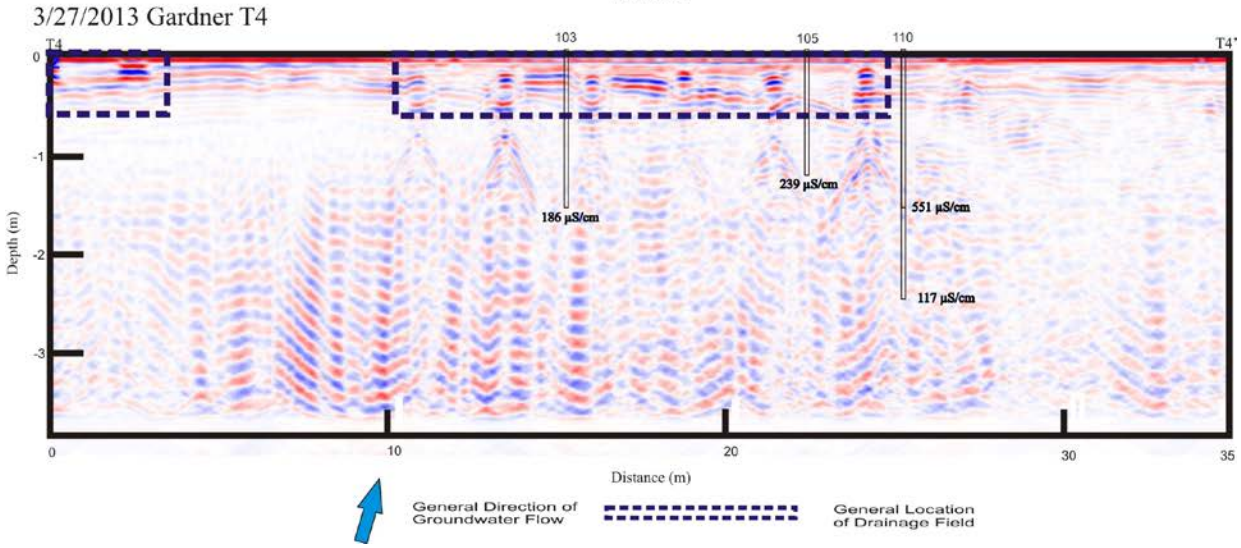

Appendix 2. Geophysics Map Site 100 ER transects near stream (T1), across DF (T2), and upgradient (T3)

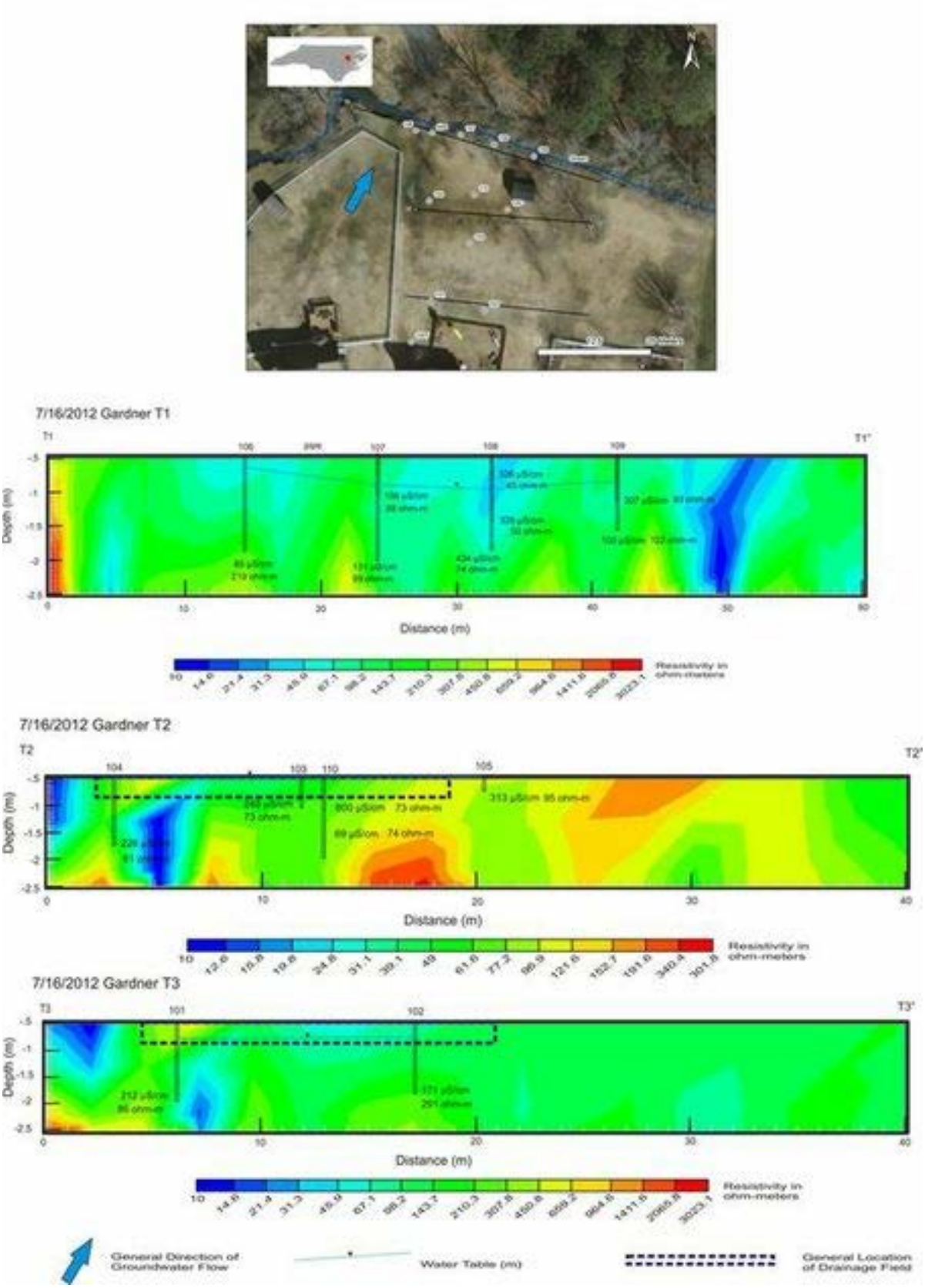

Appendix 2. Geophysics Maps (GPR transects at JWS with drainfield area in dashed line).

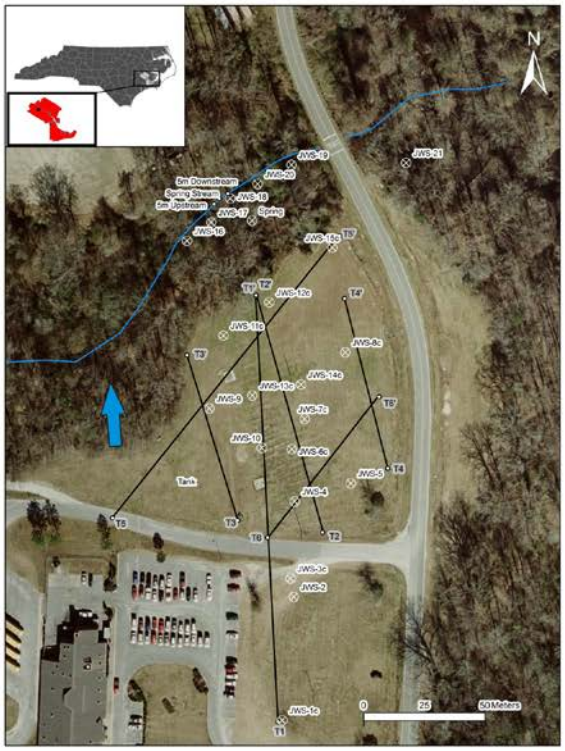

9/10/2012 JWS T1

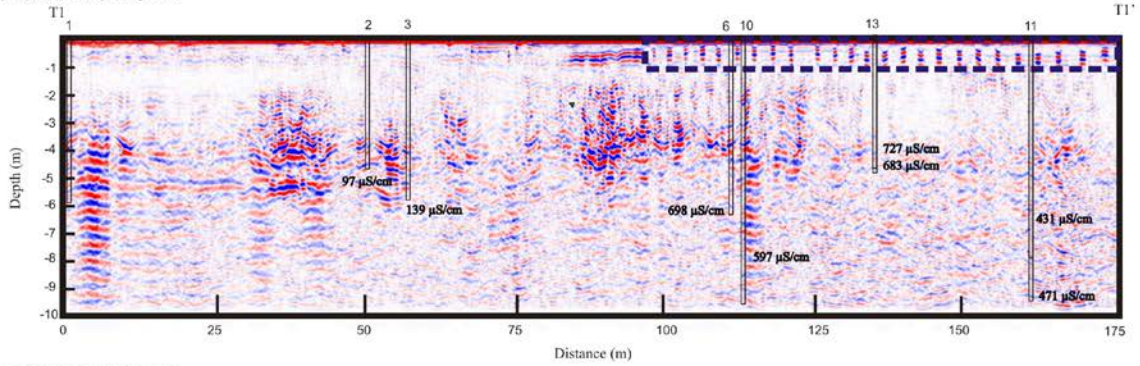

11/19/2012 JWS T1

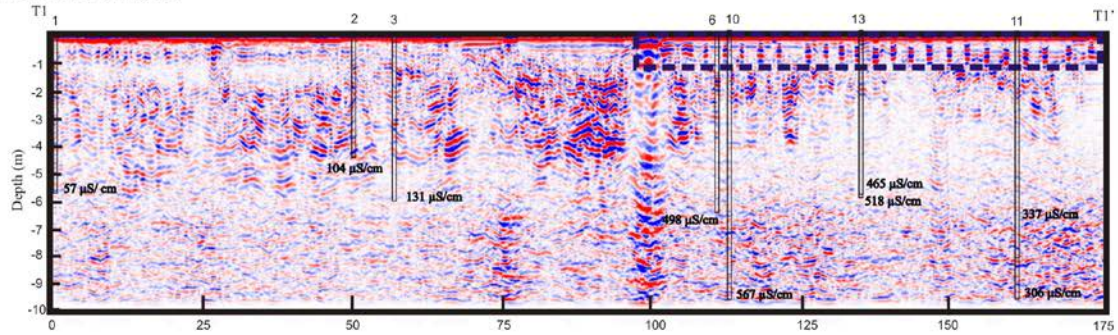

Appendix 2. Geophysics Maps (ER transects at JWS with drainfield area in dashed line).

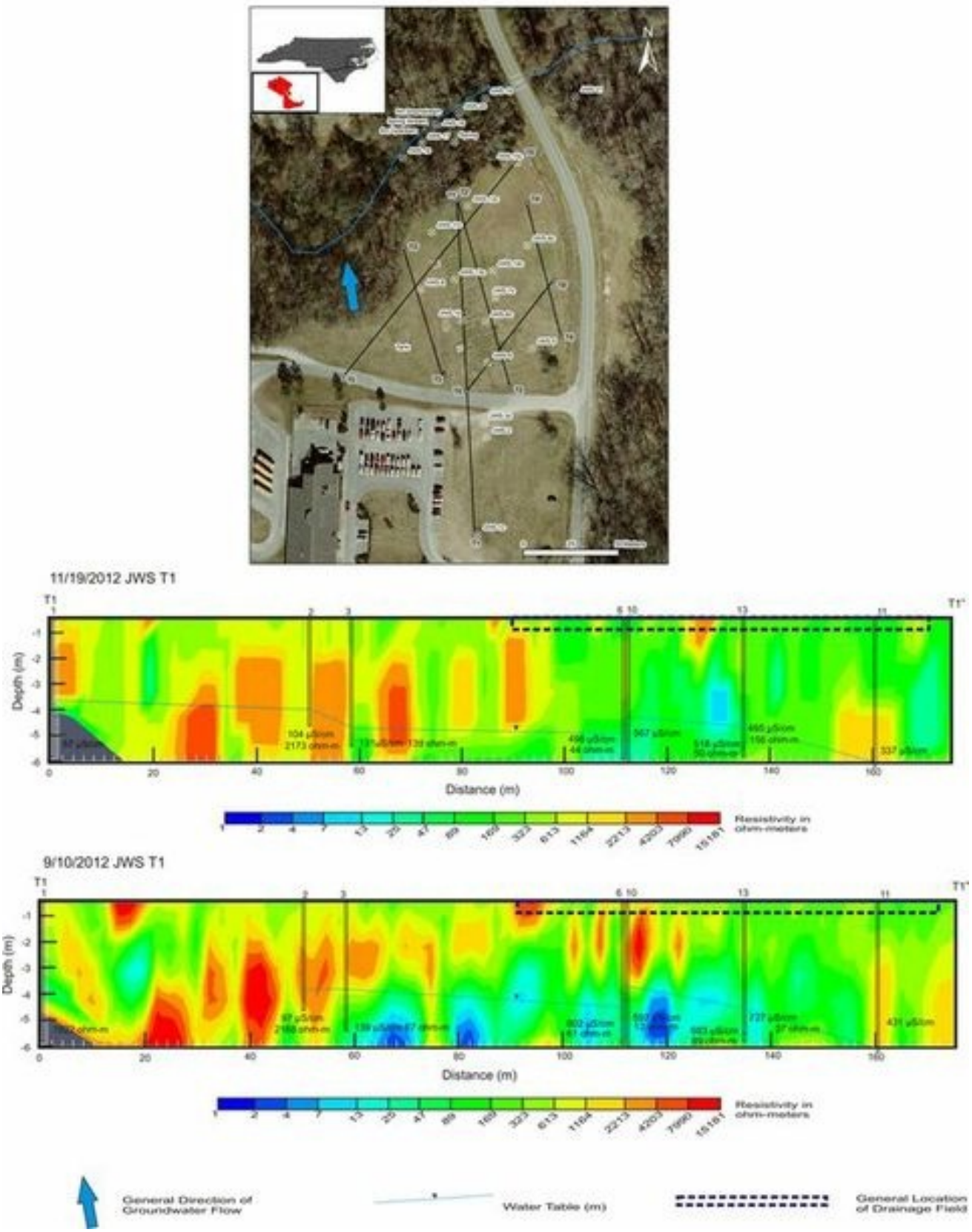

Appendix 2. Geophysics Maps (GPR transects at WCH with drainfield area in dashed line).

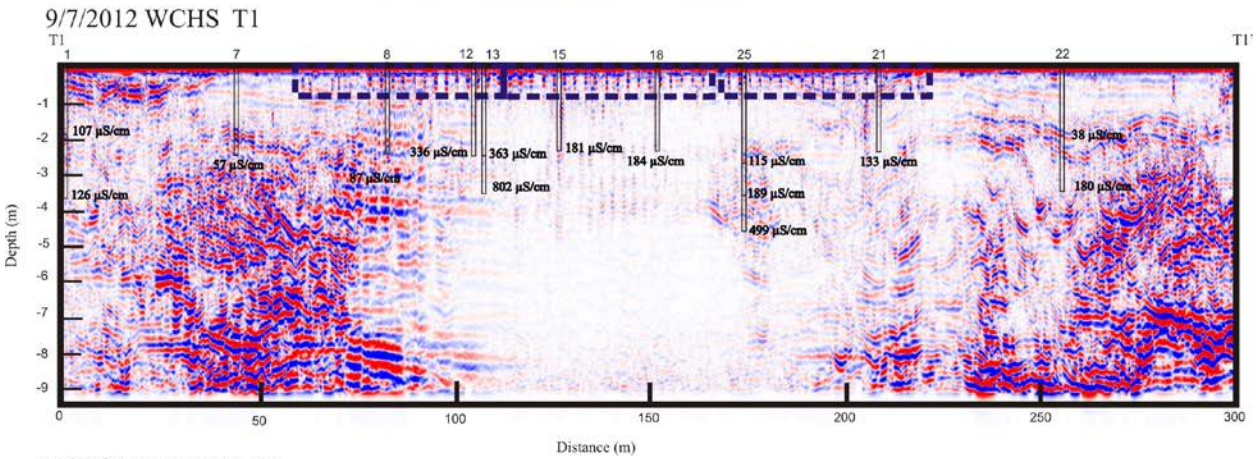

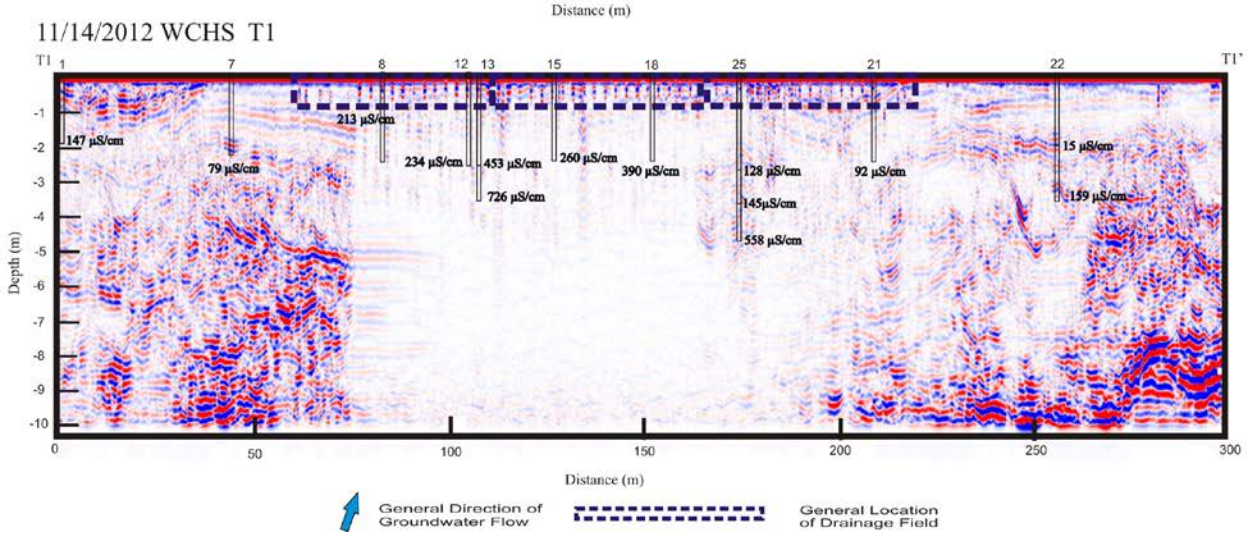

Appendix 2. Geophysics Maps (ER transects at WCH with drainfield area in dashed line).

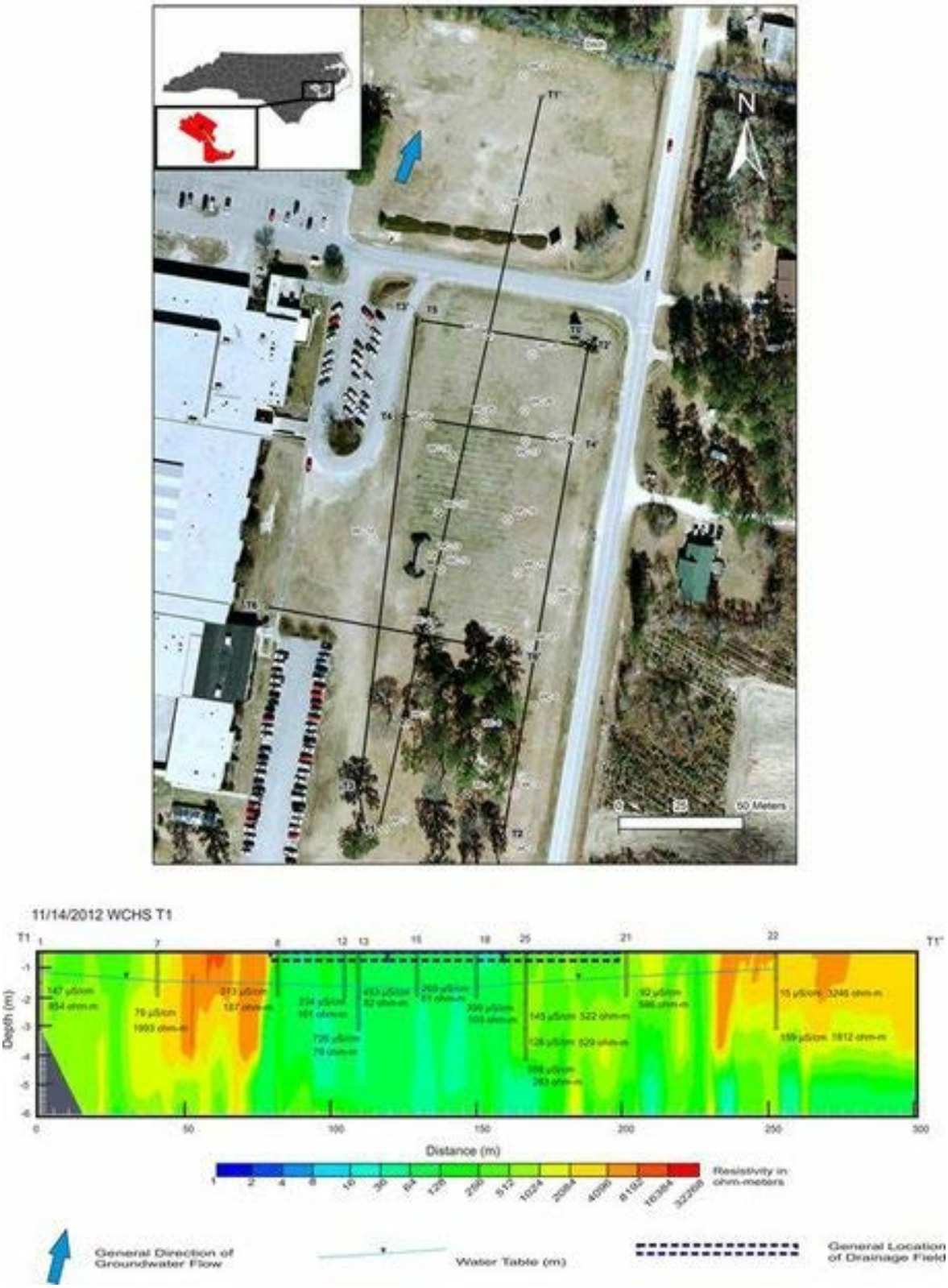

Appendix 2. Geophysics Maps (ER transects at WCH with drainfield area in dashed line).

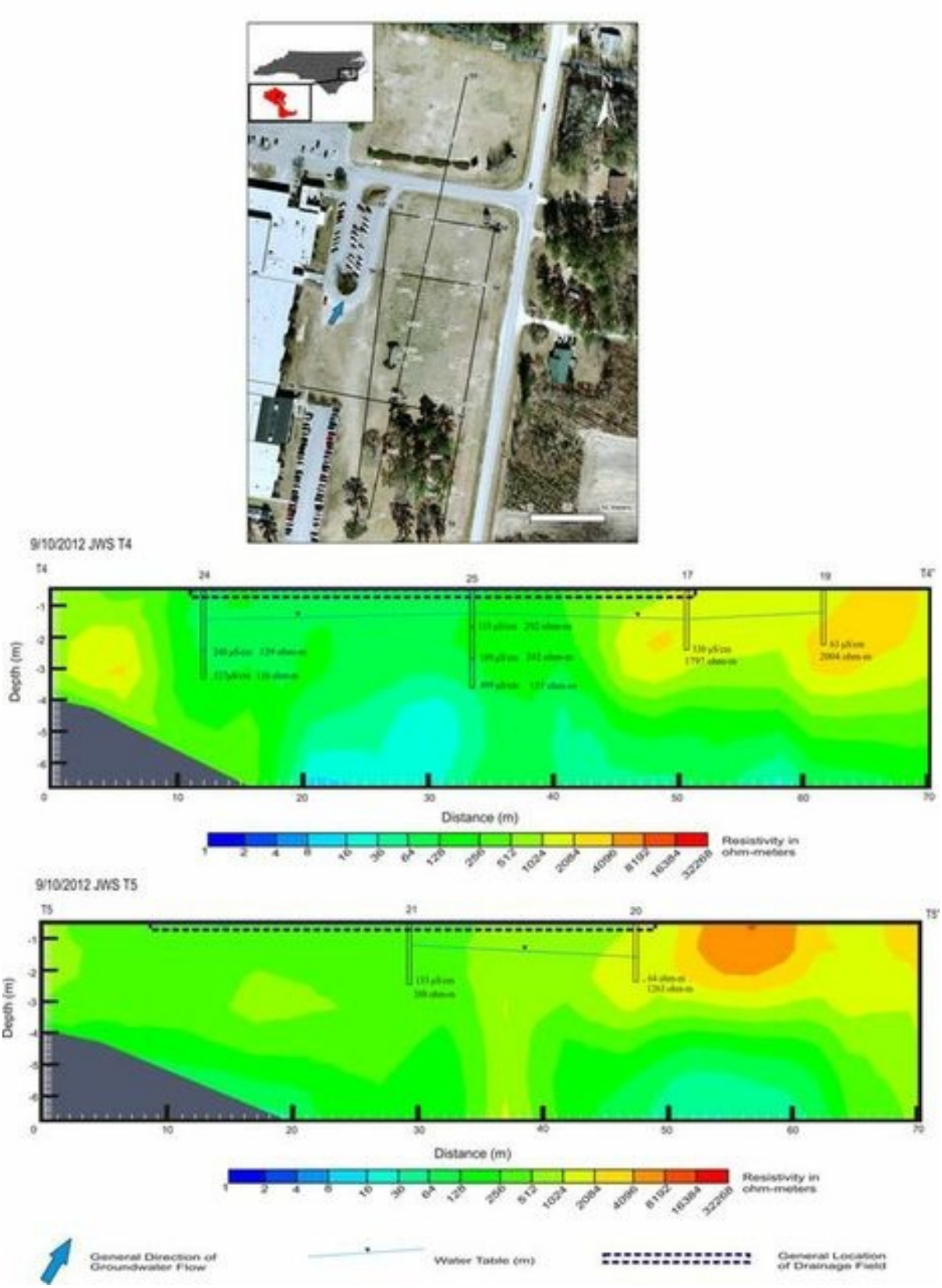

Appendix 2. Geophysics Maps (ER transects at ATFS with drainfield area in dashed line).

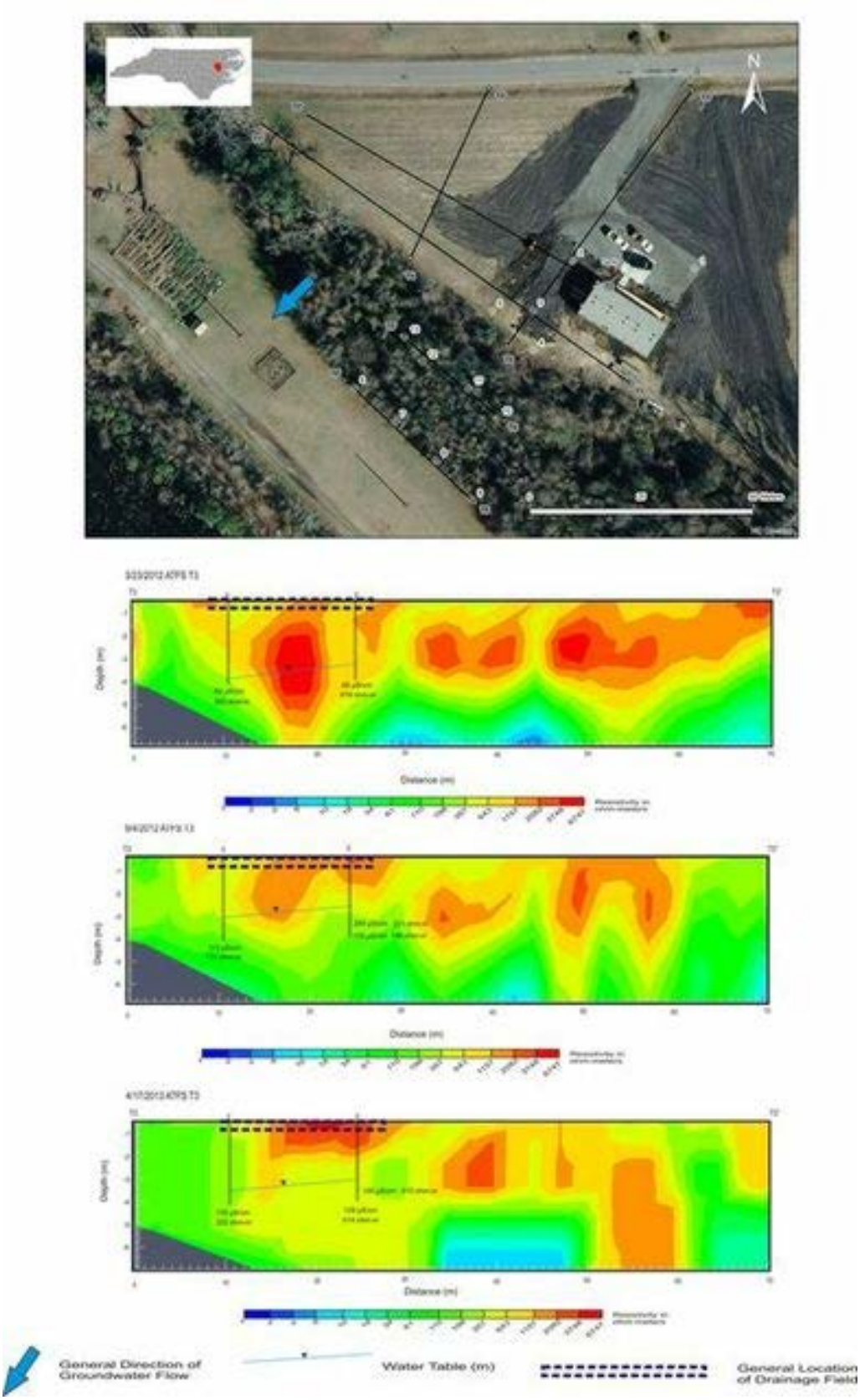

Appendix 2. Geophysics Maps (GPR transects at ATFS with drainfield area in dashed box).

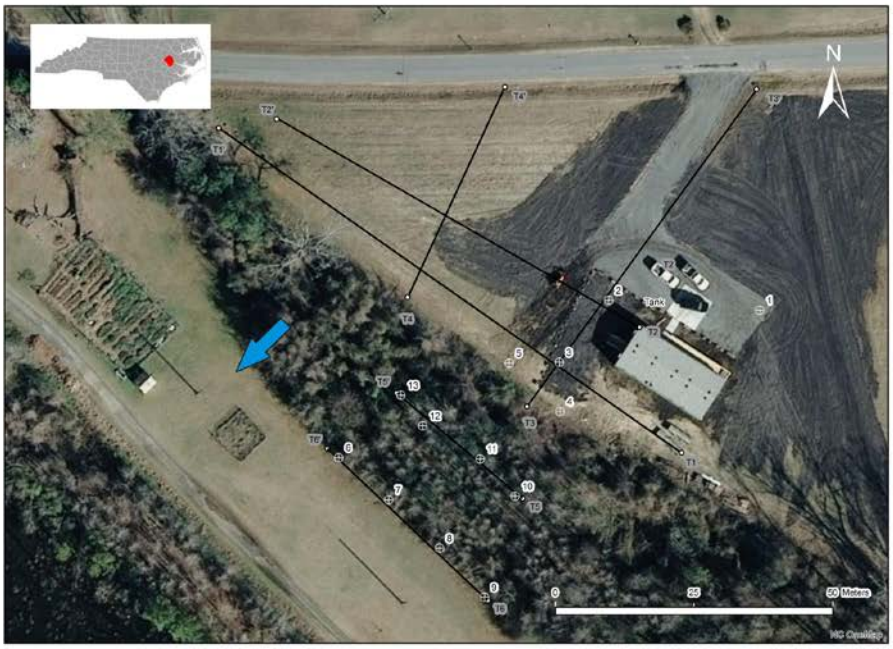

9/4/2012 ATFS T1

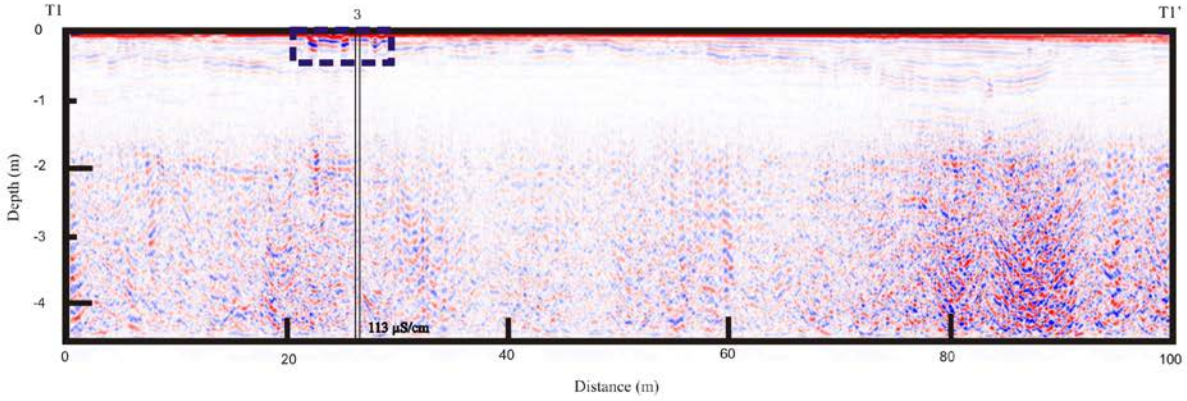

11/30/2012 ATFS T1

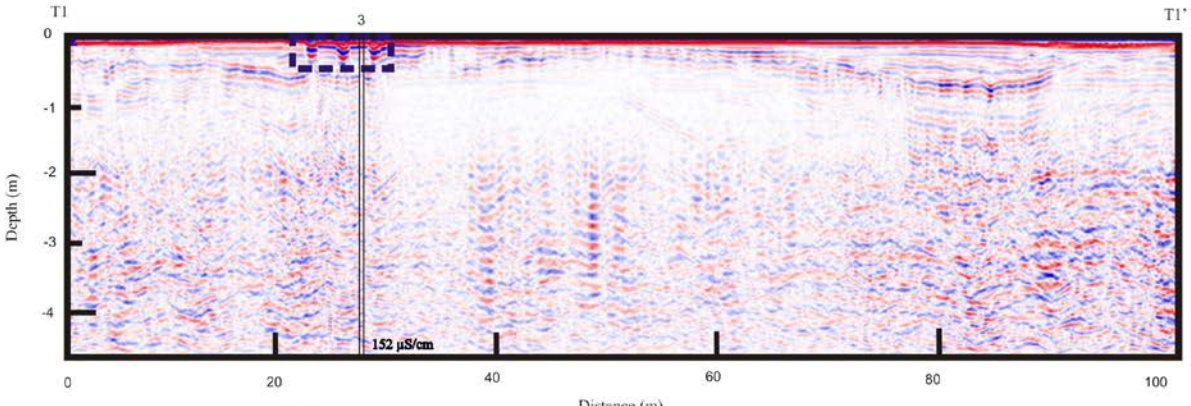

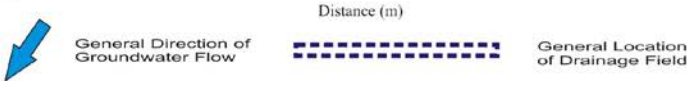

Appendix 2. Onsite system schematic for WCH showing low pressure pipe fields 1 and 2.

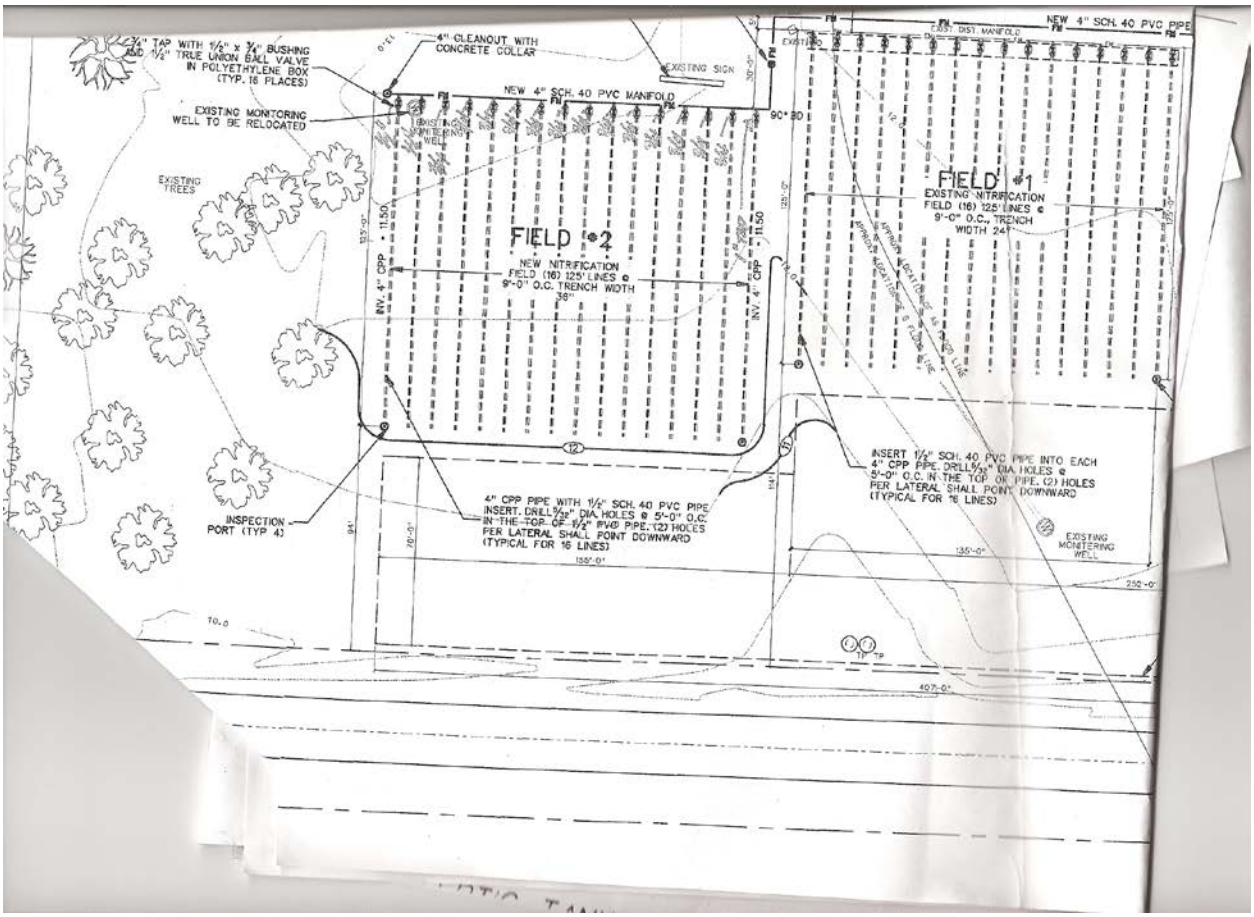

Appendix 2. Onsite system schematic for JWS

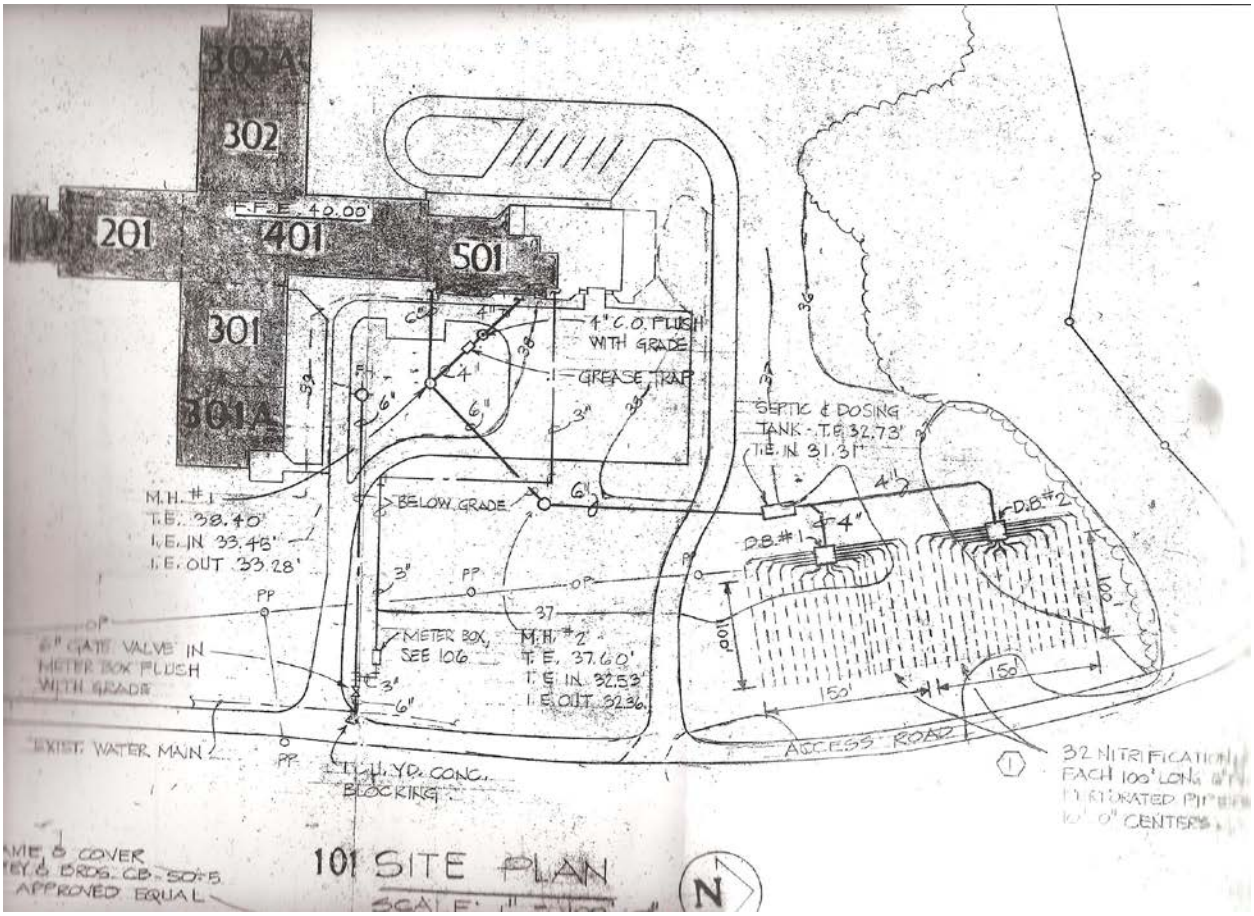

Appendix 2. Onsite system schematic for Site 100.